

People's Democratic Republic of Algeria
Ministry of Higher Education and Scientific Research
University M'Hamed BOUGARA – Boumerdes



Institute of Electrical and Electronic Engineering
Department of Power and Control

Final Year Project Report Presented in Partial Fulfilment of
the Requirements for the Degree of

MASTER

In Electrical and Electronic Engineering
Option: Power Engineering

Title:

**Mitigating Ferroresonance in MV Power
System Involving Power Transformer
and Circuit Breaker Capacitance using
Alternating Transient Program**

Presented by:

- **BEDDA ZEKRI Sad**
- **MEKKAoui Tarek**

Supervisor:

Mrs.BOUTORA.S

Registration Number:...../2016

Dedication

On the occasion of finishing my final year project, it gives me immense pleasure to express my gratitude to:

*Who helped me to reach this degree, who I cannot live without them **My Mother** and **My Father**.*

As Allah the Highest says: “And lower to them the wing of humility out of mercy” and say, “My Lord, have mercy upon them as they brought me up when I was small.”

My uncles and My aunts

***My Brothers:** Abdelmounem, Ilyes, Foudil, Ziad and especially to my heart Ahmed.*

***My lovely Sister:** “Atika”.*

***My Future Wife:** “Sara”.*

***My Supervisor:** BOU TORAJA for her help, and all who learned me even a letter.*

***My Friends:** ((especially my roommates Khaled M, Oussama T and Med ramzi CH))
My partner and best friend Tarek MEKKA OUI
and others Ali K, Bilal G, Djilani G, Hamza Z, Khaled B, ... and the list is so long.*

With Love 🌸

SAD

Dedication

*All praise to Allah, today we fold the days' tiredness and the errand
summing up between the cover of this humble work,*

*To the utmost knowledge lighthouse, to our greatest and most honored
prophet Mohamed - May peace and grace from Allah be upon him-*

*To the spring that never stops giving, to my mother who weaves my
happiness with strings from her merciful heart... to my mother.*

(Mama and Yama)

*To whom he strives to bless comfort and welfare and never stints, what he
owns to push me in the success way who taught me to promote life stairs
wisely and patiently, to my dearest father.*

*To whose love flows in my veins and my heart always remembers them, to my
brothers and sisters.*

(Mustapha, M.ishak, Hadjer, Hibaallah and Halla)

*To those who taught us letters of gold and words of jewel of the utmost and
sweetest sentences in the whole knowledge. Who reworded to us their
knowledge simply and from their thoughts made a lighthouse guides us
through the knowledge and success path, To our honored teachers and
professors.*

*To my friends Abdullah, Bachir, Bader, Baki, Belgacem, Bilal, Chouaib,
djafer, Farouk, Hachimi, Mohammed, Hamza.Z, Hamza.H, Khaled,
Maki, Masouad, Nani, Nour eldine, Omer.G, Omer.B, Ridha, Sad,
Salem, Taher, Yacine, Yacine, Zakaria and the list is so long.*

With love

TAREK

Acknowledgment

We would like to express our very great appreciation to Mrs.BOUTORA.S, our supervisor, for her patient guidance, enthusiastic encouragement and useful critiques, and for her valuable and constructive suggestions during the planning and development of this search work. Her willingness to give her time so generously has been very much appreciated.

We would also like to extend our grateful thanks to our parents and friends for their invaluable support.

A great appreciation to the library supervisors for their help in providing us the references needed.

ABSTRACT

Ferroresonance is a phenomenon usually initiated by transients in power networks resulting from switching operations or ground faults or others. Nonlinear behavior of the core of a power transformer results in magnetic saturation. Long-lasting ferroresonant state is dangerous to the equipment due to prolonged overvoltage and large overcurrents in MV windings. In this thesis, a ferroresonance solution using Alternating Transient Program, was attempted. The ferroresonant oscillations analyzed result from interaction between the power transformer and a grading capacitance of a circuit breaker. Some practical solutions are suggested and introduced after creating a ferroresonance situation, they had a considerable effect on damping and eliminating the risk of ferroresonance.

TABLE OF CONTENTS

DEDICATION	I
ACKNOWLEDGMENT	III
ABSTRACT	IV
TABLE OF CONTENTS	V
LIST OF TABLES	VII
LIST OF FIGURES	VIII
GENERAL INTRODUCTION	1
CHAPTER 01: Identifying Ferroresonance Compared To Linear Resonance	
1.1. Introduction	2
1.2. Identifying Ferroresonance Compared To Linear Resonance	2
1.3. Conclusion	8
CHAPTER 02: Understanding Ferroresonance	
2.1. Introduction	9
2.2. Types of Ferroresonance Modes	9
2.2.1. Fundamental mode	9
2.2.2. Subharmonic mode	10
2.2.3. Quasi-periodic mode	10
2.2.4. Chaotic mode	11
2.3. Causes and Effects of Ferroresonance on Power Systems	11
2.3.1. Systems Vulnerable to Ferroresonance	12
2.3.1.1. Voltage Transformer Energized Through Grading Capacitance	12
2.3.1.2. Voltage Transformers Connected to an Isolated Neutral System	13
2.3.1.3. Voltage Transformers and HV/MV Transformers with Isolated Neutral	13
2.3.1.4. Transformer Supplied by a Highly Capacitive Power System with Low Short-Circuit Power	14
2.3.1.5. Transformer Accidentally Energized in Only One or Two Phases	15
2.3.1.6. Power system grounded through a reactor	16
2.3.2. Effect of Ferroresonance on Power Systems	17

2.4. Controlling Ferroresonance	18
2.4.1. Damping Ferroresonance in Voltage Transformers	19
2.4.1.1. Voltage Transformers with one Secondary Winding	19
2.4.1.2. Voltage Transformers with two Secondary Winding	19
2.4.2. Limiting the cable length switched	20
2.5 conclusion	20
CHAPTER 03: Simulation results	
3.1. Introduction	21
3.2. The electrical power network of Haoud Berkaoui	21
3.3. Highlights about Alternative Transient Program	22
3.3.1. What is ATP?	22
3.3.2. ATPDraw	22
3.4. The real electrical circuit of Haoud Berkaoui	23
3.4.1. Description of the circuit	23
3.4.2. The characteristics of the equipment used in the Substation	24
3.4.3. ATP simulation results	25
3.5. The Case study	27
3.5.1 The effect of changing grading capacitor (Cg)	27
3.6. Practical solution	36
3.6.1. increasing the value of shunt capacitance at the transformer primary side	36
3.6.2. installing a capacitor bank at the transformer secondary side	38
3.6.3. installing a damping resistor at the transformer secondary side	41
3.7. Conclusion	44
GENERAL CONCLUSION	45
REFERENCES	
APPENDIX	

LIST OF TABLES**CHAPTER 03: Simulation results**

Table 3.1: Ferroresonance simulations results summary of maximum overvoltage for C_g	34
Table 3.2: Simulation results of maximum overvoltage for shunt capacitors.....	36
Table 3.3: Simulation results of maximum overvoltage for bank capacitors.....	39
Table 3.4: Simulation results of maximum overvoltage for damping resistor.....	42

LIST OF FIGURES

CHAPTER 01: Identifying Ferroresonance Compared with Linear Resonance

Figure 1.1: Series LC Circuit with Sinusoidal Voltage Source	2
Figure 1.2: λ -I Characteristic for a linear inductor	2
Figure 1.3: Frequency Response of a Linear LC Circuit.....	3
Figure 1.4: λ -I Characteristic for a nonlinear inductance.....	3
Figure 1.5: Frequency Response of a Nonlinear LC Circuit.....	4
Figure 1.6: Jump phenomena for variation of the amplitude of the excitation.....	5
Figure 1.7: Ferroresonant Circuit.....	5
Figure 1.8: Graphical solution of the ferroresonance circuit.....	7

CHAPTER 02: Understanding Ferroresonance

Figure 2.1: Fundamental mode of ferroresonance.....	10
Figure 2.2: Subharmonic mode of ferroresonance.....	10
Figure 2.3: Quasi-periodic mode of ferroresonance.....	11
Figure 2.4: Chaotic mode of ferroresonance.....	12
Figure 2.5: Ferroresonance of a voltage transformer connected in series with an open circuit Breaker.....	12
Figure 2.6: Ferroresonance of a VT between phase and ground in an isolated neutral system.....	13
Figure 2.7: Faulty system.....	13
Figure 2.8: Ferro-resonance of voltage transformer between phase and ground with ungrounded/isolated neutral	14
Figure 2.9: Power transformer supplied by capacitive system.....	14
Figure 2.10: Examples of unbalanced systems.....	15
Figure 2.11: PIM inductance between neutral and ground.....	16
Figure 2.12: Resonant grounding system.....	16
Figure 2.13: Damping for voltage transformer with one secondary.....	19
Figure 2.14: Damping for voltage transformer with two secondaries.....	19

CHAPTER 03: Simulation results

Figure 3.1: the geographic location of Haoud Berkaoui.....	21
Figure 3.2: Main Window Multiple Circuit windows and the floating Selection menu.....	23
Figure 3.3: The one line diagram representation.....	24
Figure 3.4: ATPDraw representation of the circuit of Haoud Berkaoui station.....	25
Figure 3.5: The values of voltages at the point A	26
Figure 3.6: The values of voltages at the point TRS, B, C and D.....	26
Figure 3.7: Voltage transformer connected in series with an open circuit breaker.....	27
Figure 3.8: The ATP model circuit used for simulation.....	28

Figure 3.9: The voltages at point TRS with $C_g = 1\text{nF}$ and 100% V_s	28
Figure 3.10: The voltages at point TRS with $C_g = 600\text{nF}$ and 100% V_s	29
Figure 3.11: The voltages at point TRS with $C_g = 2\mu\text{F}$ and 100% V_s	29
Figure 3.12: The voltages at point TRS with $C_g = 5\mu\text{F}$ and 100% V_s	29
Figure 3.13: The voltages at point TRS with $C_g = 30\mu\text{F}$ and 100% V_s	30
Figure 3.14: The voltages at point TRS with $C_g = 1\text{nF}$ and 80% V_s	30
Figure 3.15: The voltages at point TRS with $C_g = 600\text{nF}$ and 80% V_s	31
Figure 3.16: The voltages at point TRS with $C_g = 2\mu\text{F}$ and 80% V_s	31
Figure 3.17: The voltages at point TRS with $C_g = 5\mu\text{F}$ and 80% V_s	31
Figure 3.18: The voltages at point TRS with $C_g = 30\mu\text{F}$ and 80% V_s	32
Figure 3.19: The voltages at point TRS with $C_g = 1\text{nF}$ and 120% V_s	32
Figure 3.20: The voltages at point TRS with $C_g = 600\text{nF}$ and 120% V_s	33
Figure 3.21: The voltages at point TRS with $C_g = 2\mu\text{F}$ and 120% V_s	33
Figure 3.22: The voltages at point TRS with $C_g = 5\mu\text{F}$ and 120% V_s	33
Figure 3.23: The voltages at point TRS with $C_g = 30\mu\text{F}$ and 120% V_s	34
Figure 3.24: The effect of the grading Capacitance on ferroresonance.	35
Figure 3.25: The effect of the Shunt Capacitance on ferroresonance.	36
Figure 3.26: The voltages at point TRS for Case 1 with $C_s = 0.5\mu\text{F}$	37
Figure 3.27: The voltages at point TRS for case 3 with $C_s = 2.7\mu\text{F}$	37
Figure 3.28: The voltages at point TRS for Case 5 with $C_s = 5\mu\text{F}$	37
Figure 3.29: Capacitor bank at the transformer TR1 secondary side.	38
Figure 3.30: The effect of the Bank Capacitance on ferroresonance.	39
Figure 3.31: The voltages at point TRS for Case 1 with $C_b = 10\mu\text{F}$	40
Figure 3.32: The voltages at point TRS for Case 4 with $C_b = 49\mu\text{F}$	40
Figure 3.33: The voltages at point TRS for Case 7 with $C_b = 100\mu\text{F}$	40
Figure 3.34: The damping resistor at the transformer TR1 secondary side.	41
Figure 3.35: The effect of the Damping resistor on ferroresonance.	42
Figure 3.36: The voltages at point TRS for Case 5 with $R = 30\Omega$	43
Figure 3.37: The voltages at point TRS for Case 4 with $R = 25\Omega$	43
Figure 3.38: The voltages at point TRS for Case 1 with $R = 12\Omega$	43

GENERAL INTRODUCTION

GENERAL INTRODUCTION

Power quality and power disturbances have become an important increasing factor throughout electrical networks. Ferroresonance is one of these disturbances that can occur on distribution systems, causing quality and security problems.

Ferroresonance is a non-linear resonance phenomenon that can affect power networks. The abnormal rates of harmonics and transients or steady state overvoltages and overcurrents that it causes are often dangerous for electrical equipment.

The term “Ferroresonance”, which appeared in the literature for the first time in 1920, refers to all oscillating phenomena occurring in an electric circuit which must contain at least:

- 1) a non-linear inductance (ferromagnetic and saturable).
- 2) a capacitor.
- 3) a voltage source (generally sinusoidal).
- 4) low losses. [1]

Power networks are made up of a large number of saturable inductances (power transformers, voltage measurement inductive transformers (VT), shunt reactors), as well as capacitors (cables, long lines, capacitor voltage transformers, series or shunt capacitor banks, voltage grading capacitors in circuit-breakers, metalclad substations). They thus present scenarios under which ferroresonance can occur. [1]

The aim of this thesis is to identify ferroresonance and to understand it better, when it is compared to linear LC resonance. Also to describe the effects of ferroresonance on power systems, because they are considered to be catastrophic when they occur, in addition the methods of mitigating them will be discussed.

In order to demonstrate the achievement of the stated aim, we strengthen our study with simulation of one of favorable cases of this phenomenon, which is the interaction between the power transformer and circuit breaker grading capacitor in MV power system, then we try to find some practical solutions.

Chapter 1

Identifying Ferroresonance Compared To Linear Resonance

1.1. Introduction

The trend toward using higher distribution voltages and underground feeders has increased the number of instances in which ferroresonance overvoltage have been reported. [2] The problem of ferroresonance can be categorized as a nonlinear resonance which can cause damage in power distribution and transmission systems. In simple terms, ferroresonance is an LC resonance involving a nonlinear inductance and a capacitance. [3] Ferroresonance can be better understood if it is compared to linear LC resonance.

1.2. Identifying Ferroresonance Compared to Linear Resonance

A typical linear LC resonant circuit consists of an ideal inductor connected in parallel or series with an ideal capacitor. There is no damping in the circuit and the behavior of this LC combination is observed as the frequency of an applied sinusoidal voltage or current is varied. Figure 1.1 shows an example of a series LC circuit with linear elements. In this circuit L is constant and independent of current, regardless of the flux linked λ by the inductor. The relationship between the flux and the current is shown in the Figure 1.2. [3]

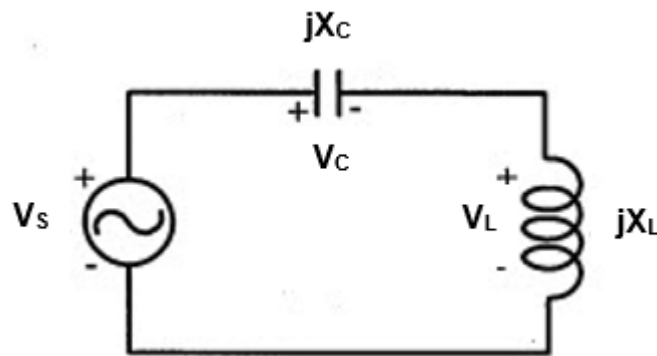


Figure 1.1: Series LC Circuit with Sinusoidal Voltage Source

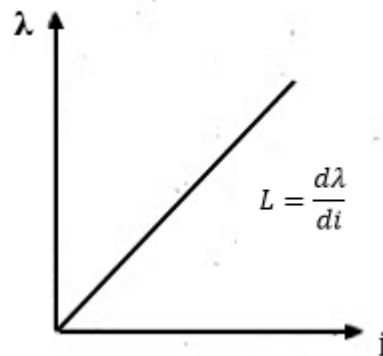


Figure 1.2: λ - i Characteristic for a linear inductor

In this circuit, the resonance occurs when the total impedance of the circuit $jX_L - jX_C$ equal to zero. The frequency at which this happens is $\omega_r = \frac{1}{\sqrt{LC}}$. Therefore as ω approaches ω_r , current i approaches ∞

Figure 1.3 shows the frequency response of a linear LC circuit. [3]

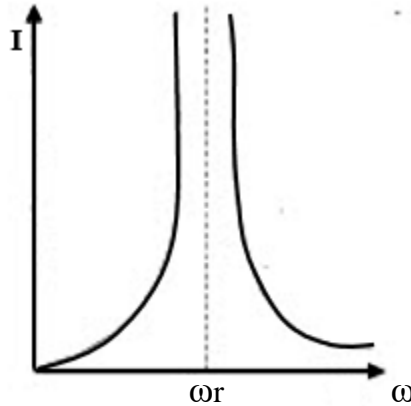


Figure 1.3: Frequency Response of a Linear LC Circuit

If damping is considered as a resistance in parallel with the inductor in the above case, the current will be limited to $i < \infty$ and the resonant frequency will be shifted to a new damped resonant frequency to $\omega = \omega_d$.

In the circuit of figure 1.1, if the linear inductance is replaced with a nonlinear saturable iron core inductor then ferroresonance can occur. A typical λ - i characteristic of such an inductor is shown in figure 1.4 which is typical for a transformer core. [3]

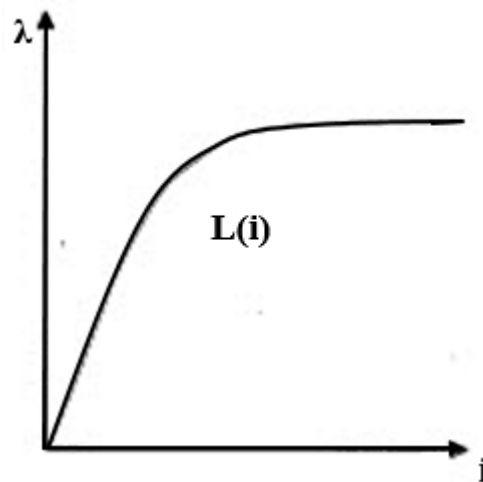


Figure 1.4: λ - i Characteristic for a nonlinear inductance

The circuit with a nonlinear inductance will have a much different type of frequency response. In this case, there is no single resonant frequency, since the frequency response characteristic will be multi-

valued. [3] Figure 1.5 shows the frequency response of a nonlinear LC circuit when there is no damping in the system.

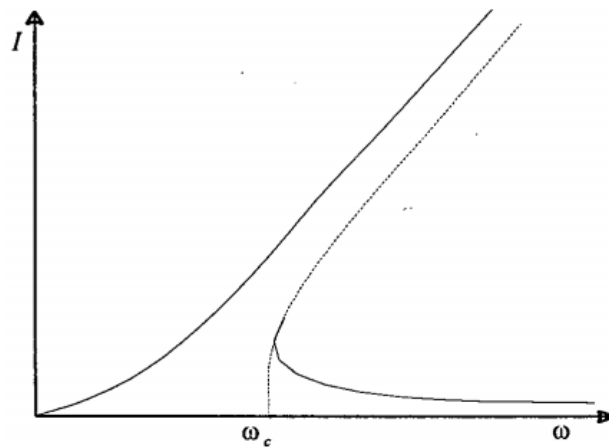


Figure 1.5: Frequency Response of a Nonlinear LC Circuit

- For $\omega > \omega_c$, there may be two stable modes of “Resonance” as well as a third unstable mode.
- For $\omega < \omega_c$ there is only one possible mode of operation.

As ω is decreased and its value passes ω_c , operation can make a sudden change or jump from one stable operating mode to another. This is one of the reasons why this type of behavior is sometimes called jump resonance.

Therefore, jump resonance refers to a condition in a sinusoidally excited system where an incremental change in the frequency of the input to the system or an incremental change in the driving voltage or in the magnitude of one of the parameters of the system causes a sudden jump in signal amplitude somewhere in the system. This jump can be one of voltage, current, flux linkage or all three.

Figure 1.6 shows the jump phenomenon when the amplitude of the excitation is varied slowly. In this diagram the effect of the damping is considered. In this figure, starting from point 1, as V_s is increased, V_L slowly increases through point 2 to point 3. As V_s is increased further, a jump takes place from point 3 to point 4 with an accompanying increase in V_L , after which V_L increases slowly with V_s . If the process is reversed, V_L decreases slowly as V_s decreases from point 5 to point 6. As V_s is decreased further, a jump from point 6 to point 2 takes place, with an accompanying decrease in V_L , after which V_L decreases slowly with decreasing V_s . Rudenberg gives a very clear explanation of this jump phenomenon based on a graphical method. [3]

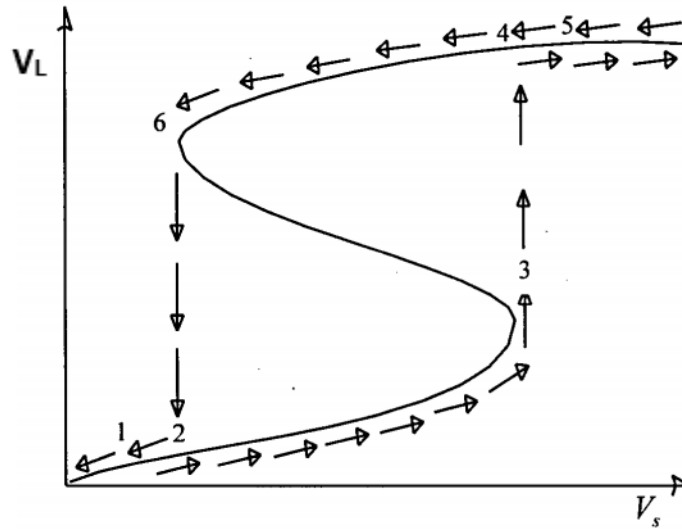


Figure 1.6: Jump phenomena for variation of the amplitude of the excitation

Consider the circuit of Figure 1.7, in which the linear inductance has been replaced with a nonlinear inductor

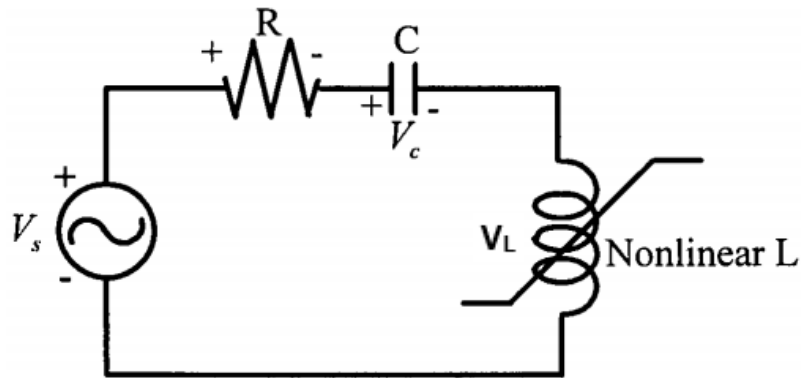


Figure 1.7: Ferroresonant Circuit

When the series resistance is ignored, the sum of the voltages around the only mesh of the circuit can be written as:

$$V_s(t) - V_c(t) - V_L(t) = 0 \quad (1.1)$$

The value of V_c can be replaced by its time-integral expression and V_L as the total derivative of $L(i)i(t)$. Then equation 1.1 can be written as:

$$V_s(t) - \frac{1}{C} \int i(t) dt - \frac{d}{dt} [L(i)i(t)] = 0 \quad (1.2)$$

Evaluating equation 1.2 and substituting $q(t) = \int i(t) dt$ will result in:

$$V_s(t) - \frac{1}{C}q(t) - L(i)\frac{d^2q(t)}{dt^2} - \frac{dq(t)}{dt}\frac{dL(i)}{di(t)} = 0 \quad (1.3)$$

From equation 1.3 it is evident that finding a closed-form solution for this nonlinear circuit will be quite difficult. This would be made more evident by adding a source impedance and by providing a complete equivalent of the transformer. Historically, methods of graphical solution represent one of the earliest attempts to explain ferroresonance. The graphical solution for the circuit of Figure 1.7, including the series resistance, can be obtained from two independent relationships for the voltage across the inductance and the capacitance. (Assuming sinusoidal variation of current). The voltage across the inductor is proportional to the frequency, and the voltage across the capacitance is proportional to the current and inversely proportional to the frequency and capacitance.

$$\begin{aligned} V_L &= \omega f(i) \\ V_C &= -\frac{I}{\omega C} \end{aligned} \quad (1.4)$$

The total magnitude of voltage for the circuit is:

$$V_s = \sqrt{(V_L + V_C)^2 + (RI)^2} \quad (1.5)$$

From equations 1.4 and 1.5, the voltage across the nonlinear inductor can be written as:

$$V_L = \sqrt{V_s^2 - (RI)^2} + \frac{I}{\omega C} \quad (1.6)$$

The first term in the right-hand side of Equation 1.6 $\sqrt{V_s^2 - (RI)^2}$ represents an ellipse whose main axes have the magnitude of V_s , and $\frac{V_s}{R}$ and the second term is a straight line having slope of $\frac{I}{\omega C}$. Adding these two quantities represents an oblique ellipse, whose intersection with the characteristic of V_L presents the three possible states of the oscillation of the circuit. Figure 1.8 shows the graphical solution for the ferroresonance circuit of Figure 1.7.

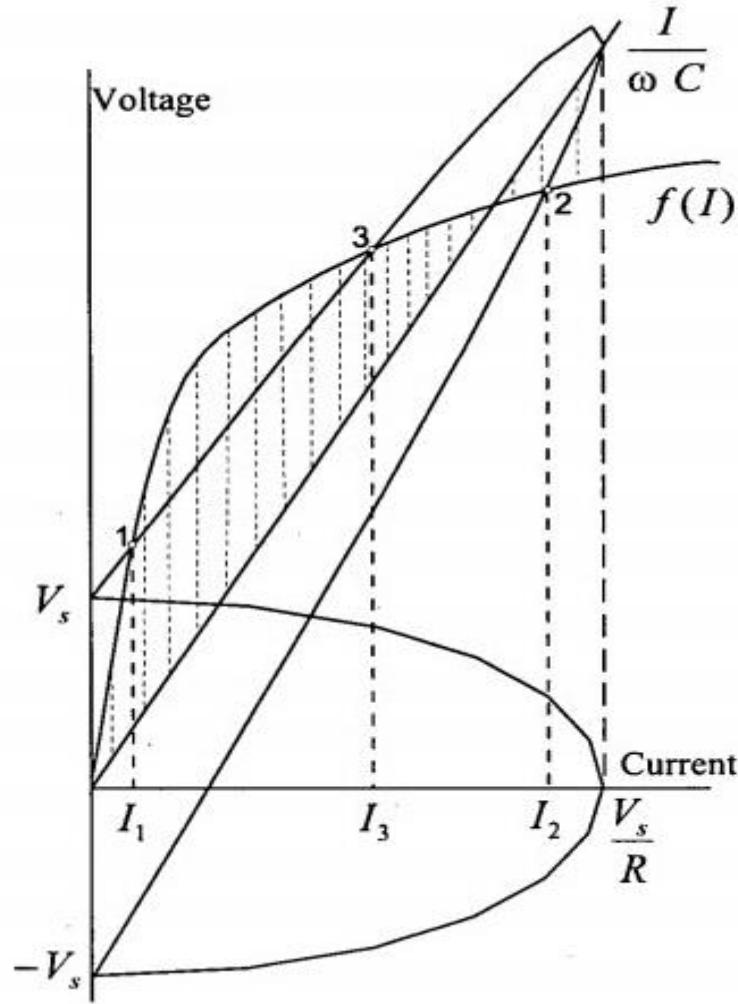


Figure 1.8: Graphical solution of the ferroresonance circuit

Points 1 and 2 in the Figure 1.8 represent the stable solutions, whereas point 3 represents an unstable solution. To show this, rewrite Equation 1.6 as:

$$(IR)^2 = V_s^2 - \left[f(I) - \frac{I}{\omega C} \right]^2 \quad (1.7)$$

If the quantity $\left[f(I) - \frac{I}{\omega C} \right]$ increases in magnitude with an increase in current, then according to equation 1.7, $(RI)^2$ tends to decrease, and this suppresses any further increase in current.

Thus stability is achieved. However, if the quantity $\left[f(I) - \frac{I}{\omega C} \right]$ decreases in magnitude, with an increase of current, the magnitude of $(RI)^2$ tends to increase and under this condition, the current continues to increase and the solution is unstable.

The dashed area in the Figure 1.8 shows the variation of the magnitude of $\left[f(I) - \frac{I}{\omega C}\right]$. And point 3 in corresponds to an unstable solution since $\left[f(I) - \frac{I}{\omega C}\right]$ decreases with an increase of current. In the same figure, points 1 and 2 represent the stable solutions. [3]

1.3. Conclusion

Therefore, we can conclude that the ferroresonance is a complex phenomenon in which there are several steady states for a given circuit, the appearance of these states is highly sensitive to system parameters values and the initial conditions. Small variations in a system parameters or a transient may cause a sudden jump between two very different steady states and initiate one of the ferroresonance modes. These modes will be discussed in next chapter with the causes of this phenomenon, and its effects on power system, then how to control it to prevent its happening.

Chapter 2

Understanding Ferroresonance

2.1. Introduction

In the previous chapter, the discriminative difference between the linear resonance and ferroresonance has been described. This chapter introduces types of ferroresonance modes, there are several modes of ferroresonance with varying physical and electrical displays, some have very high voltages and currents while others have voltages close to normal. In addition, it describes the effects of ferroresonance on power systems. Because they are considered to be catastrophic when they occur, finally the methods of mitigating them will be discussed.

2.2. Types of Ferroresonance Modes

All experience of waveforms appearing on power systems, experiments conducted on reduced system models together with numerical simulations, enable classification of ferroresonance states into four different types. This classification corresponds to the steady state condition, i.e. once the transient state is over, as it is difficult for a ferroresonant circuit to distinguish the normal transient state from ferroresonant transient states. However, this in no way implies that transient ferroresonance phenomena do not present a risk for electrical equipment. Dangerous transient overvoltages can occur during several system periods after an event (for example energizing of an unloaded transformer) and persist for several power system cycles. Basically, there are four types of steady-state responses, a ferroresonance circuit can possibly have, they are the fundamental mode, subharmonic mode, quasi-periodic mode and chaotic mode. [1] Each of the classifications and its characteristics are depicted in from Figure 2.1 to Figure 2.4.

The type of ferroresonance can be identified either by the spectrum of the current and voltage signals, or by a stroboscopic image obtained by measuring current I and voltage V at a given point of the system and by plotting in plane v, i the instantaneous values at instants separated by a system period. [1]

2.2.1. Fundamental mode

The periodic response has the same period, T as the power system. The frequency spectrum of the signals consists of fundamental frequency component as the dominant one followed by decreasing contents of 3rd, 5th, 7th and n^{th} odd harmonic. In addition, this type of response can also be identified by using the stroboscopic diagram of Figure 2.1 (c) which is also known as Poincarè plot, which can be obtained by simultaneously sampling of voltage, v and current, i at the fundamental frequency. [4] Figure 2.1 below shows the diagrams to explain fundamental mode.

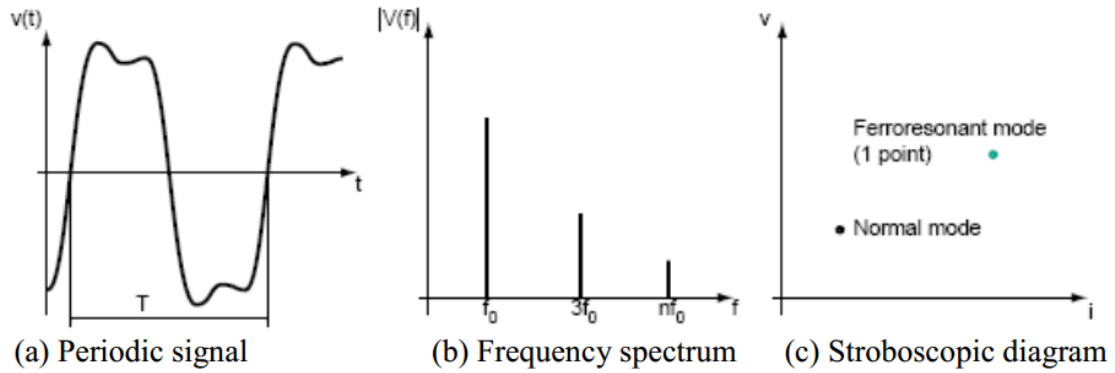


Figure 2.1: Fundamental mode of ferroresonance.

2.2.2. Subharmonic mode

In this type of ferroresonance signals has a period which is multiple of the source period, nT . The fundamental mode of ferroresonance is normally called a Period-1 (i.e. $f_0/1$ Hz) ferroresonance and a ferroresonance with a sub-multiple of the power system frequency is called a Period- n (i.e. f_0/n Hz) ferroresonance. Alternatively, the frequency contents are described having a spectrum of frequencies equal to f_0/n with f_0 denoting the fundamental frequency and n is an integer. With this signal, there are n points exist in the stroboscopic diagram which signifies predominant of fundamental frequency component with decreasing harmonic contents at other frequencies. [4] Figure 2.2 below shows the diagrams to explain Subharmonic mode.

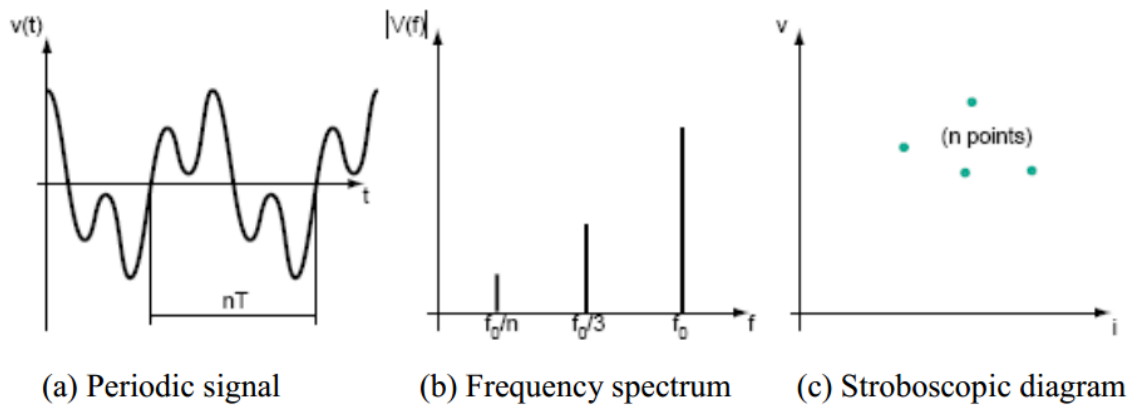


Figure 2.2: Subharmonic mode of ferroresonance.

2.2.3. Quasi-periodic mode

This kind of signal is not periodic. The frequency contents in the signal are discontinuous in the frequency spectrum, whose frequencies are defined as: $nf_1 + mf_2$ (where n and m are integers and f_1/f_2 an irrational real number). This type of response displays a feature employing a close cycle of dotted points on the stroboscopic plot.

The set of points (closed curve) in the diagram is called an attractor to which all close by orbits will asymptotically approach as $t \rightarrow \infty$, that is, in the steady state. [5] Figure 2.3 below shows the diagrams to explain Quasi-periodic mode.

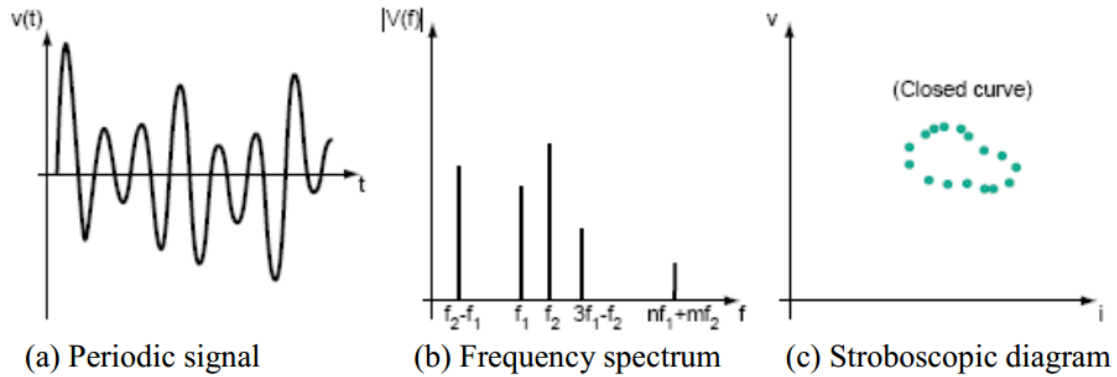


Figure 2.3: Quasi-periodic mode of ferroresonance.

2.2.4. Chaotic mode

This mode has a signal exhibiting non-periodic with a continuous frequency spectrum i.e. it is not cancelled for any frequency. The stroboscopic plot consists of n points surrounding an area known as the strange attractor which appears to skip around randomly. [4] Figure 2.4 below shows the diagrams to explain Chaotic mode.

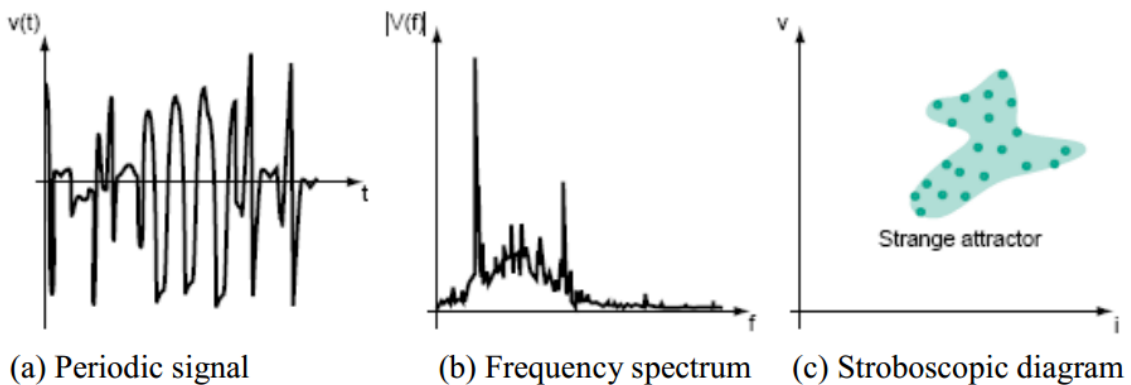


Figure 2.4: Chaotic mode of ferroresonance.

2.3. Causes and Effects of Ferroresonance on Power Systems

In the preceding section, the characteristics and features of each of the four distinctive ferroresonance modes have been highlighted. In this section we will focus firstly on causes of ferroresonance which are many but they can be generalized as below:

- Transients.
- Phase-to-ground , phase-to-phase faults.
- Circuit breaker opening and closing.
- Transformer energizing and de-energizing.

The main cause of ferroresonance cannot be known beforehand and it is generally found out by analyzing events in the power system prior to ferroresonant oscillations. [1] In addition, ferroresonance can cause undesirable effects on power system components which will be discussed.

2.3.1. Systems Vulnerable to Ferroresonance

In the modern power systems, there are many sources of capacitances, nonlinear inductances and wide range of operating setups. Configurations that may allow ferroresonance to happen are endless. But there are some typical configurations that may lead to ferroresonance. [1]

2.3.1.1. Voltage Transformer Energized Through Grading Capacitance

Switching operations may cause ferroresonance in voltage transformers which are connected between phases and ground. A sample case is illustrated in figure 2.5; Opening of circuit breaker D started ferroresonance by causing capacitance C (all the capacitances to ground) to discharge through voltage transformer. Through grading capacitance C_d , source delivers enough energy to maintain oscillation. [1]

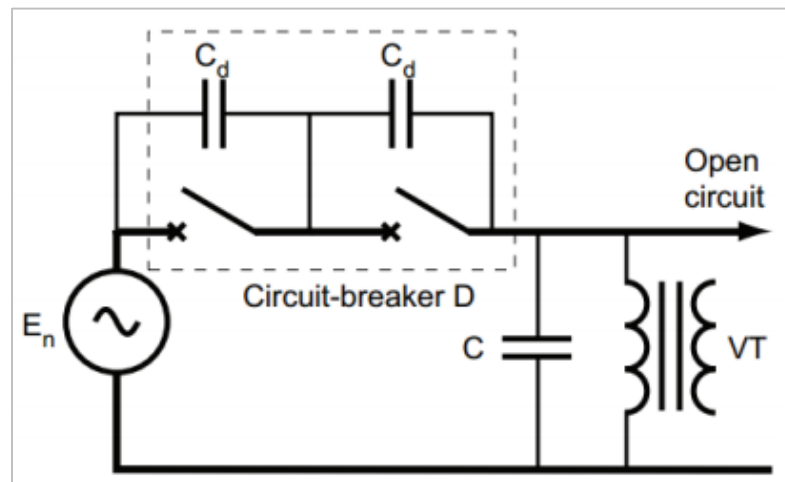


Figure 2.5: Ferroresonance of a voltage transformer connected in series with an open circuit breaker

2.3.1.2. Voltage Transformers Connected to an Isolated Neutral System

Transients due to switching operations or ground faults may start ferroresonance by saturating iron core of voltage transformers shown in figure 2.6. This grounding system can be chosen on purpose or the system can become neutral isolated from a loss of system grounding due to different reasons. A system operator may think there is a phase-to-ground fault in the system because of neutral point displacement and potential rise respect to ground on one or two phases. [1]

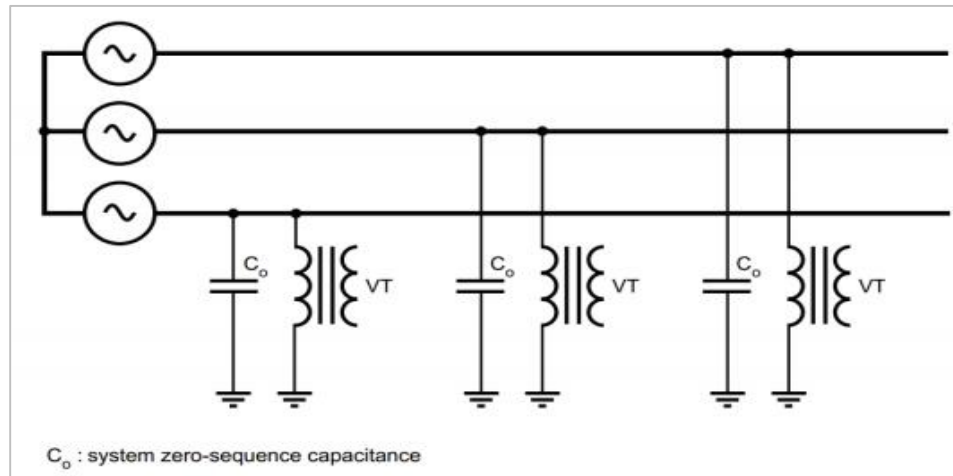


Figure 2.6: Ferroresonance of a VT between phase and ground in an isolated neutral system

2.3.1.3. Voltage Transformers and HV/MV Transformers with Isolated Neutral

There is possibility of ferroresonance when HV and MV neutrals are ungrounded. When a ground fault happens in HV side, high potential is obtained at HV neutral point. With the help of capacitive effect between primary and secondary, over-voltages appears on MV side. [1] Conditions for ferroresonance is formed with voltage source E_0 , capacitances C_e and C_0 and magnetizing inductance of a voltage transformer in figure 2.7 and figure 2.8.

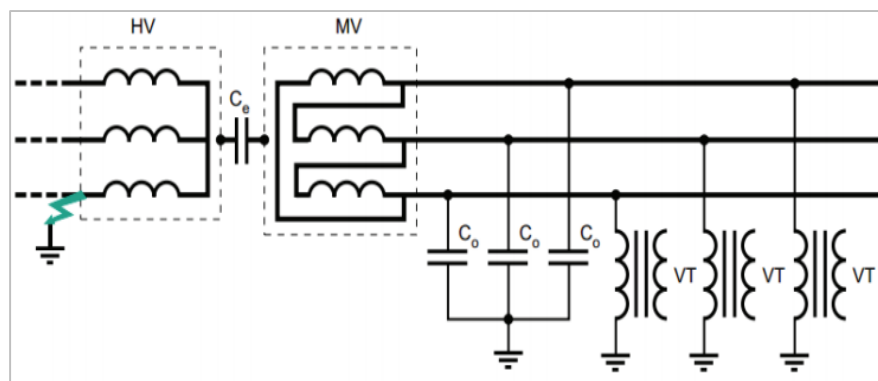


Figure 2.7: Faulty system

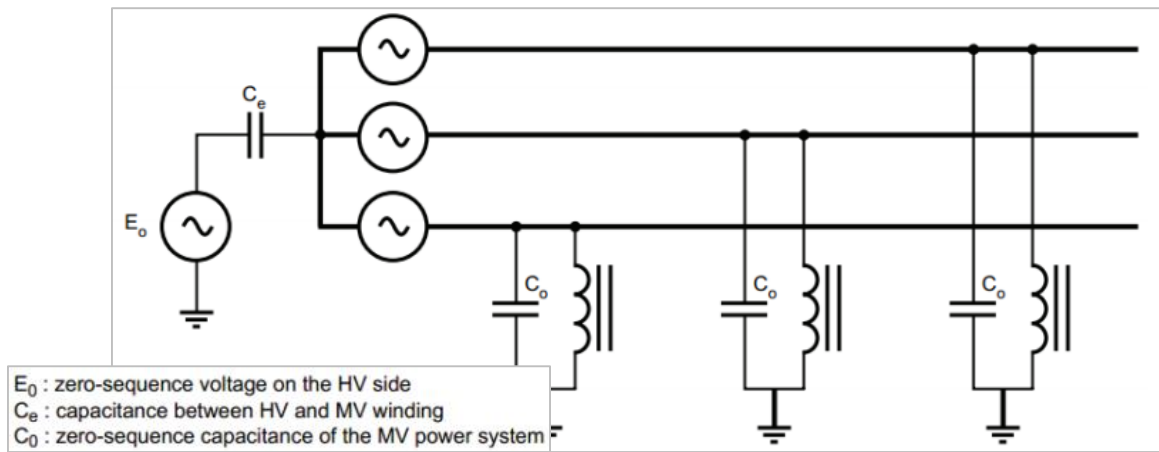


Figure 2.8: Ferro-resonance of voltage transformer between phase and ground with ungrounded/isolated neutral

2.3.1.4. Transformer Supplied by a Highly Capacitive Power System with Low Short-Circuit Power

As shown in figure 2.9 when an unloaded power transformer is connected to a relatively low short-circuit power source through underground cable or long overhead line, ferroresonance may happen. [1]

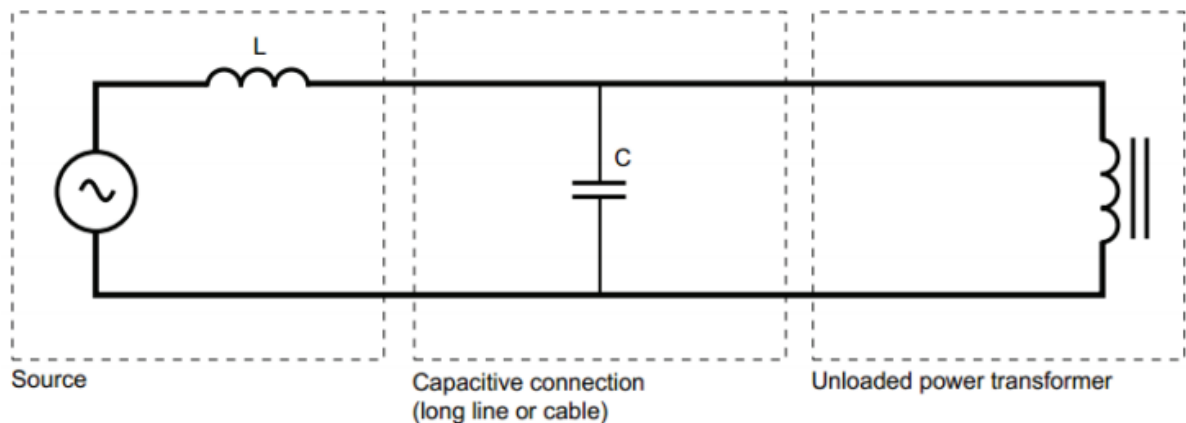


Figure 2.9: Power transformer supplied by capacitive system

With the experience from the past, it is concluded that system with features below are in danger of ferroresonance [1];

- Voltage transformer connected between phase and ground on an isolated neutral system
- Transformer fed through capacitive lines
- Non-multi pole breaking
- Unloaded or lightly loaded voltage transformers

2.3.1.5. Transformer Accidentally Energized in Only One or Two Phases

These setups can happen when one or two of the source phases are disconnected while the transformer is lightly loaded. System capacitances in figure 2.10 may consist of underground cables or overhead lines. Primary of the transformers can be delta connected or wye connected with isolated or grounded neutral. Because of switching operations, ferroresonant configurations are formed. Factors that are relevant is given below [1];

- Phase-to-phase and phase-to-ground capacitances
- Primary and secondary windings connections
- Voltage source grounding

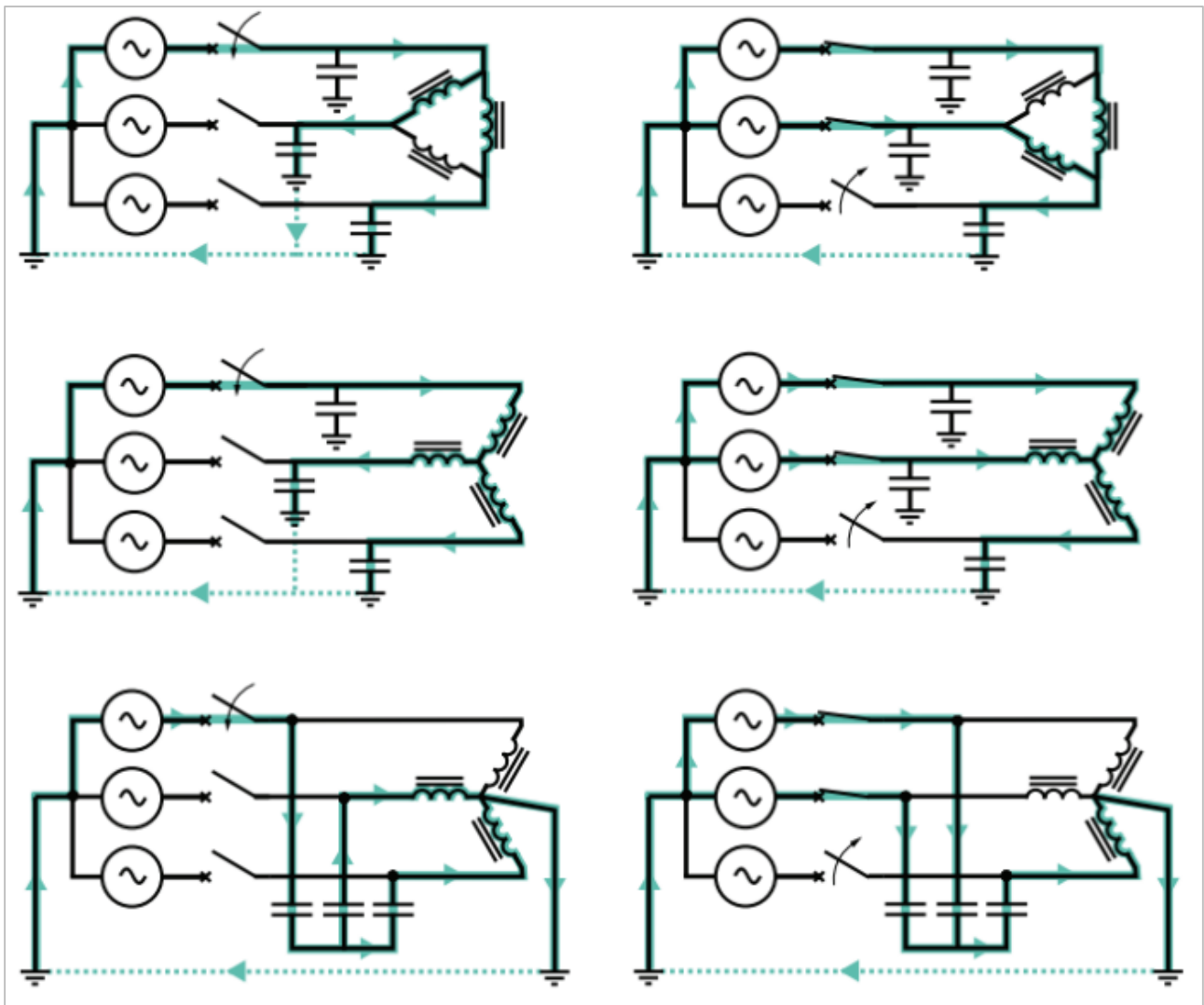


Figure 2.10: Examples of unbalanced systems

2.3.1.6. Powersystem grounded through a reactor

In LV systems, Permanent Insulation Monitors (PIMs) are used to measure insulation impedance by injecting direct current between system and ground. Their impedance is inductive and it may contribute to ferroresonance oscillations. Any potential rise in neutral point may cause ferroresonance between inductance of PIM and capacitances of the system. [1]

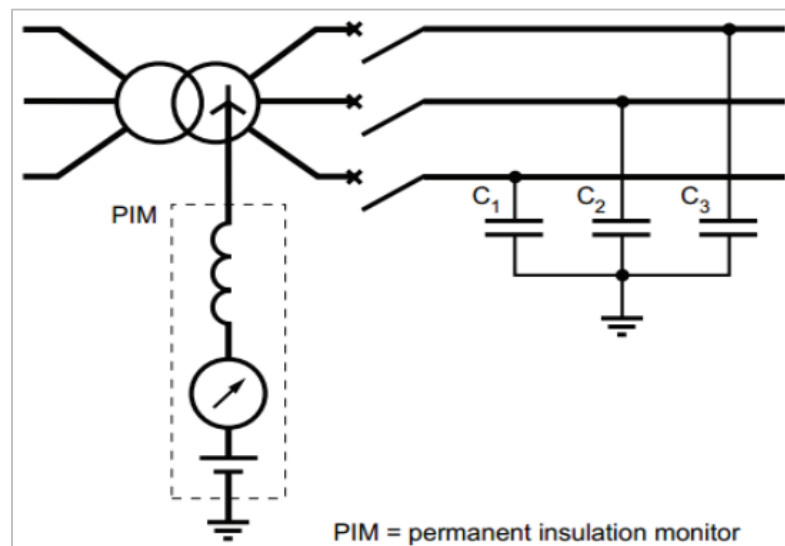


Figure 2.11: PIM inductance between neutral and ground

In MV systems, a coil of inductance L is used between MV neutral of a HV/MV transformer and ground to limit ground fault currents. Excitation of ferroresonance of the circuit consisting inductance L and zero-sequence capacitances may happen because of natural dissymmetry of transformer and capacitances shown in figure 2.12. [1]

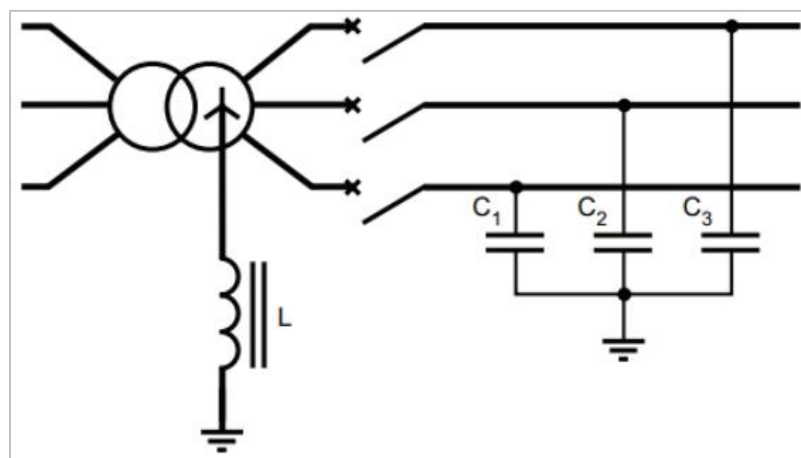


Figure 2.12: Resonant grounding system

2.3.2. Effects of Ferroresonance on Power Systems

As it may be seen hereinafter, due to the different factors involved in the ferroresonance phenomenon, when it occurs the situation can be rather disconcerting. That is why it is so important to identify the most common symptoms of a ferroresonance situation which are summarized as follows:

- High permanent over voltages of differential mode (phase-to-phase).
- High permanent over currents.
- High permanent distortions of voltage and current waveforms.
- Displacement of the neutral point voltage.
- Transformer heating.
- Loud noise in transformers and reactances.
- Damage of electrical equipments (capacitor banks, voltage transformers etc...).
- Untimely tripping of protection devices.

Some of the effects are not only special to ferroresonance; an initial analysis can be done by looking at voltage waveforms. If it is not possible to obtain recordings or if there are possible interpretations for effects, not only system configuration should be checked but also events prior to ferroresonance. Following step is to determine if three conditions are met in order ferroresonance to happen;

- Co-existence of capacitances and non-linear inductances
- Existence of a point whose potential is not fixed (isolated neutral, single phase switching)
- Lightly loaded system (unloaded power or voltage transformers)

If any of these conditions are not met, ferroresonance is said to be very unlikely [1].

In reference [6], ferroresonance occurred because of switching operations during commissioning new 400-kV substation where grading capacitance of a circuit breaker involved. It is reported that two voltage transformers are driven into sustained ferroresonance state. Ferroresonance experienced in Station Service Transformer during switching operations by firstly opening the circuit breaker and then the disconnecter switch located at the riser pole surge arrester [7]. Oscillations caused explosion of surge arrester.

In reference [8], explosion of a voltage transformer is reported. One of the buses was removed because of installing of new circuit breaker and current transformer, at the same time maintenance and line trip testing were conducted. Voltage transformers on the de-energized bus were energized by near on-operation bus bar through grading capacitors.

2.4. Controlling Ferroresonance

According to CIGRE technical brochure no. 569, mitigation techniques applicable to the power transformer are grouped into three basic approaches [18]:

- Avoid circuit parameters or operating conditions favouring ferroresonance
- Minimize the energy transfer that is required to sustain the ferroresonant oscillations
- Control the duration of ferroresonance by the operational switching

Based on these approaches, four kinds of the mitigation techniques are derived as follows:

- (a) An increase of the capacity of shunt capacitance at the transformer primary side.
- (b) An insertion of the capacitor bank at the transformer secondary side.
- (c) An installation of the resistive load bank at the transformer secondary side.
- (d) A change of the transformer saturation characteristics with the low flux density.

International standards state that resonance over voltages should be prevented or limited, those voltage values cannot be taken basis for insulation design. So in theory, current design of insulations and surge arresters do not provide protection against ferroresonance [9].

There are some researches on dynamical damping of ferroresonance, prototypes are introduced [10], [11] but the most common used practice is static damping with damping resistors.

In case of power transformers whose are fed through capacitive lines, the best solution proposed is avoiding risky situations when active power delivery is less than 10% of the transformer rated power [1]

For configurations in figure 2.10, following practical solutions are advised [1];

- Lowering capacitance between circuit breaker and transformer
- Avoiding use of transformers at 10% of its rated capacity
- Avoiding no-load energizing
- Prohibiting single-phase operations

For MV power systems grounded through a reactor figure 2.12, overcompensation of power frequency capacitance component of the ground fault current can be done or a resistive component to increase losses can also be added [1].

2.4.1. Damping Ferroresonance in Voltage Transformers

As mentioned before, voltage transformers connected between phase and ground in neutral isolated systems is dangerous for ferroresonance oscillations to happen. It is advised that avoid wye-connections of voltage transformer primaries with grounded neutral by leaving neutral of primaries ungrounded or using delta connection instead [12], [13]. If wye-connection for primaries is used, only way left to damp a possible oscillation is to introduce load resistances.

2.4.1.1. Voltage Transformers with one Secondary Winding

Even though resistors will consume power during operation, damping resistors are used to damp possible ferroresonant oscillations in figure 2.13. Recommended minimum values of resistance R and power rating of resistor P_R are calculated with rated values of transformer in (2.1) and (2.2) [13], [1].

$$R = \frac{U_s^2}{k \cdot P_t - P_m} \quad \text{..... (2.1)}$$

$$P_R = \frac{U_s^2}{R} \quad \text{..... (2.2)}$$

where; U_s : rated secondary voltage (V)

k : factor between 0.25 and 1 regarding errors and service conditions

P_t : voltage transformer's rated output (VA)

P_m : power required for measurement (VA)

2.4.1.2. Voltage Transformers with two Secondary Windings

There is also an option to have two secondaries in voltage transformers. One is for measurement and second one is especially for damping (tertiary winding). The advantage to have damping resistors in the open delta connected secondary winding is that it is only active during unbalanced operation. During the balanced operation no current circulates in open delta. Recommended minimum values of resistance R and power rating of resistor P_R are calculated with rated values of transformer in (2.3) and (2.4) [13], [1].

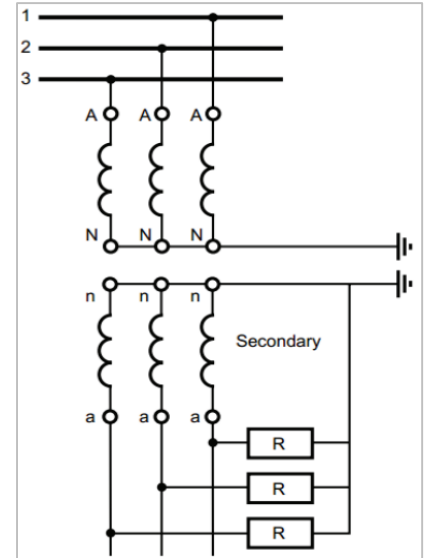


Figure 2.13: Damping for voltage transformer with one secondary.

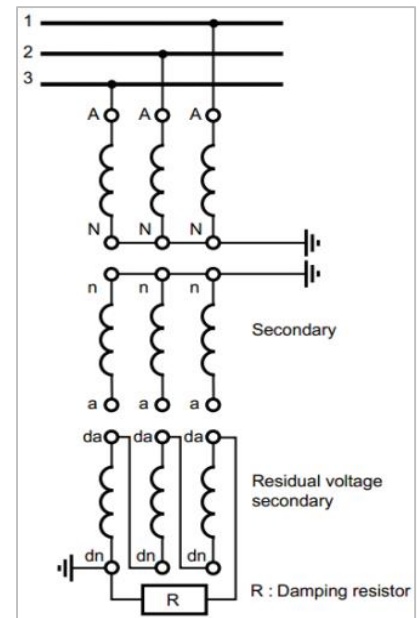


Figure 2.14: Damping for voltage transformer with two secondaries.

$$R = \frac{3\sqrt{3} U_s^2}{P_e} \dots\dots\dots (2.3)$$

$$P_R = \frac{(3U_s)^2}{R} \dots\dots\dots (2.4)$$

where; **Us**: rated voltage of the tertiary winding (V)

Pe: rated thermal burden of tertiary winding (VA) is the apparent power than voltage transformer can supply without exceeding thermal constraints.

2.4.2. Limiting the cable length switched

Limiting the cable length to be less than the length established by the Baitch Ferroresonance Critical Cable Length will limit the overvoltage that may occur to $(1 + \sqrt{3})$ times phase-to-earth voltage. The effect of iron losses will tend to result in the overvoltage being less than $(1 + \sqrt{3})$ times phase-to-earth voltage.

There are some issues on ferroresonance as follows:

- Isolating a power transformer from the grid during ferroresonance oscillations using a disconnector between the transformer and the circuit breaker
- Effectiveness of surge arresters for the actual ferroresonance.
- Varying residual flux of the iron core in a power transformer

2.5 conclusion

At the end of this chapter, the appearance of various types of ferroresonance oscillations in a power system was presented. Then we have discussed some typical configurations that may lead to destructive effects that make us care about it and looking hardly for controlling it. In the next chapter we will analyze and make simulation to the first vulnerable configuration to this phenomenon in section 2.3.1.1 using ATP program trying to damp it.

Chapter 3

Simulation results

3.1. Introduction

In practice the ferroresonant oscillations may be initiated by momentary saturation the core of the inductive element resulting from e.g. switching operation or other type of event resulting in a transient overvoltage in the system. The undamped ferroresonant oscillations in power system are dangerous to the equipment installed due to large overcurrents and/or overvoltages which may ultimately lead to permanent equipment damage. [14]

In this chapter numerical simulations of the ferroresonance phenomenon in the MV inductive voltage transformer are presented. The ferroresonant oscillations analyzed result from interaction between the voltage transformer and a grading capacitance of a circuit breaker. [14] our simulation will be analyzed on electrical power network of Haoud Berkaoui using Alternative Transient Program.

3.2. The electrical power network of Haoud Berkaoui

The region of Haoud Berkaoui represents one of ten principles hydrocarbons productive zones of Algerian desert. It is situated at 35 Km to south west of Wilaya of Ouregla. Figure 3.1 shows the geographic location of Haoud Berkaoui. [15]

The electrical power network implemented by Schneider Electric as part of the electrification project of Haoud Berkaoui is composed of three high-voltage substations. Which are located in Guellala, Haoud Berkaoui and Benkahla; they are powered by 60kV from the Algerian national electricity company Sonelgaz. Each substation is composed of control buildings, premises and equipment home building separate GIS and thus protecting the metal-clad high-voltage SF6. The transformers are located outside the boxes in walls separated by firewalls.[15]

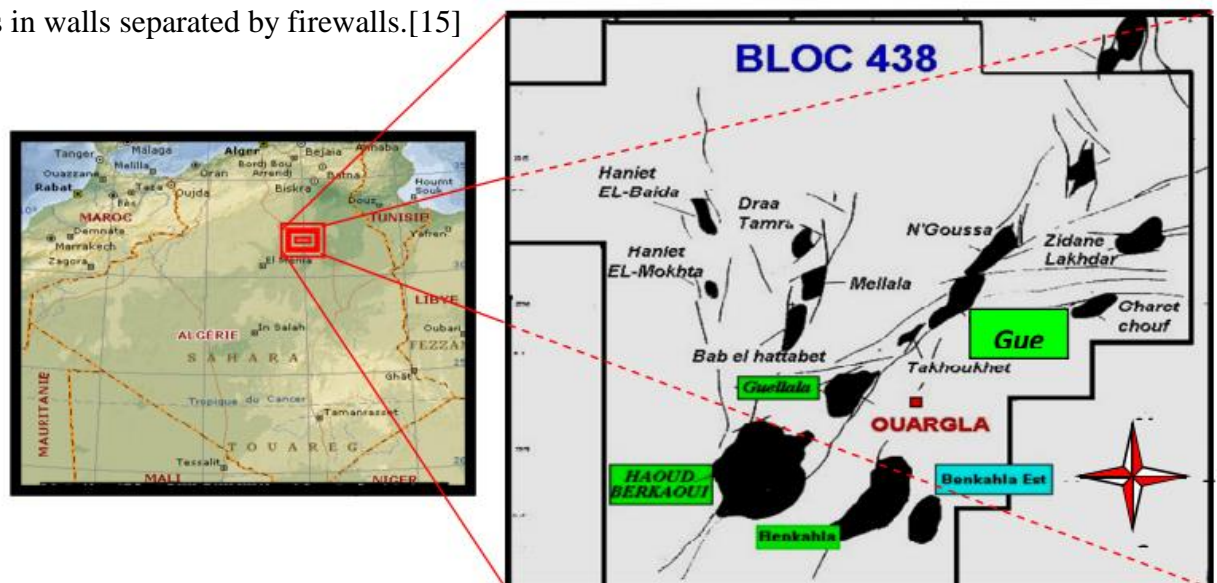


Figure 3.1: the geographic location of Haoud Berkaoui.

3.3. Highlights about Alternative Transient Program

Transient analysis of electrical circuits is as important as steady-state analysis. When transients occur, the currents and voltages in some parts of the circuit may many times exceed those that exist in normal behavior and may destroy the circuit equipment in its proper operation. A number of simulation tools have been developed in the last few years, especially for steady state simulations. Few programs are able to accurately determine the response of a system to a transient; one of these programs is ATP. [16]

3.3.1. What is ATP ?

ATP is a universal program system for digital simulation of transient phenomena of electromagnetic as well as electromechanical nature. With this digital program, complex networks and control systems of arbitrary structure can be simulated. ATP has extensive modelling capabilities and additional important features besides the computation of transients. It has been continuously developed through international contributions. ATP was formed after a disagreement over commercialization in 1984 and has been continuously developed by both Drs. W.Scott Meyer and Tsu-huei Liu. [17]

ATP program calculates variables of interest within electric power systems as functions of 3 to solve the differential equations of system components in the time domain. Non-zero initial conditions can be determined either automatically by a steady state, phasor solution or they can be entered by the user for some components.

ATP has many models including rotating machines, transformers, surge arresters, transmission lines and cables. With this digital program, complex networks of arbitrary structure can be simulated. Analysis of control systems, power electronics equipment and components with nonlinear characteristics such as arcs and corona are also possible. Symmetric or asymmetric disturbances are allowed, such as faults, lightning surges, or any kind of switching operations including commutation of valves. Calculation of the frequency response of phasor networks is also supported. [17]

3.3.2. ATPDraw

ATPDraw is a graphical, mouse- driven preprocessor to ATP. It helps creating and editing the model of the electrical circuit the user wants to simulate interactively. In the program the user can construct an electric circuit, by selecting predefined components from an extensive library. The preprocessor then creates the corresponding ATP input file, automatically in correct format.

ATPDraw has a standard Windows user interface. Figure 3.2 shows the main window of ATPDraw containing two open circuit windows. ATPDraw supports multiple documents and offers the user to work on several circuits simultaneously along with the facility to copy information between the circuits. The size of the circuit window is much larger than the actual screen, as is indicated by the scroll bars of each circuit window. [17]

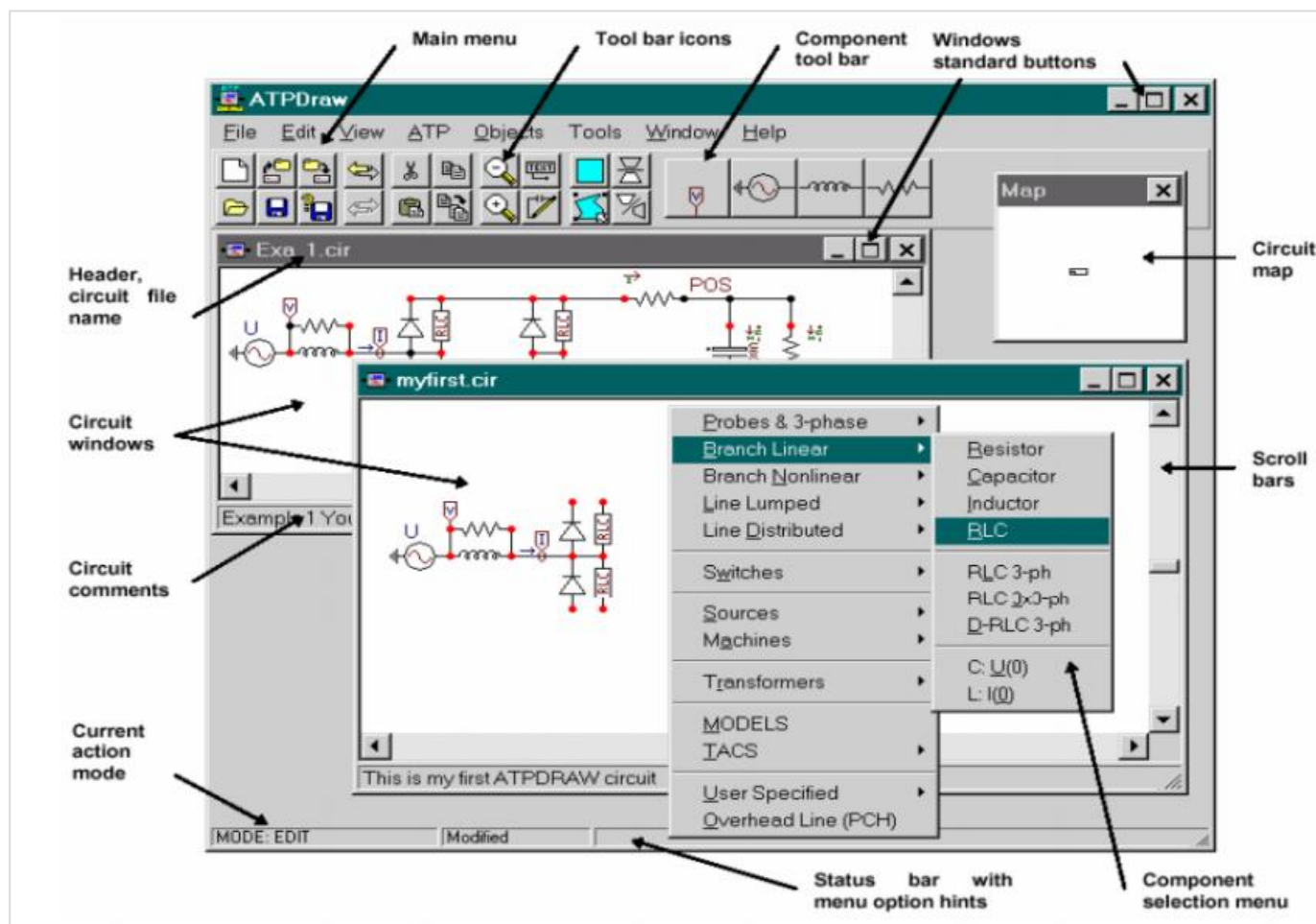


Figure 3.2: Main Window Multiple Circuit windows and the floating Selection menu.

3.4. The real electrical circuit of Haoud Berkaoui

3.4.1. Description of the circuit

Figure 3.3 shows the single line diagram of Haoud Berkaoui. It is formed by a generator as source followed by transmission line connected to two big transformers in parallel, there are two transformers 30/5.5 KV with rated power 6300 KVA each, both connected to 5.5KV bus bare. This bus bare feeds:

- Two motors of the compressors of rated power 2060 KW for each one.
- Two transformers 5.5/0.4 KV of rated power 500 KVA used for lightning, motors, air conditioning, 220 volts sources.

- One motor feeds pump Security 315KW.
- Water injection unit which feeds three electro-pumps of rated power 560 KW. [15]

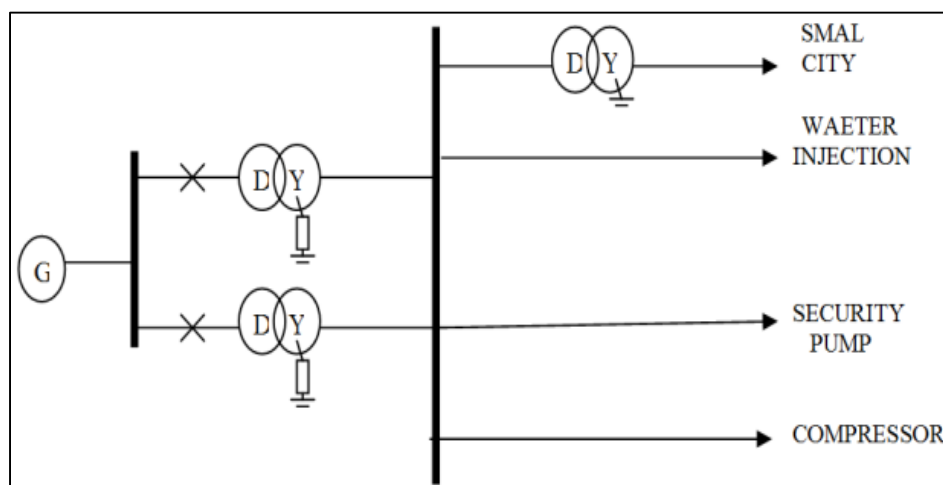


Figure 3.3: The one line diagram representation.

3.4.2. The characteristics of the equipment used in the Substation:

All important parameters which have been taken even from the station or from the Web site of the companies that have made those instruments are listed below:

❖ Two transformer TR1 and TR2 (MV):

- Rated power: 6300 KVA
- Primary voltage: 30000 V
- Secondary voltage: 5750 V
- Primary current: 121,24 A
- Secondary current: 632,57 A

❖ A Transformers TR3 (LV):

- Rated power: 250 KVA
- Primary voltage: 5500 V
- Secondary voltage: 400 V
- Primary current: 24 A
- Secondary current: 358.9 A

❖ Three motors feed three pumps for water injunction:

- Number of phases: Three
- Rated power: 560 KW
- Voltage: 5500 V
- Current: 69,5 A
- Frequency: 50 Hz
- Cos Φ : 0,88
- Rotation speed: 1494 rev/min
- Weight: 4600 Kg
- Type of connection: Star

❖ Two motors feed two compressors:

- Number of phases: Three
- Rated power: 2060 KW
- Voltage: 5500 V
- Current: 242,7 A
- Frequency: 50 Hz
- Cos Φ : 0,93
- Rotation Speed: 2986 rev/min
- Weight: 8400 Kg
- Type of connection: Star

❖ **One motor feeds a security pump:**

- | | | |
|-----------------------------------|-----------------------|----------------------------|
| - Number of phases: Three | - Rated power: 315 KW | - Voltage: 5500 V |
| - Current: 40,6 A | - Frequency: 50 Hz | - Cos Φ : 0,86 |
| - Speed of rotation: 1488 rev/min | - Weight: 2420 Kg | - Type of connection: Star |

❖ **The consumption parameters of the city (RLC):**

- | | |
|------------------------------|---------------------------------|
| - The real power: 103.09 KW | - The reactive power: 49.93 VAR |
| - The rated power: 114.55 VA | - Power factor: 90.0% |
| | - The efficiency: 97.0% |

3.4.3. ATP simulation results

In our simulation, ATPDraw software has been used to draw the circuit which is shown in figure 3.4. Synchronous machine has been represented as source of 30KV, the two transformers are 30/5.5KV, the small transformers are 5.5/0.4KV, the induction motor of 0.4KV and the loads are the RL equivalent circuit of the used light, pumps water injection...etc. The detailed elements of the ATPDraw circuit are given in the appendix.

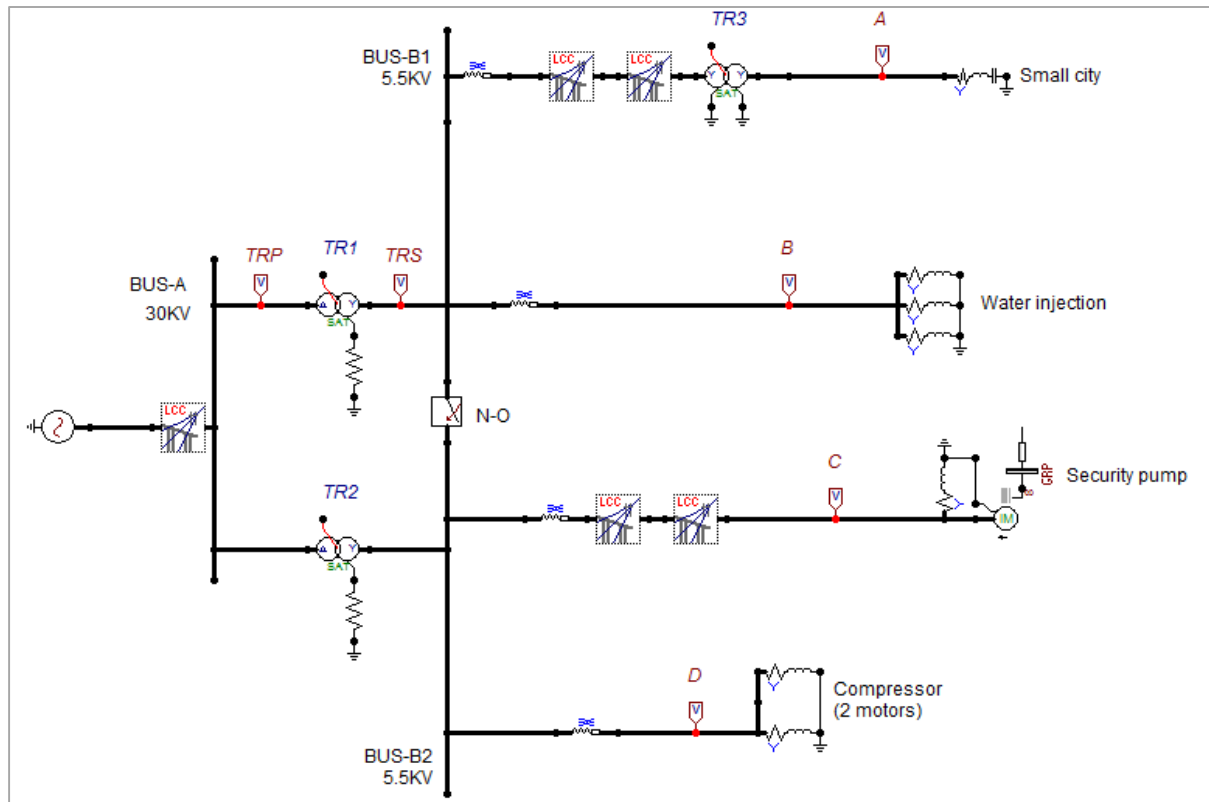


Figure 3.4: ATPDraw representation of the circuit of Haoud Berkaoui station.

Figures 3.5 and 3.6 below show the steady state of the network, after checking the voltage waveform at points TRS, A, B, C and D for the loads.

➤ **The simulation result at point A:**

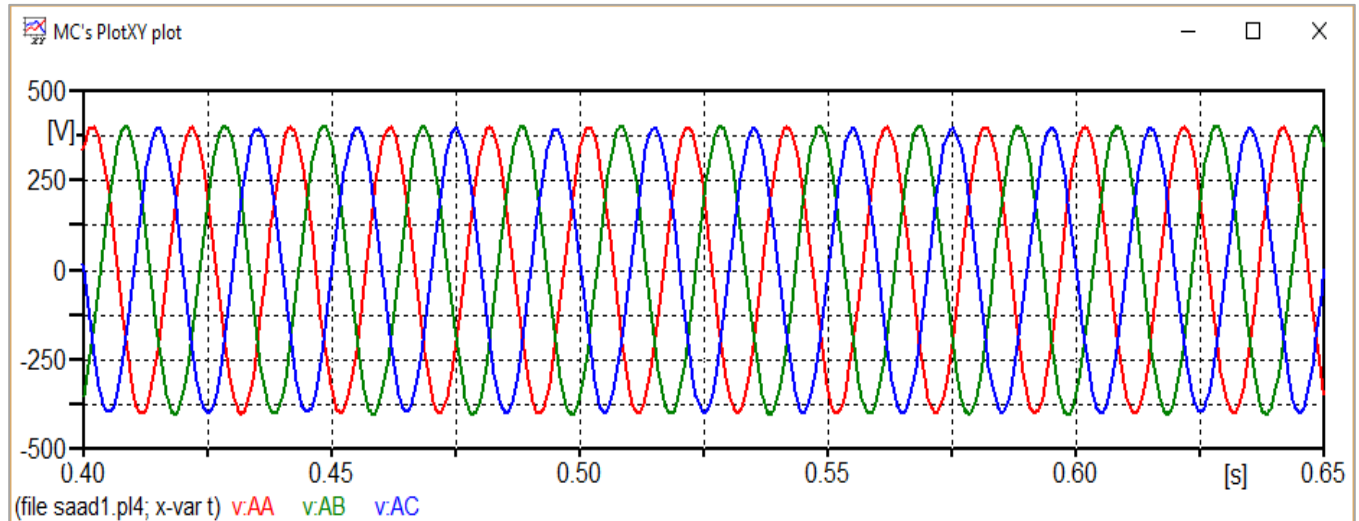


Figure 3.5: The values of voltages at the point A.

Where the peak values of the three phases (A, B and C) at point A are: $V_A = 380 \text{ V}$

➤ **The simulation result at points TRS, B, C and D:**

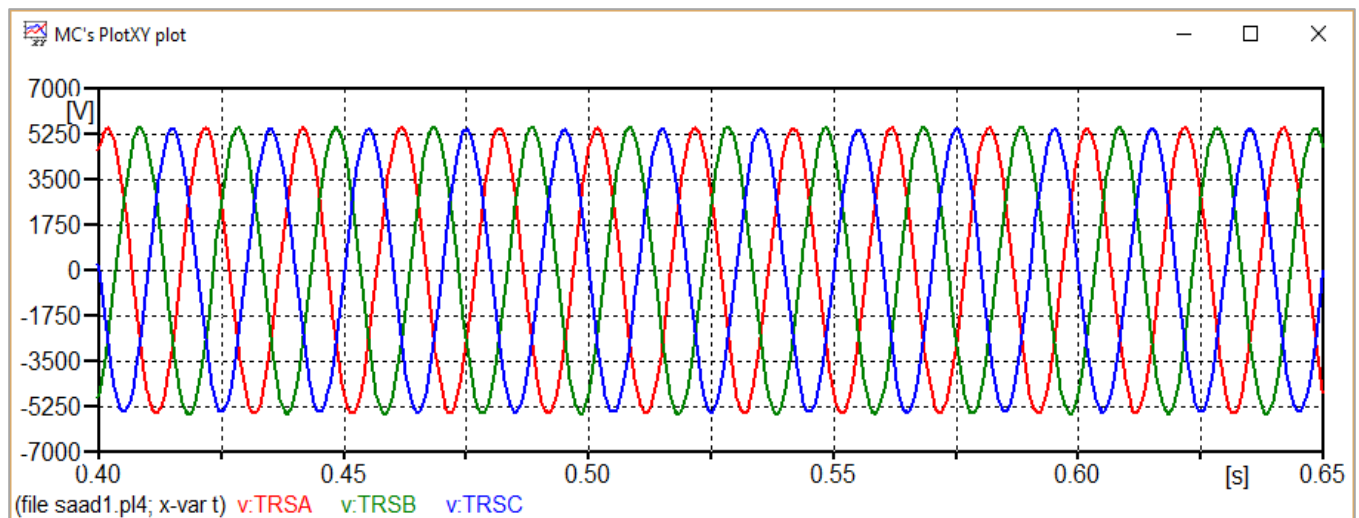


Figure 3.6: The values of voltages at the point TRS, B, C and D.

Where the peak values of the three phases (A, B and C) are: $V_{TRS} = V_B = V_C = V_D = 5.5 \text{ kV}$

3.5. The Case study

Switching operations may cause ferroresonance in voltage transformers which are connected between phases and ground. A sample case of voltage transformer energized and de-energized through Grading capacitance of circuit breaker is illustrated in Figure 3.7.

Opening of circuit breaker D starts ferroresonance by causing capacitance C (all the capacitances to ground) to discharge through voltage transformer. Through grading capacitance C_d , source delivers enough energy to maintain oscillation.

Following is the circuit equipment condition:

- i. Before switching (Transformer energized)
 - Circuit breaker was close.
- ii. After switching (Transformer de-energized)
 - Circuit breaker was open.

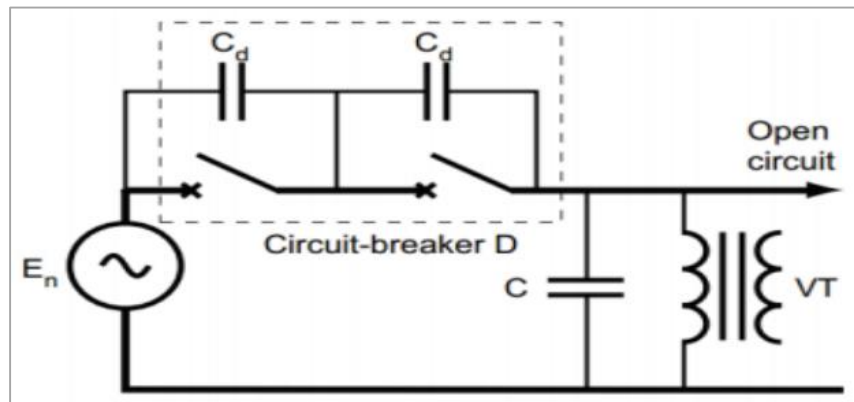


Figure 3.7: Voltage transformer connected in series with an open circuit breaker.

3.5.1 - The effect of changing grading capacitor (C_g):

In order to see the effect of the circuit breaker grading capacitance values on the occurrence of ferroresonance we have connected a circuit breaker consisting of its grading capacitance (C_g) at the primary side of the big transformers as shown in the gray area in Figure 3.8.

The commissioning of the system of Figure 3.8 was conducted as follows: the energization of the VT's from the 30 kV busbar when the circuit breaker (CB) were close and then de-energized the VT's by opening the circuit breaker (CB). The effect after the switching events has thus reconfigured the circuit into ferroresonance condition involving the interaction between the circuit breaker's grading capacitor and the transformers.

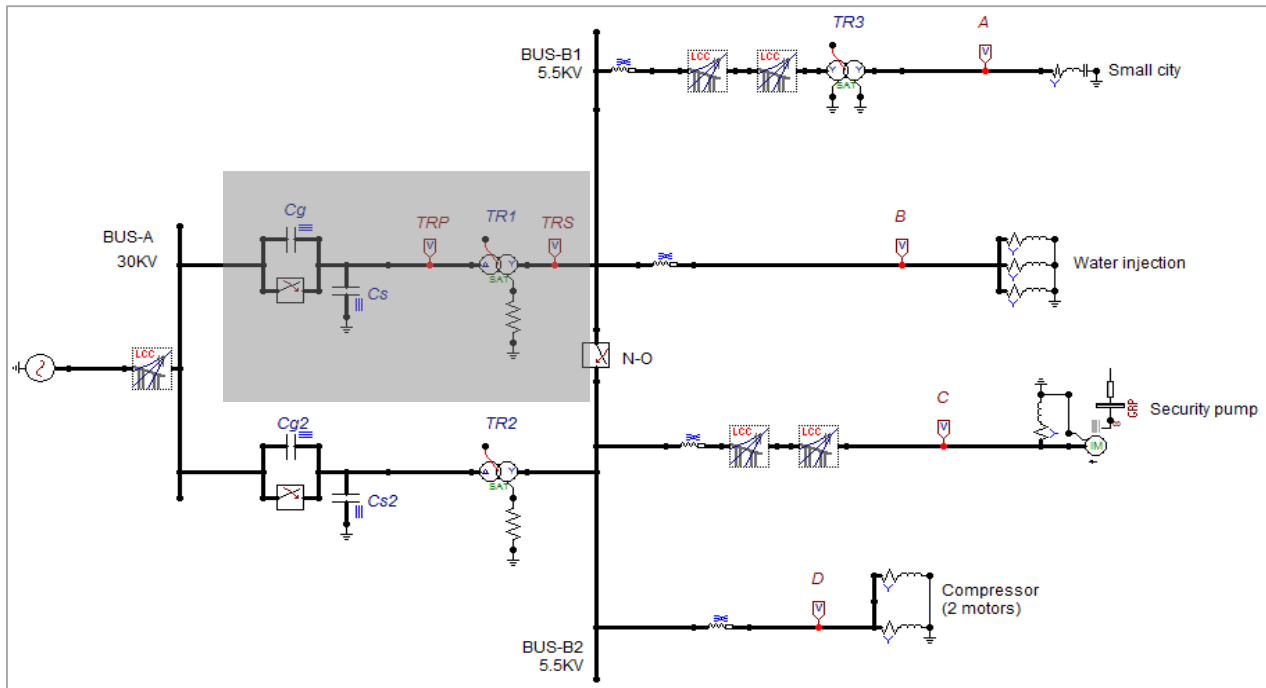


Figure 3.8: The ATP model circuit used for simulation

- Simulation results:

In order to look into the effect of grading capacitance on ferroresonance, let us look at a wider view by having the grading capacitance (C_g) varied. We assume also the variation of the coming voltage from the generation station, the network voltage values for which the ferroresonance risk will be verified are: 80%, 100% and 120% of the rated voltage V_s (30Kv). The ferroresonant response was verified for opening the switch parallel to the C_g at the $t = 0.5$ s.

The voltage waveforms across the transformer TR1 (MV power transformer) with network voltage 100% $V_s = 30$ Kv are recorded as shown below:

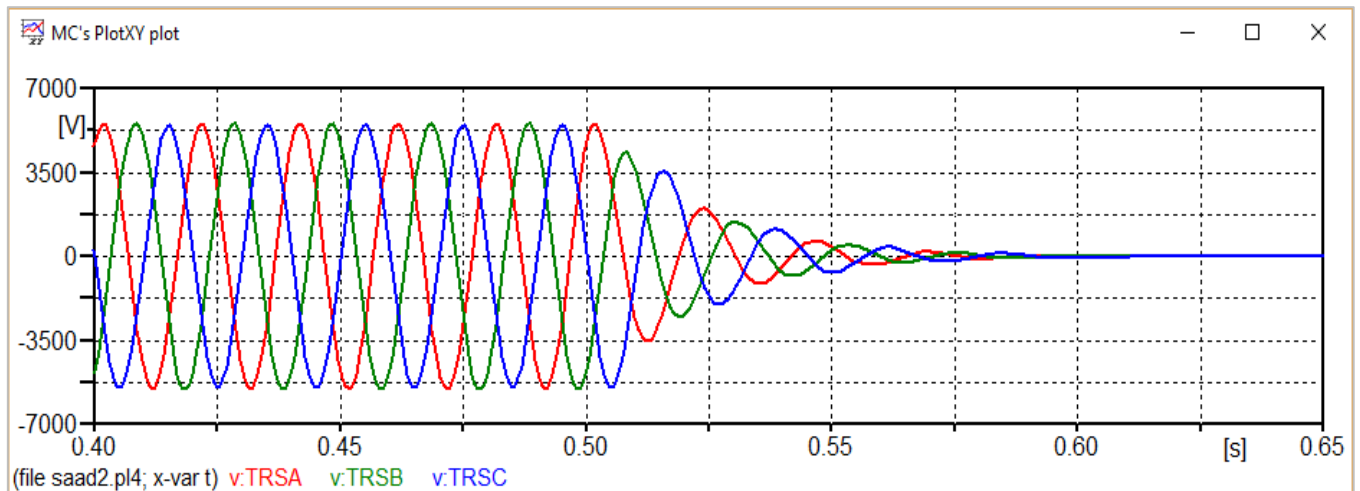


Figure 3.9: The voltages at point TRS with $C_g = 1\text{nF}$ and 100% V_s

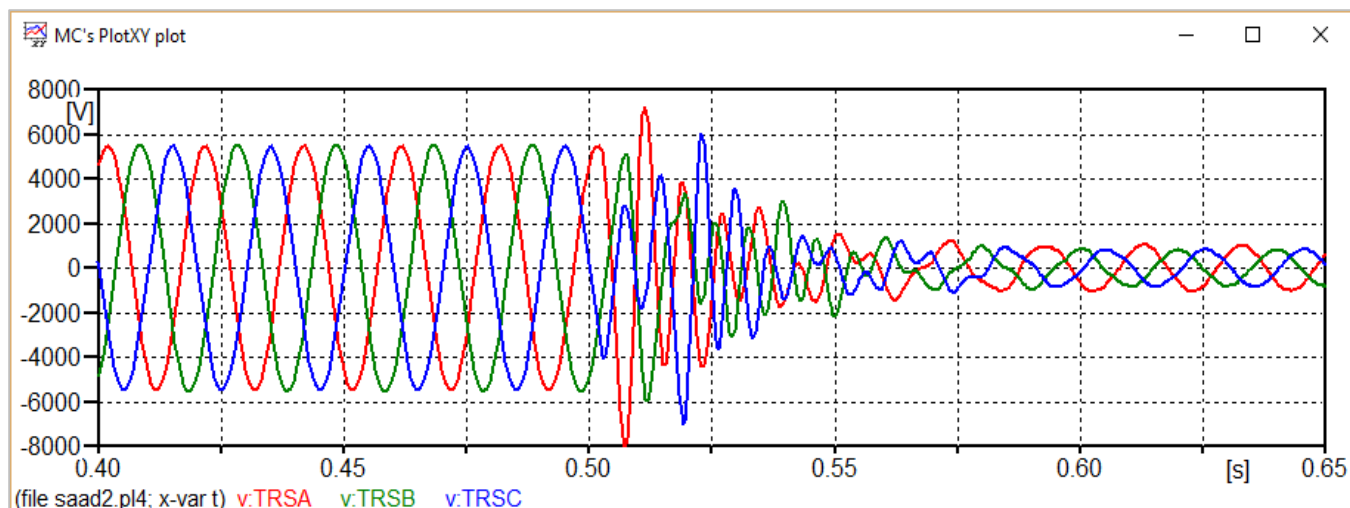


Figure 3.10: The voltages at point TRS with $C_g = 600\text{nF}$ and 100% V_s

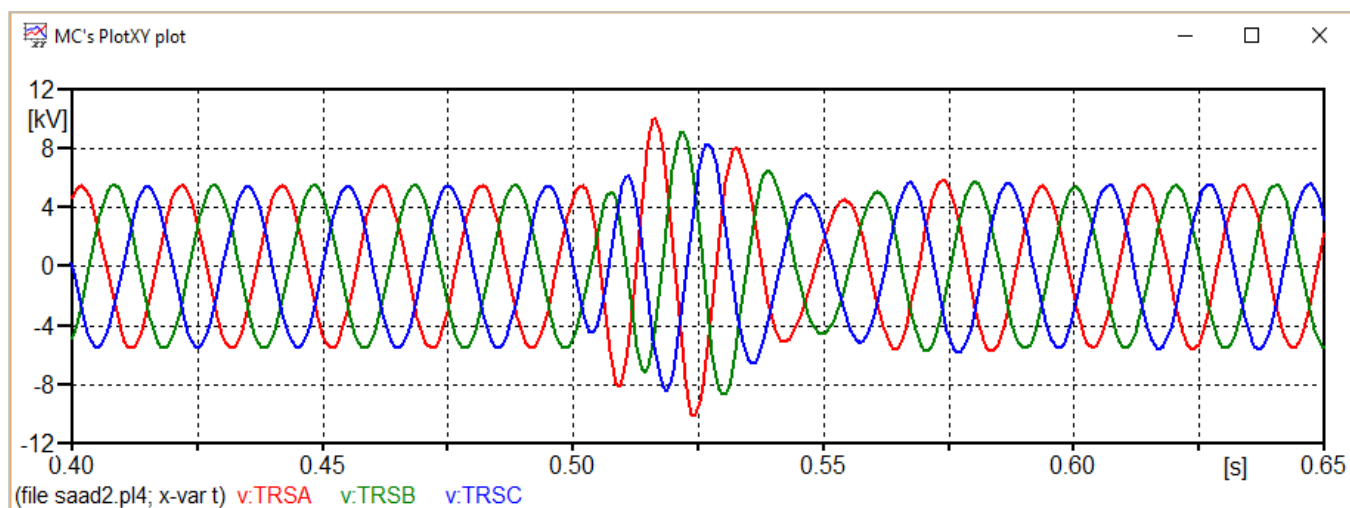


Figure 3.11: The voltages at point TRS with $C_g = 2\mu\text{F}$ and 100% V_s

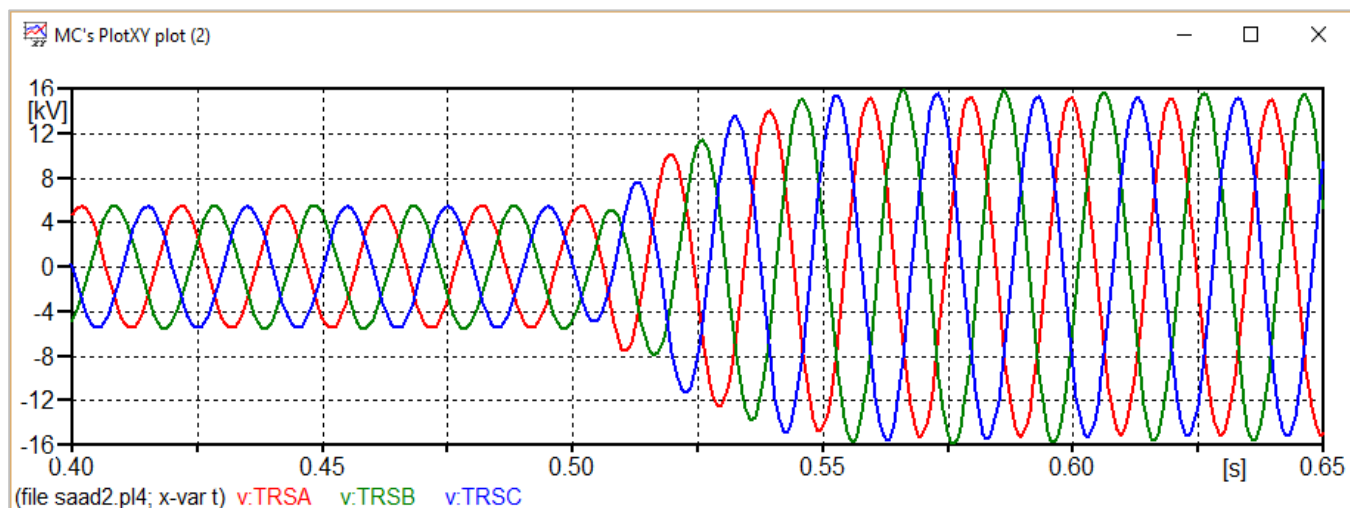


Figure 3.12: The voltages at point TRS with $C_g = 5\mu\text{F}$ and 100% V_s

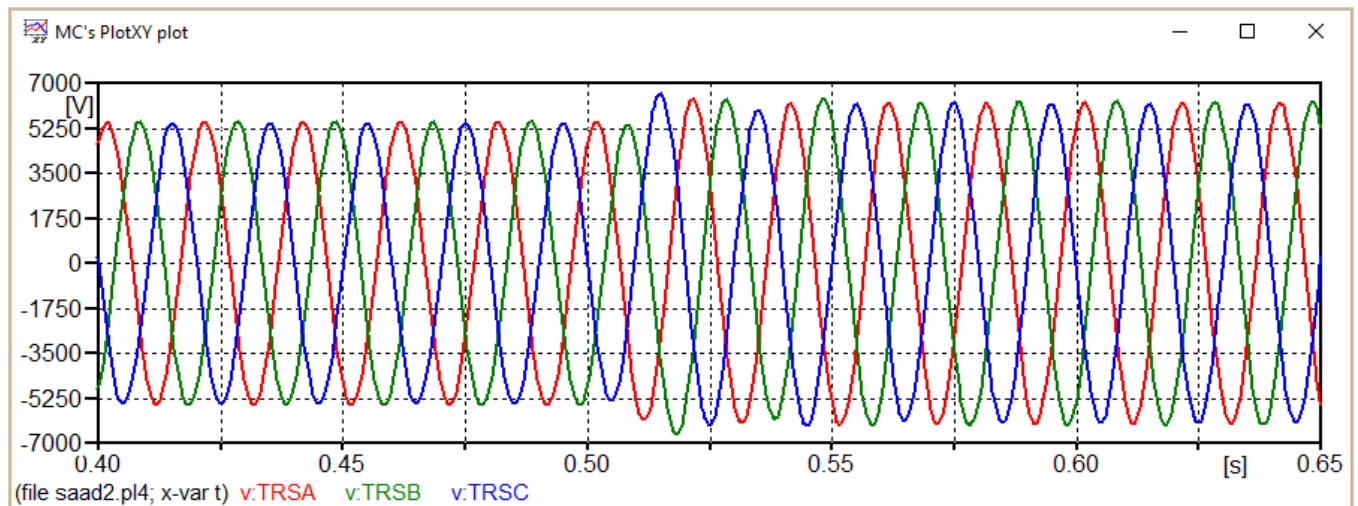


Figure 3.13: The voltages at point TRS with $C_g = 30\mu\text{F}$ and 100% V_s .

Comments: In all the above waveforms. It could be seen that for V_s values of 100%, the ferroresonance may exist for $C_g = 0.6\mu\text{F}$ and above until the value $C_g = 30\mu\text{F}$, it will appear overvoltage start to be less and extremely equal to the secondary voltage of TR1.

Now we vary the network voltage down to 80% $V_s = 24\text{ Kv}$, then we record the voltage waveforms across the transformer TR1 as shown below:

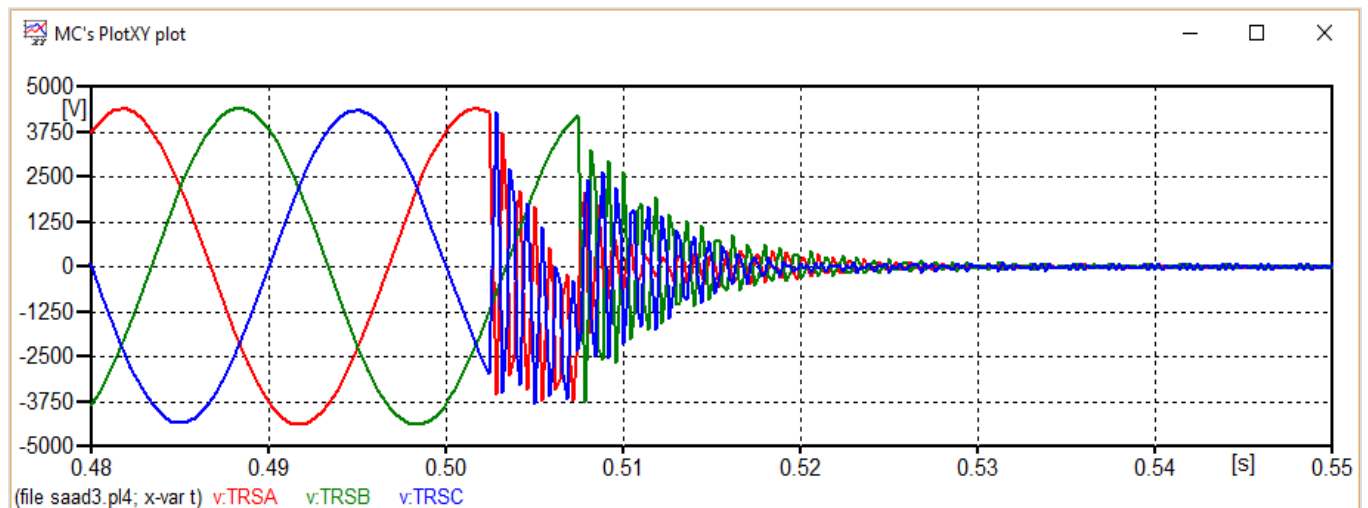


Figure 3.14: The voltages at point TRS with $C_g = 1\text{ nF}$ and 80% V_s .

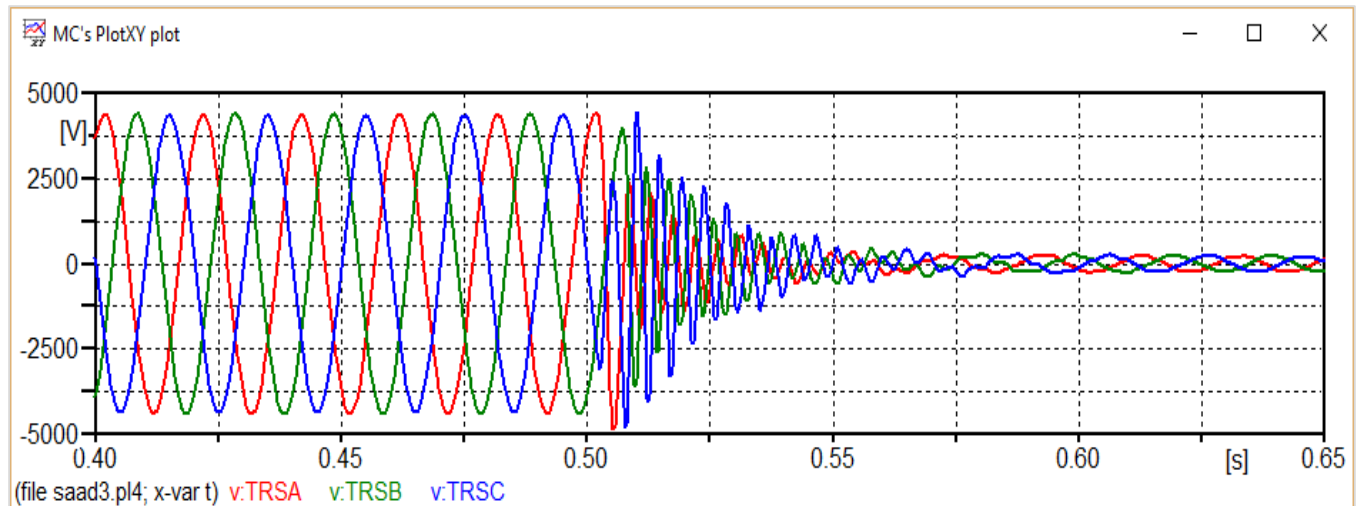


Figure 3.15: The voltages at point TRS with $C_g = 600\text{nF}$ and 80% V_s .

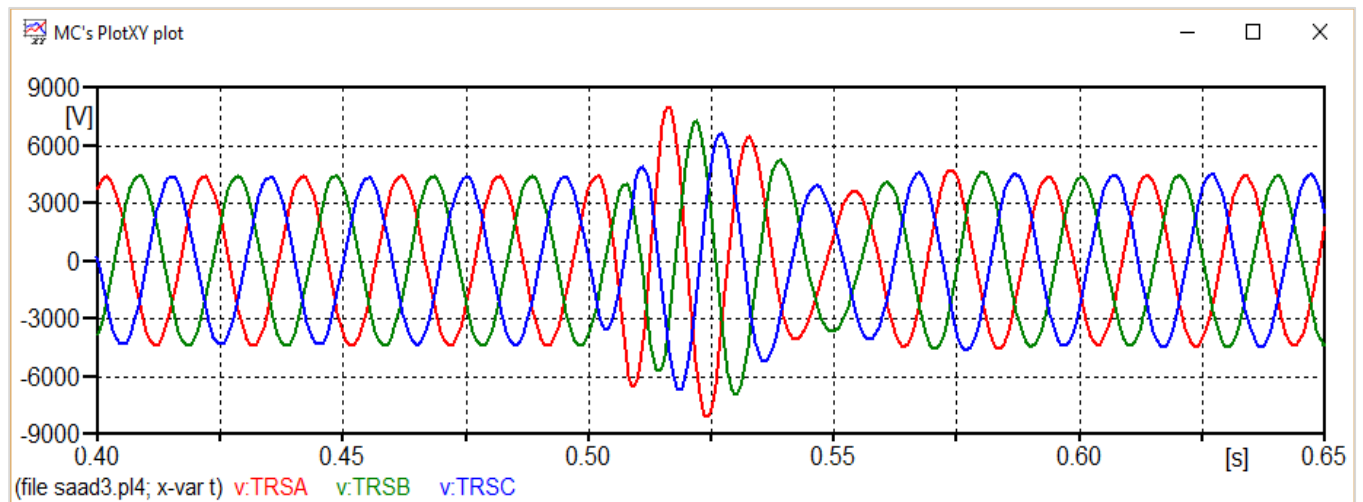


Figure 3.16: The voltages at point TRS with $C_g = 2\mu\text{F}$ and 80% V_s .

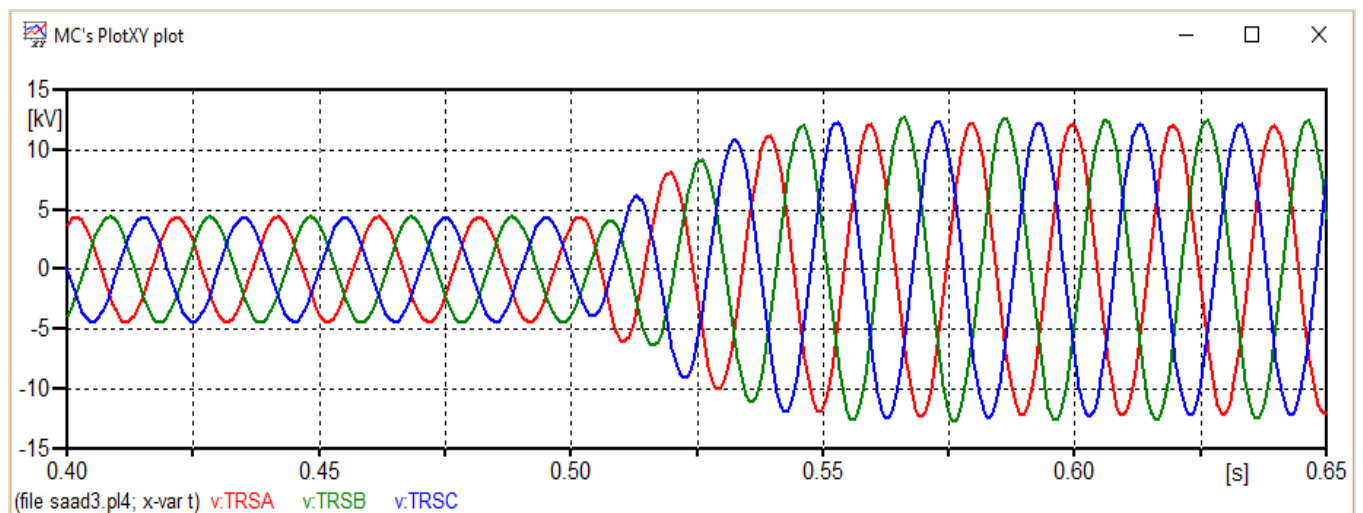


Figure 3.17: The voltages at point TRS with $C_g = 5\mu\text{F}$ and 80% V_s .

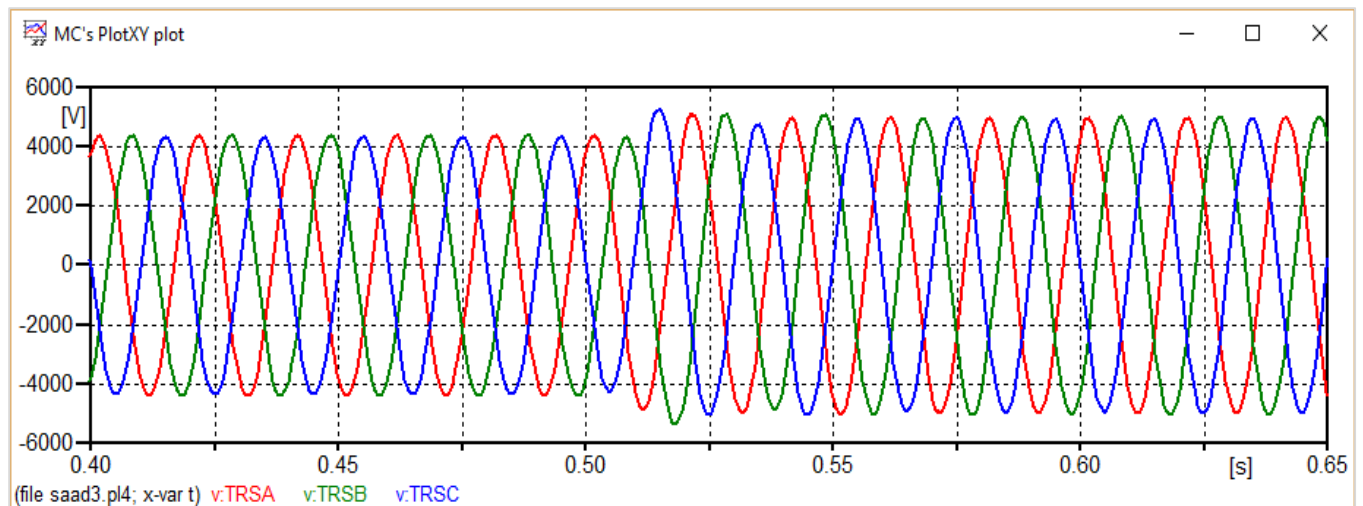


Figure 3.18: The voltages at point TRS with $C_g = 30\mu\text{F}$ and 80% V_s .

Comments: In the above waveforms from figure 3-14 to 3-18. It could be seen that for V_s values of 80%, the ferroresonance doesn't exist for $C_g = 0.6\mu\text{F}$ as it is for V_s values of 100%, it exists for $C_g = 2\mu\text{F}$ and above until the value $C_g = 30\mu\text{F}$, it will appear overvoltage start to be less and extremely equal to the secondary voltage of TR1.

Now we vary the network voltage up to 120% $V_s = 36\text{ Kv}$, then we record the voltage waveforms across the transformer TR1 as shown below:

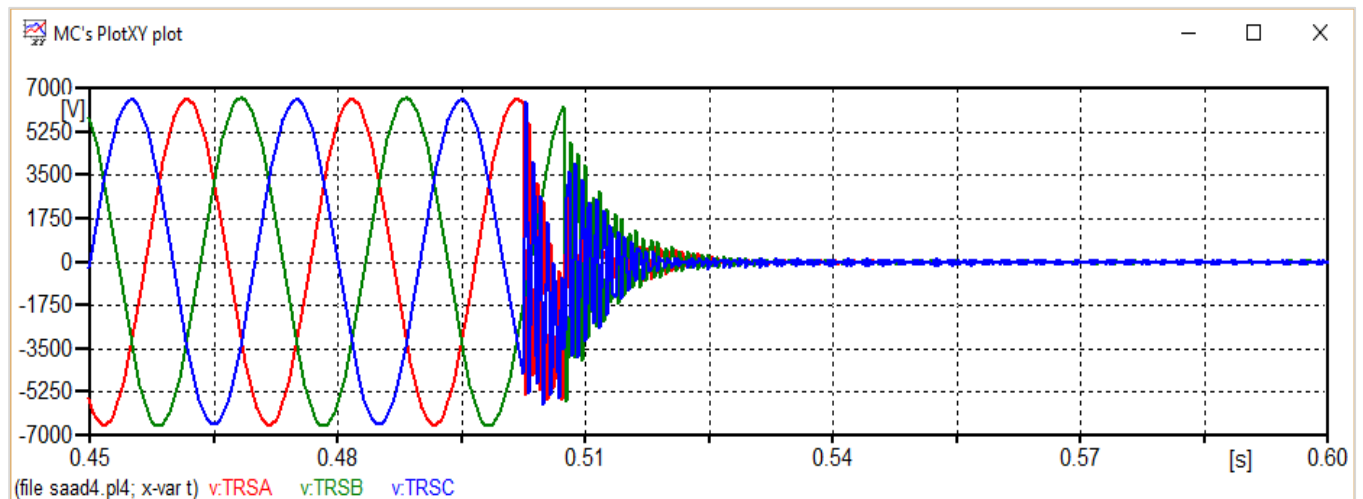


Figure 3.19: The voltages at point TRS with $C_g = 1\text{nF}$ and 120% V_s .

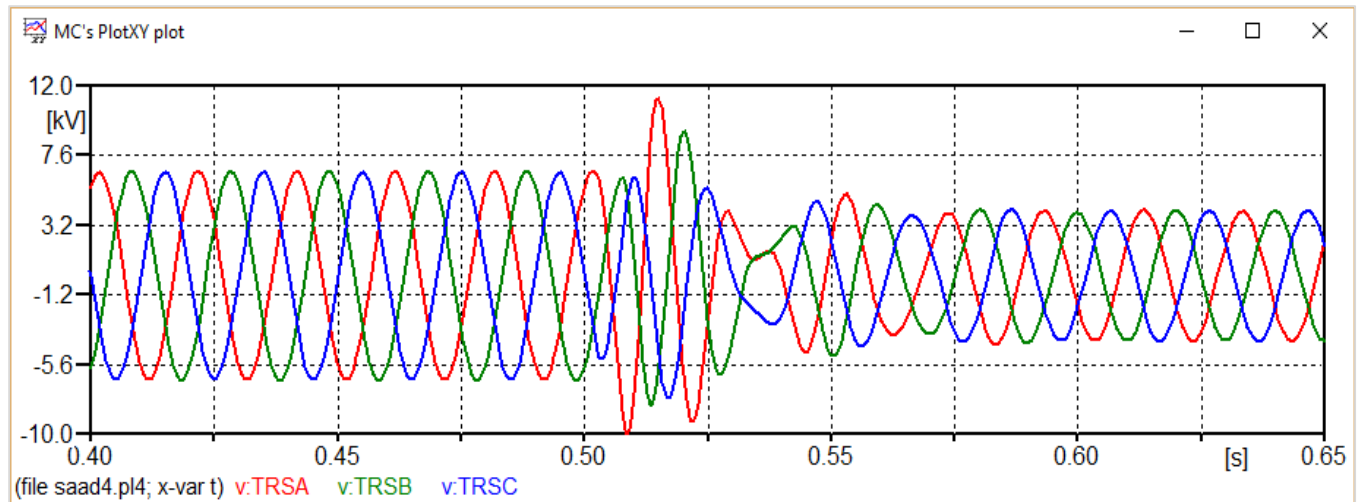


Figure 3.20: The voltages at point TRS with $C_g = 10\text{ nF}$ and 120% V_s .

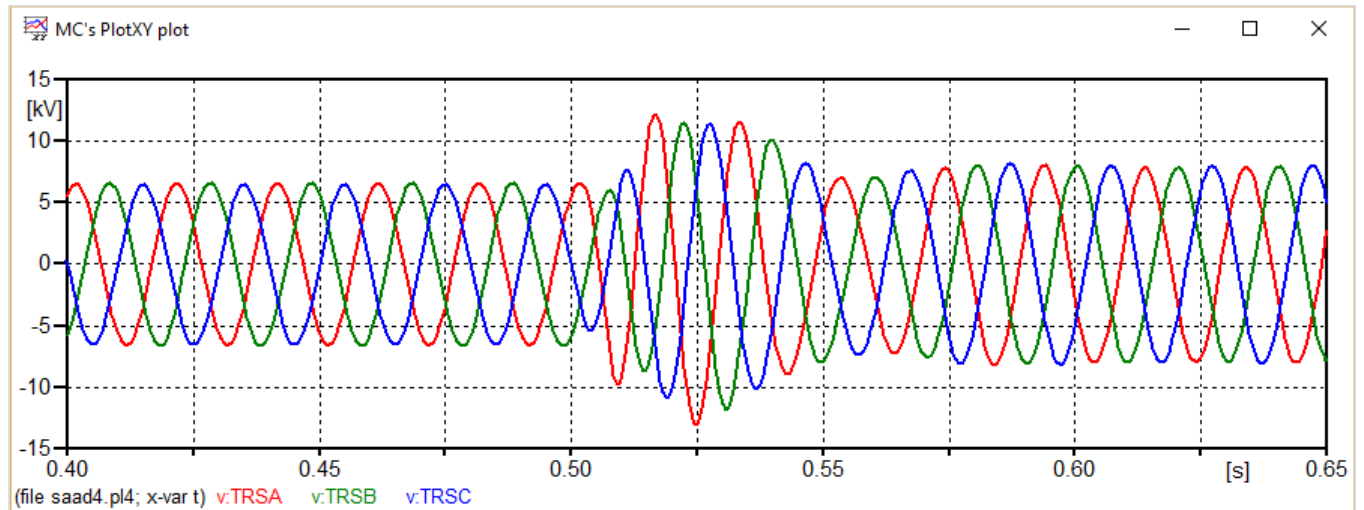


Figure 3.21: The voltages at point TRS with $C_g = 2\text{ }\mu\text{F}$ and 120% V_s .

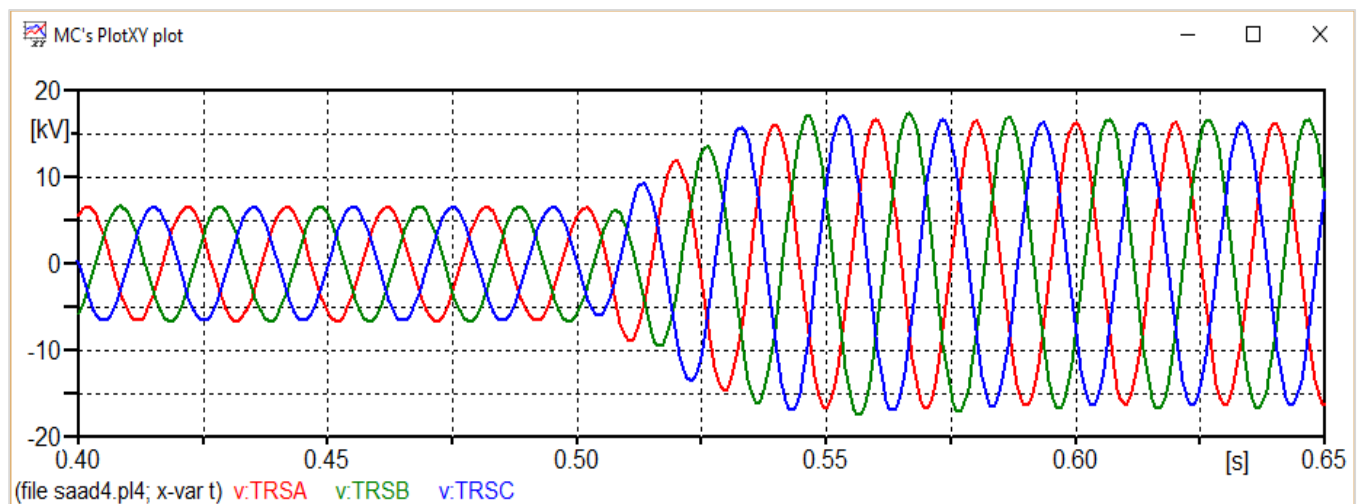


Figure 3.22: The voltages at point TRS with $C_g = 5\text{ }\mu\text{F}$ and 120% V_s .

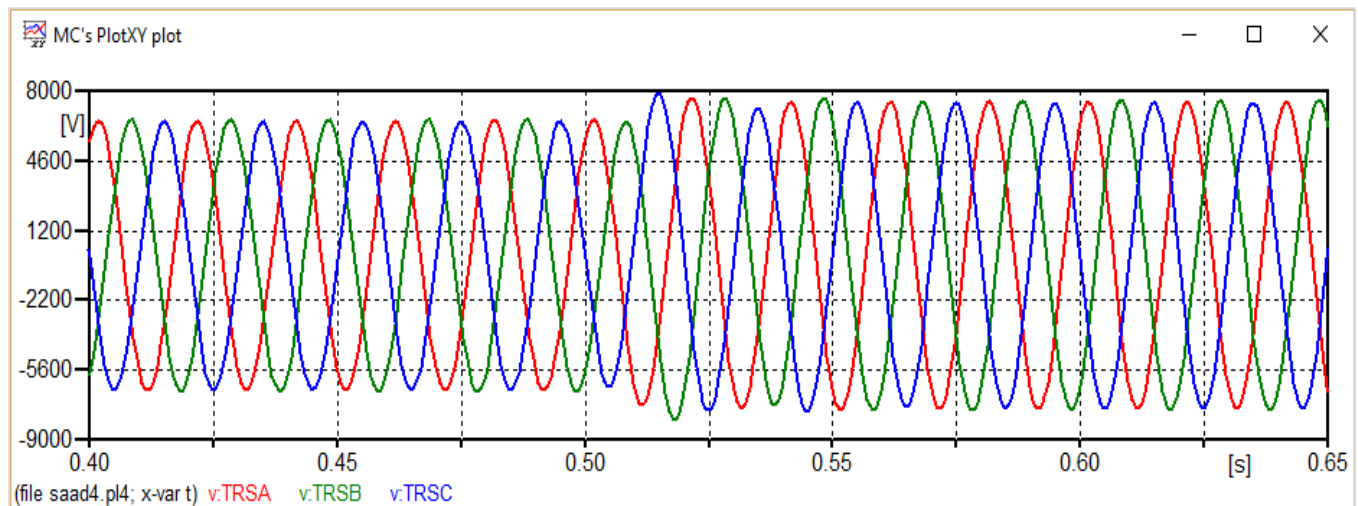


Figure 3.23: The voltages at point TRS with $C_g = 30\mu\text{F}$ and 120% V_s .

Comments: In the above waveforms from figure 3-19 to 3-23. It could be seen that for the extreme value of $V_s = 120\%$ however, a potential risk of ferroresonance was identified for $C_g = 10\text{nF}$ and above, until the value $C_g = 50\mu\text{F}$, it will appear overvoltage start to be less and extremely equal to the secondary voltage of TR1.

After performing all the simulations to identify the ferroresonant combination of V_s and C_g values. This ferroresonant region is clearly shown in Table 1 below, summarizing the results of the peak value of overvoltage.

	80% V_s	100% V_s	120% V_s
1nF	NO (0 pu)	NO (0 pu)	NO (0 pu)
10nF	NO (0 pu)	NO (0 pu)	YES (1.3 pu)
600nF	NO (0 pu)	YES (1.5 pu)	YES (1.6 pu)
2 μF	YES (1.8 pu)	YES (2 pu)	YES (2.1 pu)
2.5 μF	YES (2.1 pu)	YES (2.3 pu)	YES (2.5 pu)
5 μF	YES (2.85 pu)	YES (2.9 pu)	YES (3.1 pu)
10 μF	YES (2.1 pu)	YES (2.2 pu)	YES (2.3 pu)
15 μF	YES (1.35 pu)	YES (1.4 pu)	YES (1.6 pu)
30 μF	NO (1.2 pu)	NO (1.25 pu)	YES (1.4 pu)
50 μF	NO (1 pu)	NO (1 pu)	NO (1.2 pu)

Table 3.1: Ferroresonance simulations results summary of maximum overvoltage for C_g .

We have plotted the corresponding graph of this table:



Figure 3.24: The effect of the grading Capacitance on ferroresonance.

General comments:

Finally, we conclude that the best values of grading capacitor which insure a high speed switching for the circuit breaker are: $C < 1\text{nF}$ for the three cases of Vs

Also the interval of grading capacitance which causes overvoltage more than 1.5 per unit:

$$2\mu\text{F} < C < 10\mu\text{F}$$

The Figure 3.24 referred that for values greater than $15\mu\text{F}$ it will appear overvoltage start to be less and less because the resistance of the capacitor was being smaller every time which damp out the extra power of the system.

Varying the value of the source voltage has its effect on ferroresonance especially at the small values of C_g as shown above in the red region (Figure 3.24) and table 3.1, which in the case of 80% Vs the risk

of ferroresonance is suppressed at $C_g = 600\text{nf}$, unlike what exist in the other cases. Also the opposite in the case of 120% V_s , which the risk of ferroresonance extended to $C_g = 10\text{nf}$.

3.6. Practical solution

3.6.1. Increasing the value of shunt capacitance at the transformer primary side

As mentioned in section 2.4, increasing the capacity of shunt capacitance at the transformer primary side is one of the ferroresonance mitigation techniques.

In order to confirm its effectiveness, we create a ferroresonance situation at it is optimum, by fixing the value of grading capacitor $C_g = 5\mu\text{F}$ as we see in figure 3.12, then we try to change the value of the shunt capacitor C_s at the transformer primary side. The simulation results are summarized in Table 3.2, and Figures 3.26, 3.27 and 3.28 show voltage waveforms at transformer secondary side for case 1 with ferroresonance, the threshold in case 3 and its elimination in case 5.

Industry analysts have empirically assumed that when the voltage exceeds 1.25 pu, the system is said to be “in ferroresonance” [19].

Cases	Capacitor (μF)	Maximum overvoltage (pu)	state
1	0.5	2.4	In ferroresonance
2	2.5	1.3	In ferroresonance
3	2.7	1.25	Threshold
4	3	1.15	Non ferroresonance
5	5	0.8	Non ferroresonance

Table 3.2: Simulation results of maximum overvoltage for shunt capacitors.

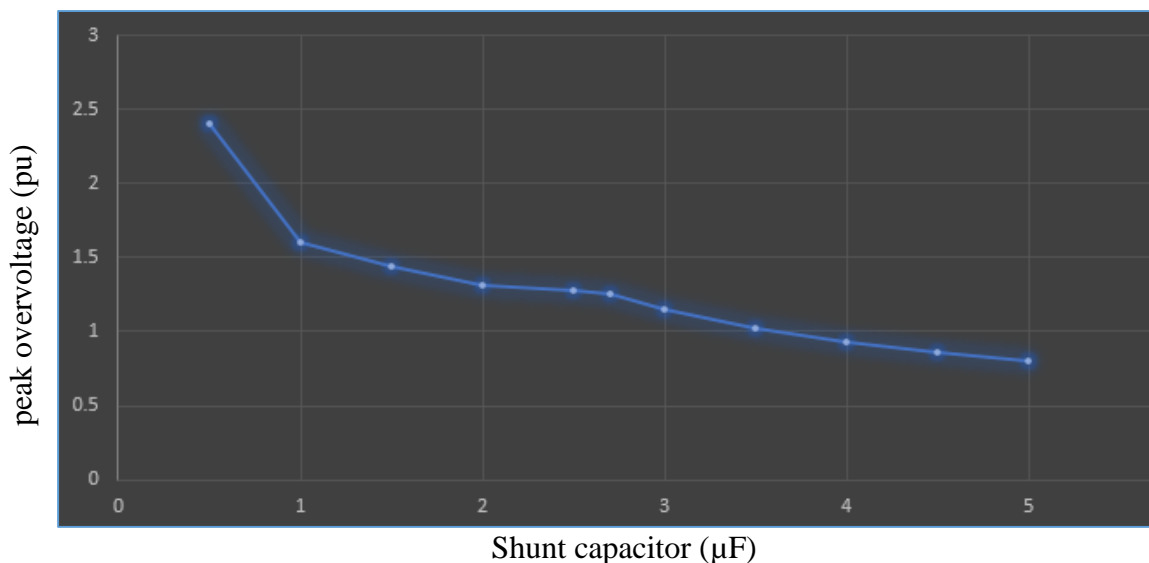


Figure 3-25: The effect of the Shunt Capacitance on ferroresonance.

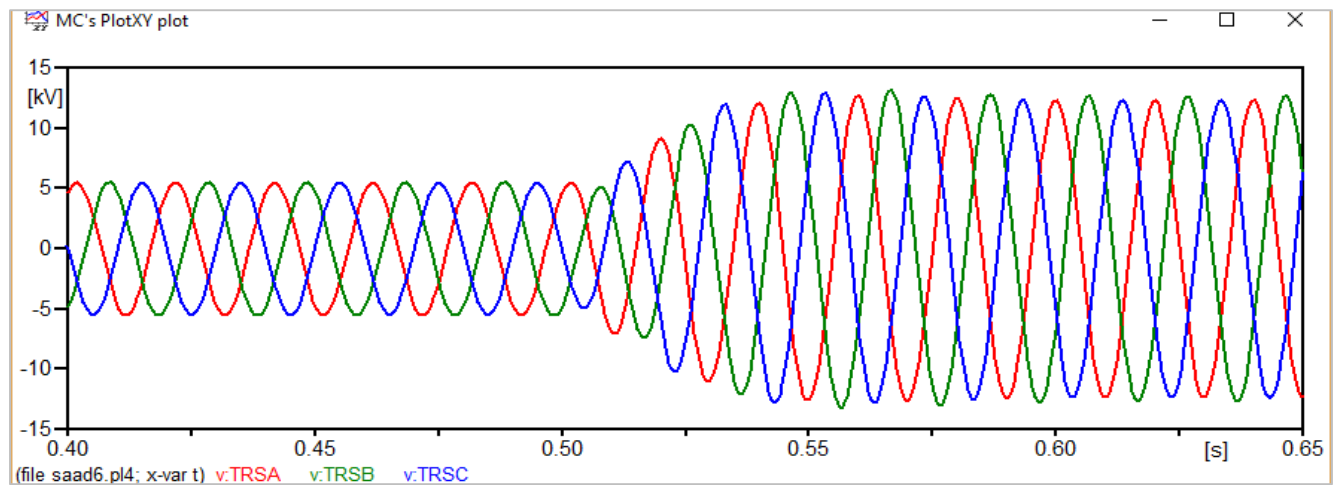


Figure 3.26: The voltages at point TRS for Case 1 with $C_s = 0.5 \mu\text{F}$

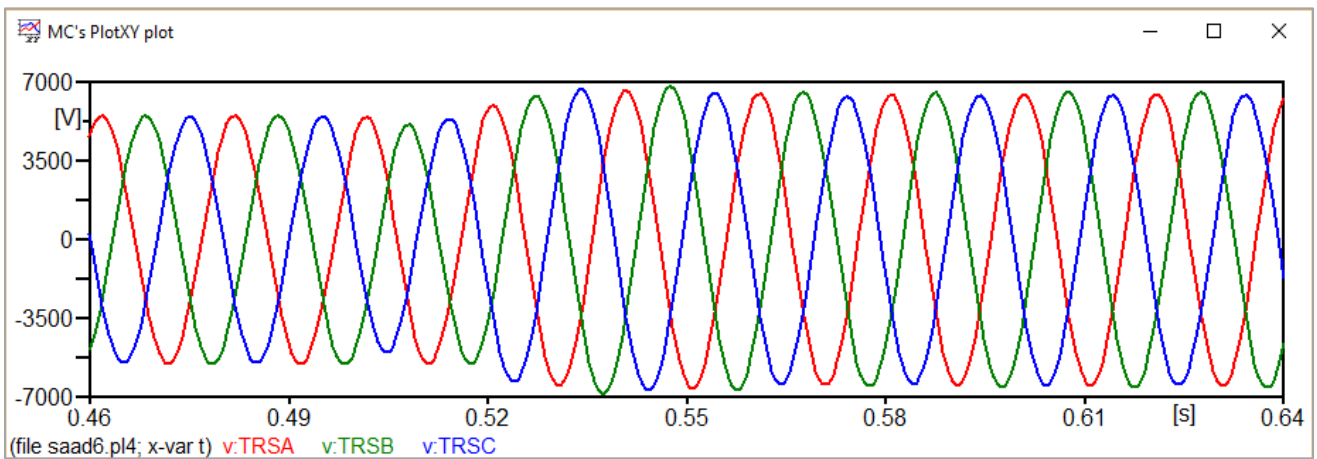


Figure 3.27: The voltages at point TRS for case 3 with $C_s = 2.7 \mu\text{F}$

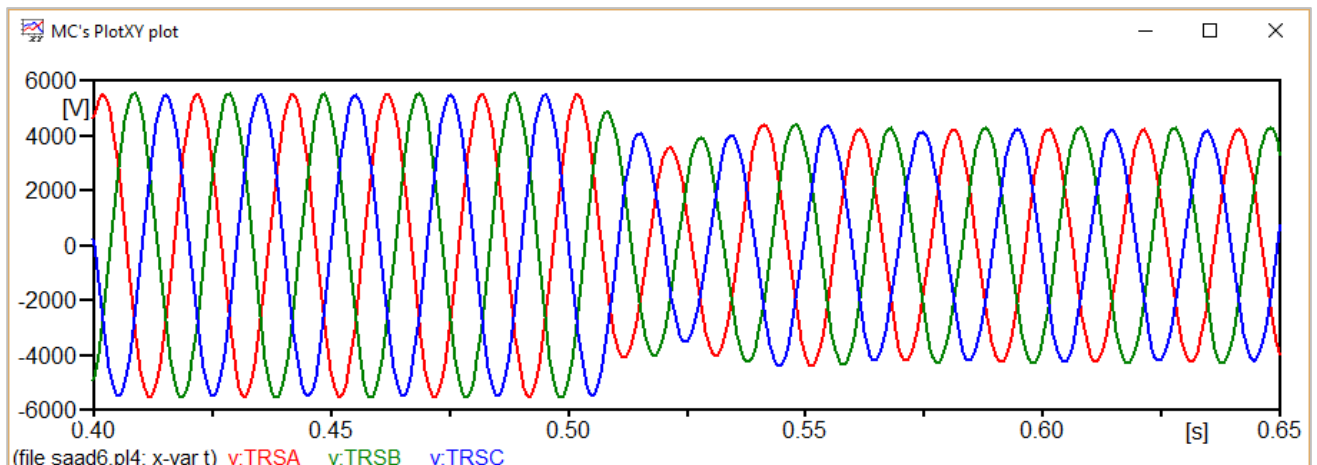


Figure 3.28: The voltages at point TRS for Case 5 with $C_s = 5 \mu\text{F}$

Comments:

According to industry analysts, we see from the table 3.2 and figure 3.25 above that the value of **Cs = 2.7 μF** is the threshold value, and ferroresonance can be avoided by installing the shunt capacitor **Cs ≥ 2.7μF** in this study case. But in the case of **Cs < 2.7 μF** the ferroresonance is reduced slowly when Cs increased from small values until 2.7 μF.

The increasing at the value of shunt capacitance connected in the transformer primary side is very effective to reduce the risk of ferroresonance. Despite the high cost of implementation, it is one of the best solutions if the transformer secondary side is not accessible.

3.6.2. Installing a capacitor bank at the transformer secondary side

The second solution is to install the capacitor bank to suppress ferroresonance. As many papers and technical reports propose the insertion of the capacitor bank at the delta connected tertiary winding [20]. This can only be applicable to the power transformers with tertiary winding terminals. It is considered that the capacitor bank C_b is located at the transformer secondary side in the study because the transformer applied to this study does not have tertiary winding as shown in gray region in figure 3.29.

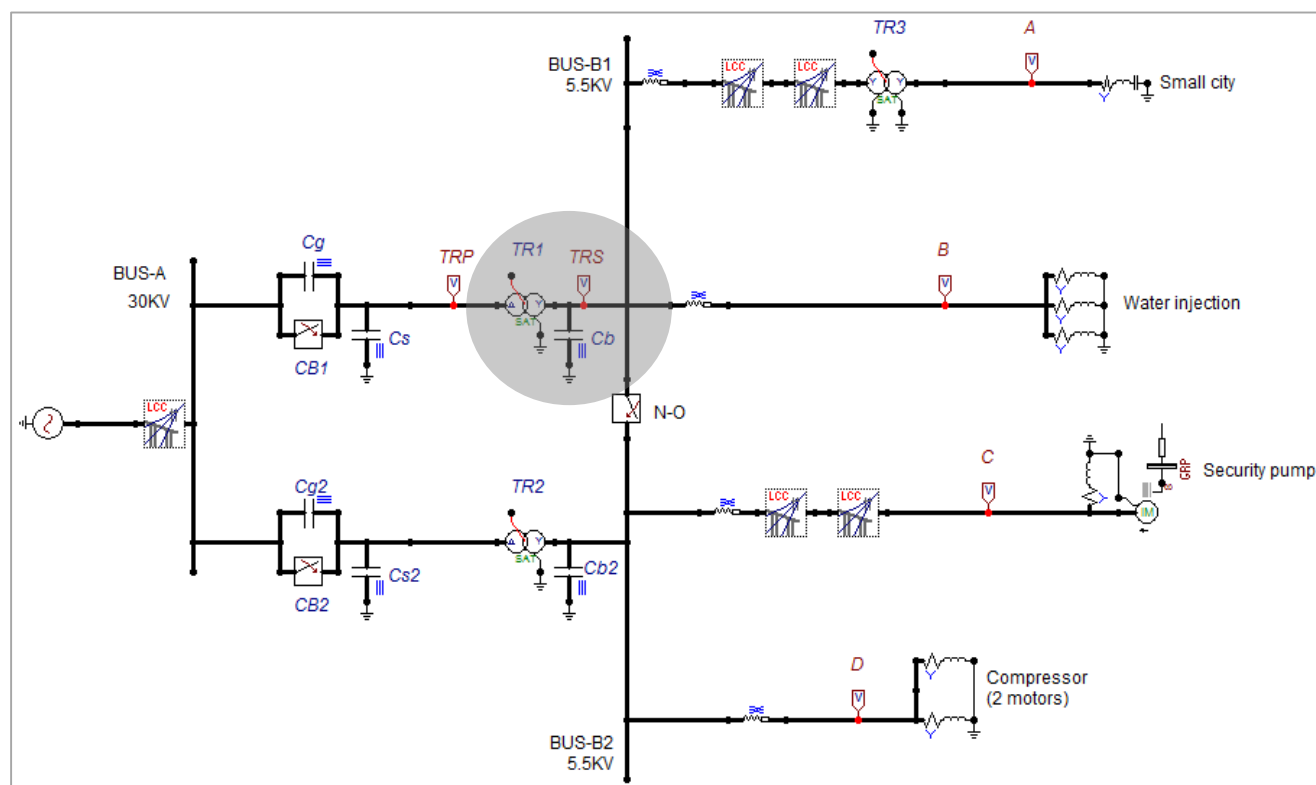


Figure 3.29: Capacitor bank at the transformer TR1 secondary side.

In order to confirm its effectiveness, we create a ferroresonance situation at it is optimum, by fixing the value of grading capacitor $C_g = 5\mu\text{F}$ as we see in figure 3.12, then we try to change the value of the bank capacitor C_b at the transformer secondary side (see figure 3-29). The simulation results are summarized in Table 3.3, and Figures 3.31, 3.32 and 3.33 show voltage waveforms at transformer secondary side for case 1 with ferroresonance, the threshold in case 4 and its elimination in case 7.

Cases	Capacitor (μF)	Maximum overvoltage (pu)	state
1	10	1.8	In ferroresonance
2	40	1.35	In ferroresonance
3	45	1.29	In ferroresonance
4	49	1.25	Threshold
5	50	1.24	Non ferroresonance
6	60	1.15	Non ferroresonance
7	100	0.87	Non ferroresonance

Table 3.3: Simulation results of maximum overvoltage for bank capacitors.

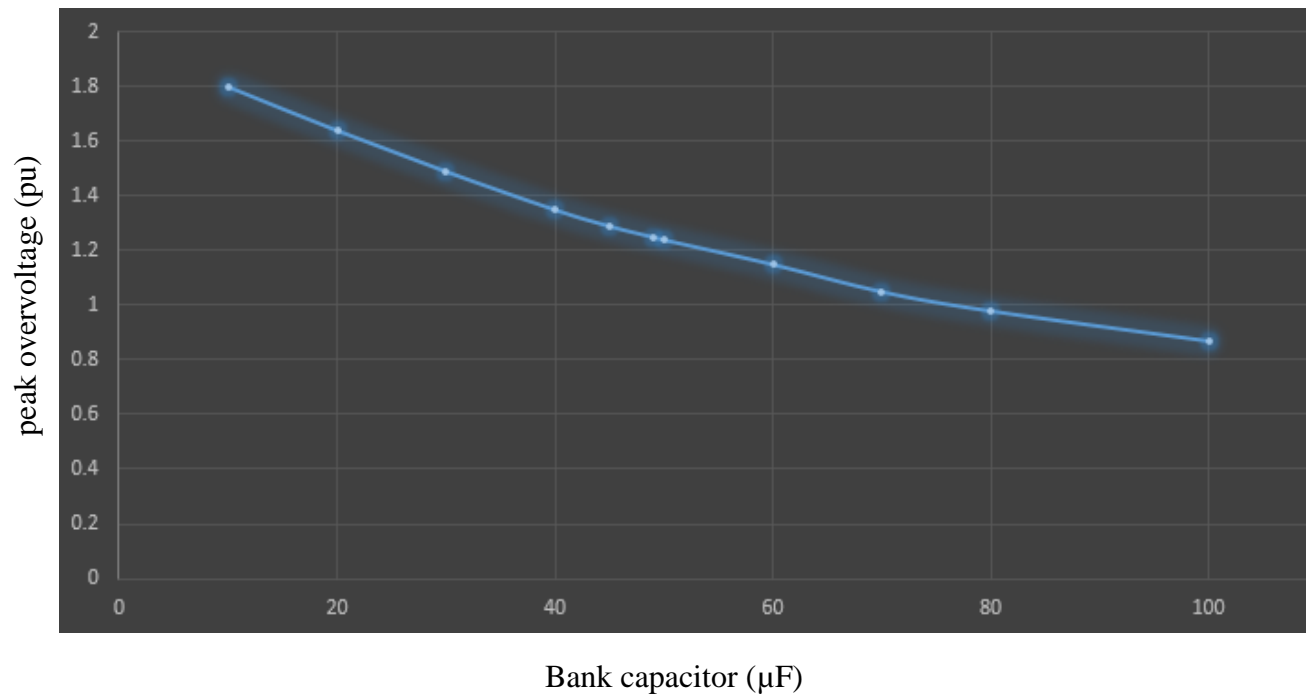


Figure 3.30: The effect of the Bank Capacitance on ferroresonance.

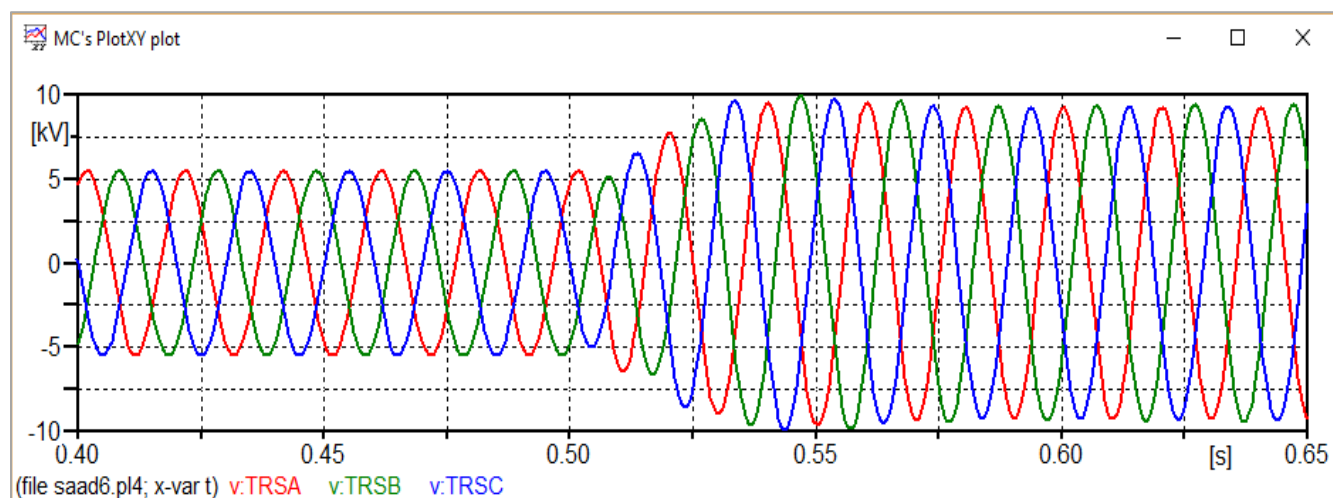


Figure 3.31: The voltages at point TRS for Case 1 with $C_b = 10 \mu\text{F}$

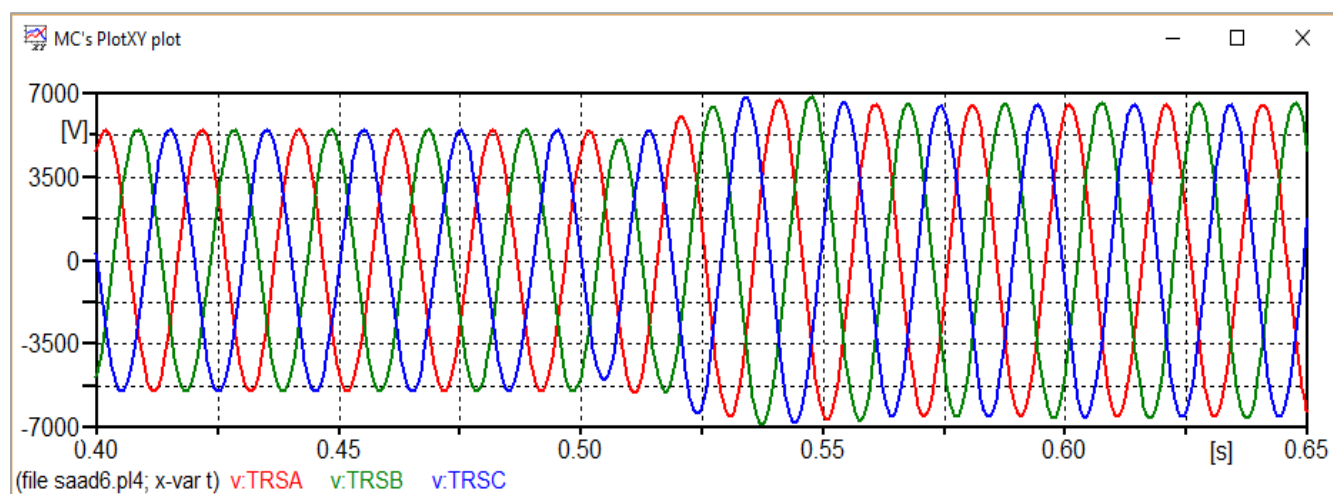


Figure 3.32: The voltages at point TRS for Case 4 with $C_b = 49 \mu\text{F}$

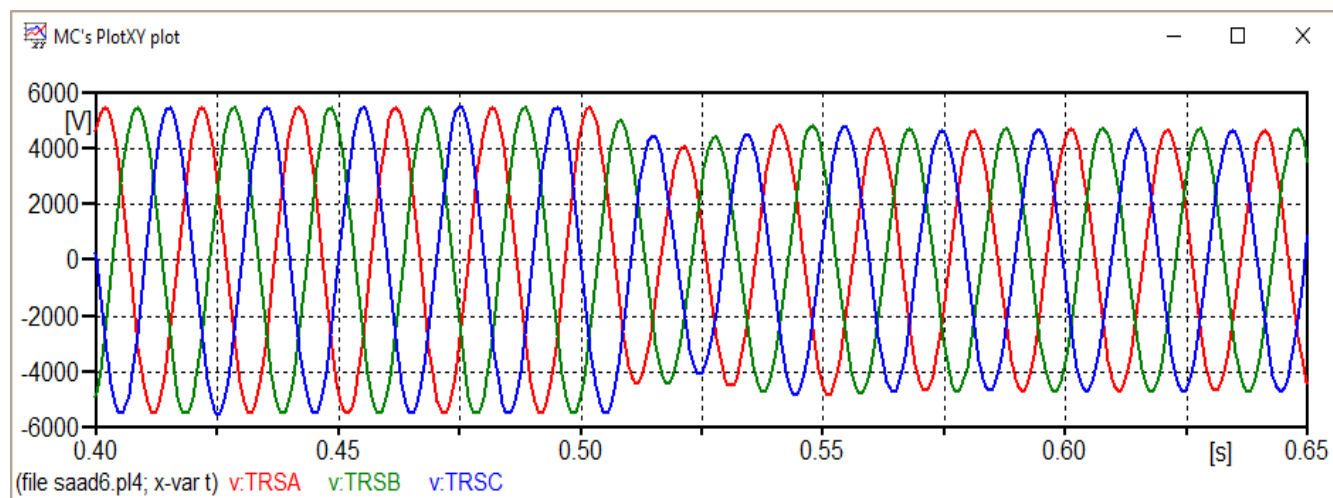


Figure 3.33: The voltages at point TRS for Case 7 with $C_b = 100 \mu\text{F}$

Comments:

According to industry analysts, we see from the table 3.3 and Figure 3.30 above that the value of $C_b = 49 \mu\text{F}$ is the threshold value, and ferroresonance can be avoided by installing the bank capacitor $C_b \geq 49 \mu\text{F}$ in this study case. But in the case of $C_b < 49 \mu\text{F}$ the ferroresonance is reduced slowly when C_s increased from small values until $49 \mu\text{F}$.

It can be observed that the high capacity of the capacitor bank is very effective on the suppression of ferroresonance. This countermeasure has the disadvantages such as its higher cost and the possibility of explosion in practice. In other words, the capacitor bank at the transformer secondary side can significantly reduce the risk of ferroresonance, however it also has disadvantages as well.

3.6.3. Installing a damping resistor at the transformer secondary side

Historically, the most commonly used mitigation method is a resistor connected to the transformer TR1 secondary side as shown in figure 3.34. The zero-sequence voltage present at the resistor terminals results in the zero-sequence current resulting from the ferroresonant oscillations.

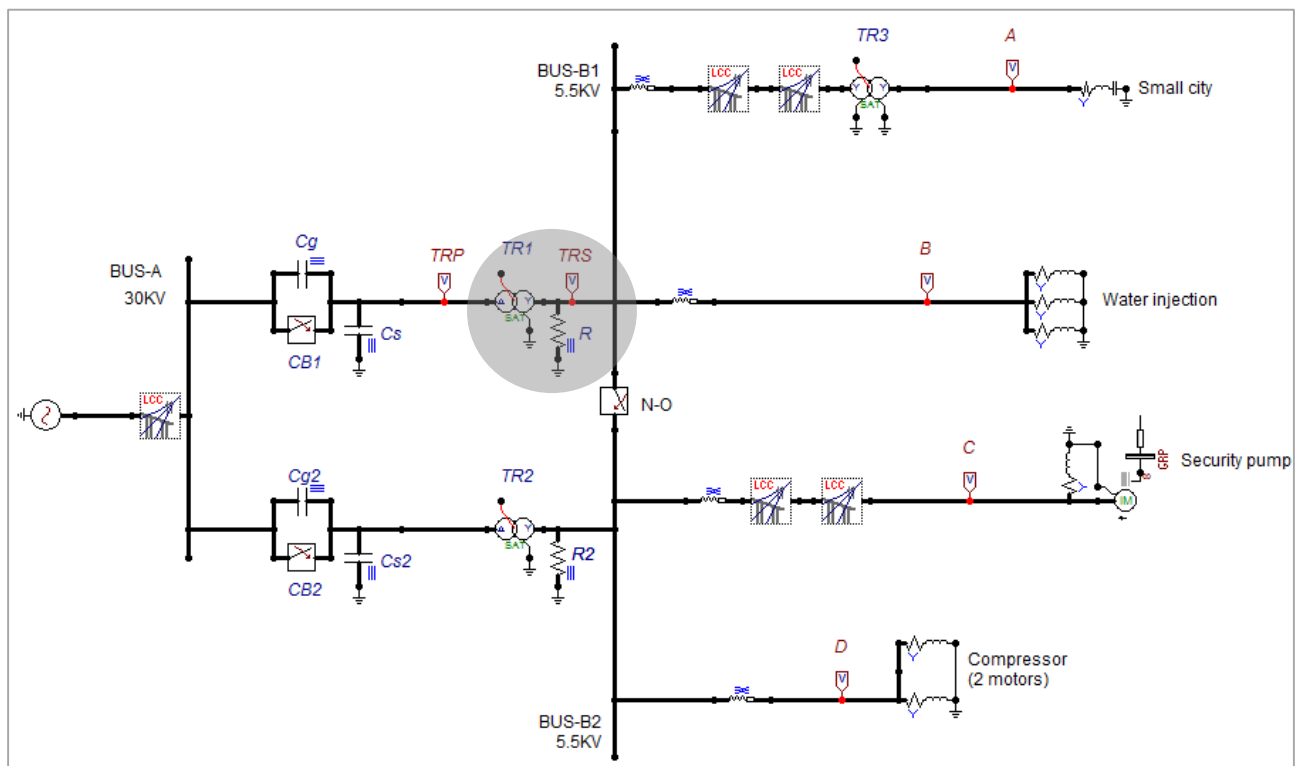


Figure 3.34: The damping resistor at the transformer TR1 secondary side.

This simple method, however, has a limited applicability in the case of the modern, compact constructions of the VTs, utilizing low-loss magnetic materials since typical core losses (oriented steel) are lower than 50 W, which has little effect on the damping properties.

Both computer simulations and experiments showed in many cases that the resistance value needed for efficient damping of the ferroresonant oscillations is very small ($R < 20 \Omega$) and the resulting power dissipated in the damping resistor is greater than several hundreds of watts.

Now we try to see the effect of this method we try to vary R around the value of 20Ω , table 3.4 summarizes the simulation results and figures 3.36, 3.37 and 3.38 show voltage waveforms at transformer secondary side for case 5 with ferroresonance, the threshold in case 4 and its elimination in case 1.

Cases	Resistor (Ω)	Maximum overvoltage (pu)	state
1	12	0.9	Non ferroresonance
2	15	1.1	Non ferroresonance
3	20	1.18	Non ferroresonance
4	25	1.25	Threshold
5	30	1.29	In ferroresonance

Table 3.4: Simulation results of maximum overvoltage for damping resistor.

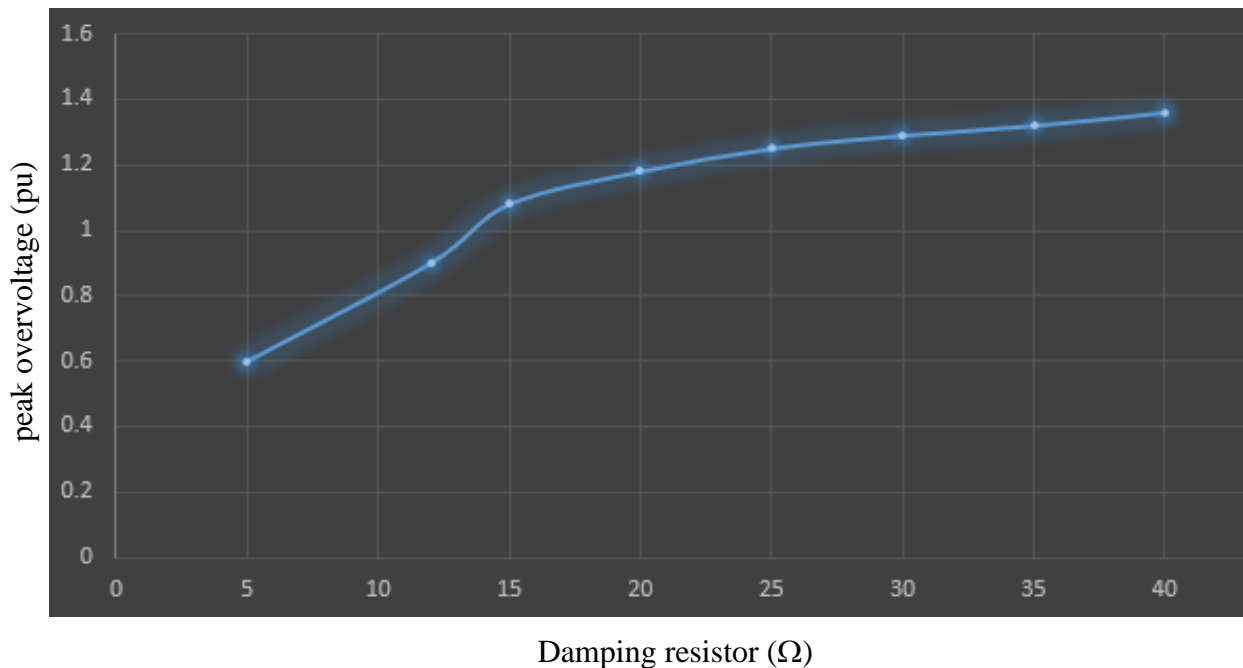


Figure 3.35: The effect of the Damping resistor on ferroresonance.

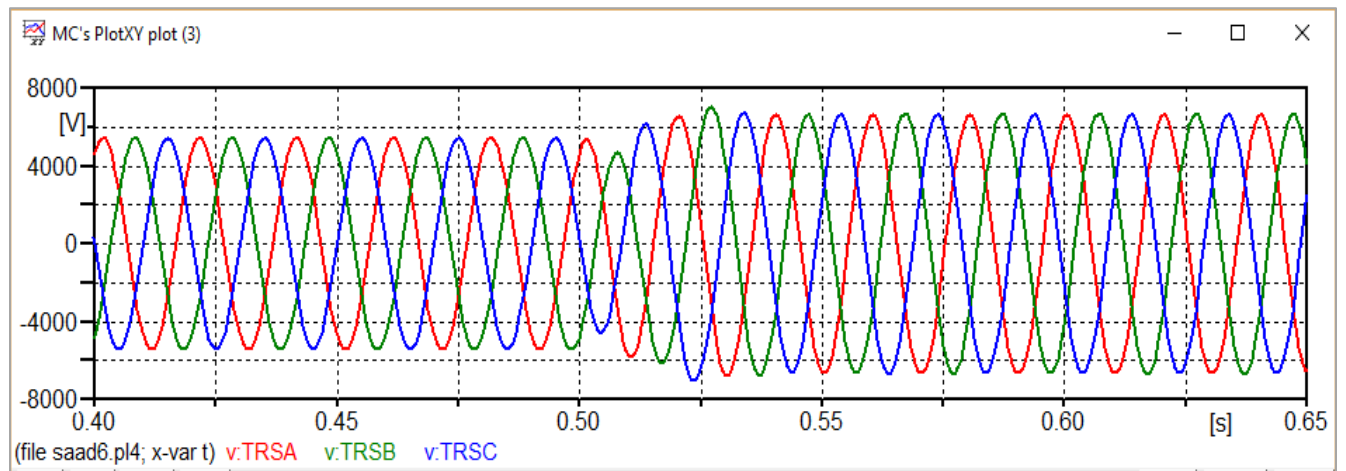


Figure 3.36: The voltages at point TRS for Case 5 with $R = 30 \, \Omega$

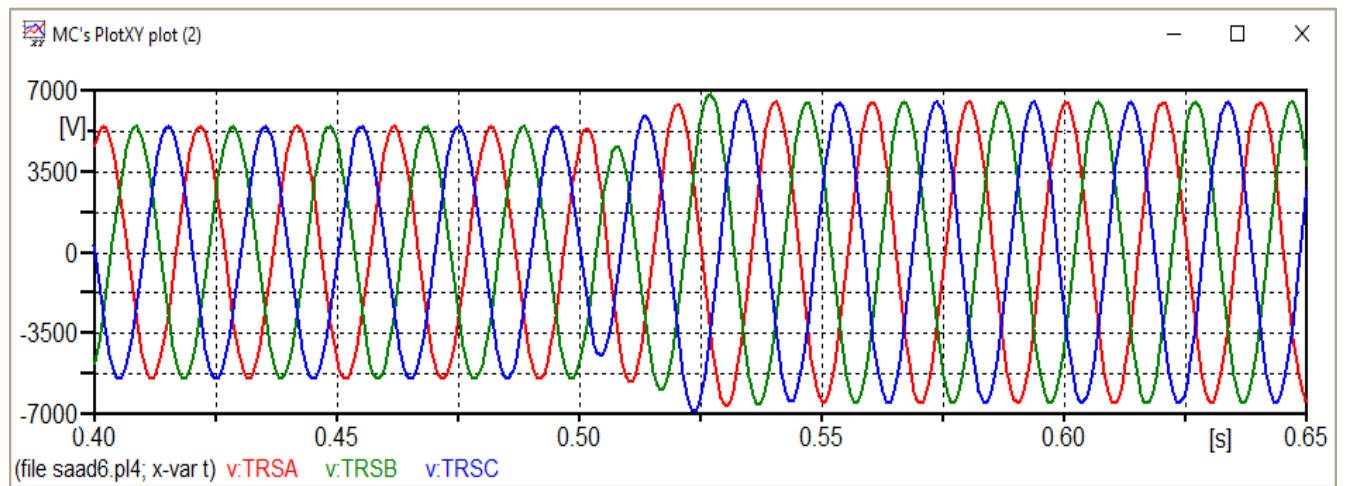


Figure 3.37: The voltages at point TRS for Case 4 with $R = 25 \, \Omega$

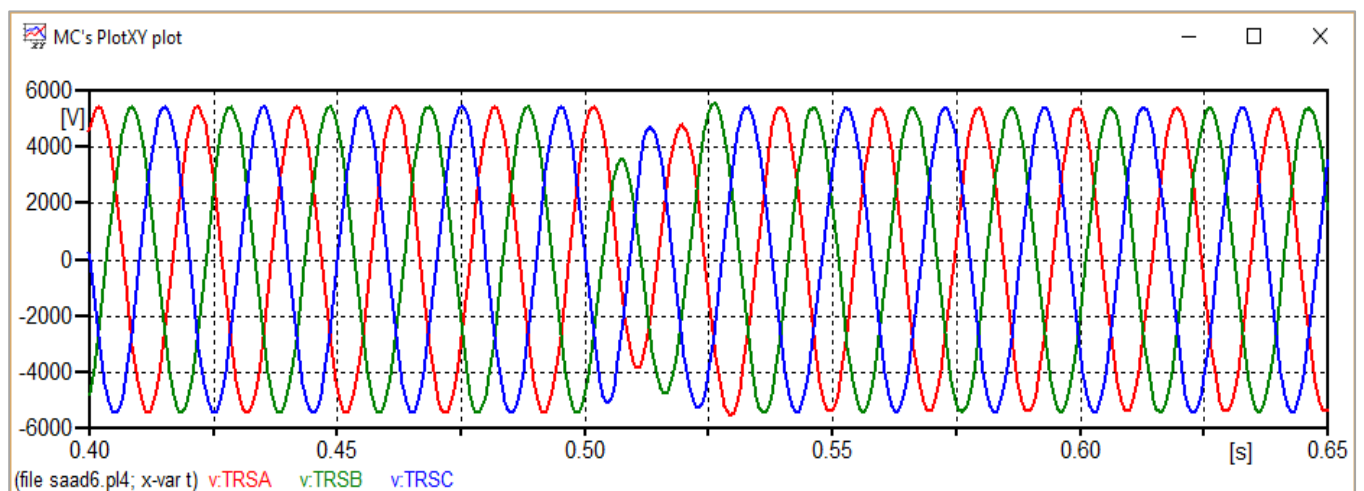


Figure 3.38: The voltages at point TRS for Case 1 with $R = 12 \, \Omega$

Comments:

Table 3.4 and Figure 3.35 shows the simulated effectiveness of the ferroresonant oscillations damping with the resistor. It can be seen that the use of the resistor $R = 12\Omega$ eliminate the ferroresonance with peak voltage $V = 0.9$ pu, and the use of the value of R larger than approximately 12Ω has a small influence on avoiding the ferroresonance, until the threshold $R = 25\Omega$ the ferroresonance is observed.

However, in practice, using a damping resistor of such a low value results in a risk of thermal damage of the VTs during abnormal network asymmetry resulting from prolonged earth faults. There are other known methods of preventing ferroresonance, such as the use of a saturable inductor in series with a damping resistor.

This approach, despite its applicability in high-voltage (HV) capacitive VTs with an intermediate inductive VT, is practically not used in the MV voltage transformers. The use of the R–L circuit overcomes the thermal problem in the case of the earth fault situation. However, the efficiency of damping is limited (it conducts current only above the saturation level of the inductor) and, thus, a very precise design of the damping circuit for a specific VT type is required.

3.7. Conclusion

The analysis presented in this chapter on the case study example showed the approach applicable to studying the potential of the ferroresonant behavior of the real power network. we have seen almost the parameters that can affect ferroresonance which are the grading capacitor of the circuit breaker and the source voltage.

The use of the ATP environment can be used to identify the potential ferroresonant combinations of parameters (voltage and capacitance) and allows one to select appropriate mitigation scheme as we have seen in section 3.6.

GENERAL CONCLUSION

GENERAL CONCLUSION

Even though ferroresonance is not very common, it is a problem in power systems. To get familiar with it, it is compared to linear resonance. The ferroresonance has dangerous consequences like stable overvoltages and overcurrents. Risky configurations are mentioned and prevention of ferroresonance is discussed, because they are considered to be catastrophic when they occur.

In addition, ATPDraw software has been developed to simulate one of the critical situations for the ferroresonance to appear, which is the interaction between the grading capacitor of circuit breaker and MV power transformer. The influence of capacitance values has been analyzed through several software simulations, considering the critical capacitance values.


Some practical solutions are suggested and introduced in the ATPDraw representation of the circuit of Haoud Berkaoui station after creating a ferroresonance situation, such as installing a shunt capacitor at the transformer primary side and installing a capacitor bank or a damping resistor at the secondary side, they had a considerable effect on damping and eliminating the risk of ferroresonance.

REFERENCES

- [1] Philippe FERRACCI, "Group Schneider Cahier technique n°190, Ferroresonance", ECT190, first issued March 1998.
- [2] Schultz, R.A., "Ferroresonance in Distribution Transformer Banks on 8/34.5 kV Systems," Presented at 1964 Spring Conference, Rocky Mountain Elec. League.
- [3] Rudenberg, R., transient performance of electrical power system, McGraw-Hill Book Company, New York, NY, Copyright @ 1949.
- [4] Swee Peng Ang "Ferroresonance simulation studies of transmission systems", the university of Manchester 2010, p 20-22.
- [5] T. D. Burton, Introduction to Dynamic System Analysis, International Edition ed.: McGraw-Hill.
- [6] M. Val Escudero, I. Dudurych, and M.A. Redfern, "Characterization of ferroresonant modes in HV substation with CB grading capacitors", Electric Power Systems Research, vol. 77, pp. 1506-1513, 2007.
- [7] K. Pattanapakdee and C. Banmongkol, "Failure of Rise Pole Arrester Due to Station Service Transformer Ferroresonance", Proceedings of International Conference on Power Systems Transients, Lyon, 4-7 June 2007.
- [8] D.A.N. Jacobson, D.R. Swatek and R.W. Mazur, "Mitigating Potential Transformer Ferroresonance in a 230 kV Converter Station", Proceedings of IEEE Transmission and Distribution Conference, pp. 269-275, Los Angeles, 1996.
- [9] IEC 71 International Standard, "Insulation Co-ordination", 1996
- [10] Yunge Li, Wei Shi, Rui Qin and Jilin Yang, "A Systematical Method for Suppressing Ferroresonance at Neutral-Grounded Substations", IEEE Transactions on Power Delivery, vol. 18, no.3, July 2003.
-

- [11] L. X. Zhou and Z. D. Yin, "Research on PT Ferromagnetic Resonance and the Controllable Damping", Proceedings of IEEE Power Tech Conference, pp. 413-418, Lausanne, 1-5 July 2007.
 - [12] P. Sakarung, T. Bunyagul and S. Chatratana, "Investigation and Mitigation of Overvoltage Due to Ferroresonance in the Distribution Network", Journal of Electrical Engineering and Technology, vol. 2, no. 3, pp. 300-305, 2007.
 - [13] T. Van Craenenbroeck, D. Van Dommelen and N. Janssens, "Damping Circuit Design for Ferroresonance in Floating Power Systems", European Transactions on Electrical Power, vol. 10, no. 3, May/June 2000.
 - [14] M StoSur, W PiaSecki . M FlorkoWSki, M Fulczyk "Electrical Power Quality and Utilization, Journal Vol. XIV, No. 2, pp 49 2008.
 - [15] B. Djaafar R. Taoufik 'Investigation on Power Transformer Design' Final Year Project Report 2015.
 - [16] Earthing systems in LV, B. LACROIX, R. CALVAS, Cahier Technique Merlin Gerin n 172.
 - [17] Bienvenido Rodríguez – Medina, Marianela Santiago- Luna, "Electric Power Engineering Group UPR- Mayagüez" "ATP/EMTP Quick Guide", Mayagüez, P.R. June 18,2002.
 - [18] CIGRE Working Group C4.307, "Resonance and ferroresonance in power networks," CIGRE, Tech. Bro. TB-569, Feb. 2014.
 - [19] S. Santoso, R. C. Dugan, and P. Nedwick, "Modeling ferroresonance phenomena in an underground distribution system," in Proc. 2001 IPST.
 - [20] A. V. Ranst, J. M. Dumoulin, and N. Mabrouk, "Insulation coordination and ferroresonance study for EMAL phase II project," Tractebel Eng., Brussels, BE, Apr. 2012.
-

The definitions and parameters

➤ **Source :** 

Name: ACSOURCE - Steady-state (cosine) function (voltage) Grounded; TYPE 14.

Component: ACSOURCE

DATA	UNIT	VALUE
AmplitudeA	Volt	30000
Frequency	Hz	50
PhaseAngleA	degrees	0
StartA	sec	-1
StopA	sec	100

NODE	PHASE	NAME
AC	ABC	X0019

Copy Paste entire data grid Reset Order: 0 Label:

Comment:

Type of source: ☐ Current ☒ Voltage

Num phases: ☐ Single ☒ 3-phase ☐ 3*1-phase

Angle units: ☒ Degrees ☐ Seconds

Amplitude: ☒ Peak L-G ☐ RMS L-G ☐ RMS L-L

Grounding: ☒ Grounded ☐ Ungrounded ☐ Hide

Edit definitions OK Cancel Help

➤ **Transformer:** 

Name: Sat-Trafo - General saturable transformer. 3 phase. 2 windings, Delta, Wye .with 30° phase shifts.

Component: SATTRAFO

	Prim.	Sec.
U [V]	30000	3180
R [ohm]	0.0005	0.0005
L [mH,ohm]	0.05	0.05

Coupling: D Y

Phase shift: 30

I(0)= 0 Rm= 00000000 ☒ 3-leg core

F(0)= 2 R0= 11500 ☐ RMS ☐ 3-winding

NODE	PHASE	NAME
Primary	ABC	X0045
Secondary	ABC	S
Starpoint	ABC	X0038
Sec-N	1	X0039

Order: 0 Label:

Comment:

Output: 0 - No ☐ Hide

Edit definitions OK Cancel Help



Model: PI **Unit system:** Metric

Line/Cable Data: XLPE120

Model Data Nodes

System type
Overhead Line #Ph: 3

☐ Transposed
☐ Auto bundling
☒ Skin effect
☐ Segmented ground
☐ Real transf. matrix

Units
☒ Metric
☐ English

Standard data
Rho [ohm*m] 20
Freq. init [Hz] 50
Length [km] 0.7
☐ Set length in icon

Model Type
☐ Bergeron
☒ PI
☐ JMart
☐ Semlyen
☐ Noda

Data
☐ Printed output ☐ [C] print out

Comment: Order: 0 Label: ☐ Hide

OK Cancel Import Export Run ATP View Verify Edit defin. Help

Line/Cable Data: XLPE120

Model Data Nodes

#	Ph.no	Rin [cm]	Rout [cm]	Resis [ohm/km DC]	Horiz [m]	Vtower [m]	Vmid [m]
1	1	0	0.545	0.303	-0.75	10	8
2	2	0	0.545	0.303	0	10	8
3	3	0	0.545	0.303	0.75	10	8

Add row Delete last row Insert row copy Move

OK Cancel Import Export Run ATP View Verify Edit defin. Help



Component: UM_3

Attributes

General Magnet Stator Rotor Init

Stator coupling
Y

Pole pairs: 2

Rotor coils
d: 1 q: 1

Frequency: 50
Tolerance: 0.1885

Global
☐ Automatic
☐ Prediction

Order: 0 Label:

Comment:

Output
TQOUT 0 1 2 3
OMOUT 0 1 2 3
☒ THOUT
☒ CURR

Edit definitions OK Cancel Help

Component: UM_3

Attributes

General Magnet Stator Rotor Init

LMUD: 0.003533
LMUQ: 0.003533

Saturation
☒ none
☐ d
☐ q
☐ both
☐ symm

NODE	PHASE	NAME
Stator	ABC	P
M_NODE	1	XX0026
Neut	1	

Order: 0 Label:

Comment:

Output
TQOUT 0 1 2 3
OMOUT 0 1 2 3
☒ THOUT
☒ CURR

Edit definitions OK Cancel Help

Component: UM_3

Attributes

General Magnet Stator Rotor Init

	R [ohm]	L [H/pu]
0	0	0
d	0.01673	0.1968
q	0.01673	0.1968

NODE	PHASE	NAME
Stator	ABC	P
M_NODE	1	XX0026
Neut	1	

Order: 0 Label:

Comment:

Output

TQOUT 0 1 2 3 OMOUT 0 1 2 3 ☒ THOUT ☐ Hide ☒ CURR

Edit definitions OK Cancel Help

Component: UM_3

Attributes

General Magnet Stator Rotor Init

	R [ohm]	L [H/pu]
1	0.017405	0.1968
2	0.017405	0.1968

NODE	PHASE	NAME
Stator	ABC	P
M_NODE	1	XX0026
Neut	1	

Order: 0 Label:

Comment:

Output

TQOUT 0 1 2 3 OMOUT 0 1 2 3 ☒ THOUT ☐ Hide ☒ CURR

Edit definitions OK Cancel Help

Component: UM_3

Attributes

General Magnet Stator Rotor Init

Manual

Stator	I [A]	Rotor	I [A]
0	0	1	0
d	0	2	0
q	0		

OMEGM [rad/s]: 0 THETAM: 0

NODE	PHASE	NAME
Stator	ABC	P
M_NODE	1	XX0026
Neut	1	

Order: 0 Label:

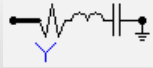
Comment:

Output

TQOUT 0 1 2 3 OMOUT 0 1 2 3 ☒ THOUT ☐ Hide ☒ CURR

Edit definitions OK Cancel Help

➤ **RLC load of the Small City:**



Name: RLCY3. Y-coupling

Independent values in phases.

Component: RLCY3

Attributes

DATA	UNIT	VALUE
L_1	mH	9.4
C_1	μF	0.01
R_2	Ohm	1.5
L_2	mH	9.4
C_2	μF	0.01
R_3	Ohm	1.5
L_3	mH	9.4
C_3	μF	0.01

NODE	PHASE	NAME
IN	ABC	RLC
OUT	1	

Copy Paste entire data grid Reset Order: 0 Label:

Comment:

Output 0 - No ☐ Hide ☐ \$Vintage,1

Edit definitions OK Cancel Help

Component: RLCY3

DATA	UNIT	VALUE	NODE	PHASE	NAME
R_1	Ohm	78	IN	ABC	W
L_1	mH	407	OUT	1	
C_1	μ F	0			
R_2	Ohm	78			
L_2	mH	407			
C_2	μ F	0			
R_3	Ohm	78			
L_3	mH	407			

Copy Paste entire data grid Reset Order: 0 Label:

Comment:

Output: 0 - No ☐ Hide ☐ \$Vintage,1

Edit definitions OK Cancel Help

Component: RLCY3

DATA	UNIT	VALUE	NODE	PHASE	NAME
R_1	Ohms	47.65	IN	ABC	SP
L_1	mH	580	OUT	1	
C_1	μ F	0			
R_2	Ohms	20			
L_2	mH	580			
C_2	μ F	0			
R_3	Ohms	20			
L_3	mH	580			

Copy Paste entire data grid Reset Order: 0 Label:

Comment:

Output: 0 - No ☐ Hide ☐ \$Vintage,1

Edit definitions OK Cancel Help

➤ **RL load of Water Injection:**



Name: RLCY3; Y-coupling,
Independent values in phases.

➤ **RL load of Security Pump:**



Name: RLCY3; Y-coupling,
Independent values in phases.

Component: RLCY3

DATA	UNIT	VALUE	NODE	PHASE	NAME
R_1	Ohm	13.55	IN	ABC	C
L_1	mH	80	OUT	1	
C_1	μ F	0			
R_2	Ohm	13.55			
L_2	mH	80			
C_2	μ F	0			
R_3	Ohm	13.55			
L_3	mH	80			

Copy Paste entire data grid Reset Order: 0 Label:

Comment:

Output: 0 - No ☐ Hide ☐ \$Vintage,1

Edit definitions OK Cancel Help

Component: LINESY_3

DATA	UNIT	VALUE	NODE	PHASE	NAME
R ₀	Ohm/m	0.5	IN1	ABC	F
L ₀	mH/m	0.1	OUT1	ABC	W1
R ₊	Ohm/m	0.005			
L ₊	mH/m	0.001			

Copy Paste entire data grid Reset Order: 4 Label:

Comment:

Lines: Length 100 [m] ☐ Hide

Edit definitions OK Cancel Help

➤ **RL load of compressor:**



Name: RLCY3; Y-coupling,
Independent values in phases.

➤ **Cable:**

Name: LINESY_3 - Symmetric RL
coupled line. Data given in positive
and zero sequence.

The parameters of the circuit breaker used in the electric substation of HAOUD BERKAOUI

TYPE		S																															
		EGB 1 20-06F		EGB 1 20-12F		EGB 1 28-06F		EGB 1 28-12F		EGB 2 12-06F		EGB 2 12-12F		EGB 2 16-06F		EGB 2 16-12F		EGB 3 12-06F		EGB 3 12-12F		EGB 3 16-06F		EGB 3 16-12F		EGB 3 25-12F							
Rated voltage	kV	7,2								12								17,5															
Rated lightning impulse withstand voltage 1,2/50 μs	kV	60								75								95															
Rated power frequency withstand voltage 1 min	kV	22								28								38															
Rated normal current	A	630	1250	630	1250	630	1250	630	1250	630	1250	630	1250	630	1250	630	1250	630	1250	630	1250	630	1250	630	1250	630	1250						
Rated short circuit breaking current	kA	20				28				12,5				16				25				12,5				16				25			
Rated short circuit making current	kA	50				70				31,5				40				63				31,5				40				63			
Rated cable-charging breaking current	A	10								25								31,5															
DC component	%	30																31															
Rated no-load transformer breaking current	A	20																															
Rated single capacitor bank breaking current	A	500																															
Rated operating sequence		0 - 0.3 s - CO - 3 min. - CO/CO - 15 s - CO																															

TYPE		SL						S						LM															
		EGB 4 12-06F		EGB 4 12-12F		EGB 4 16-06F		EGB 4 16-12F		EGB 4 20-12F		EGB 5 08-06F		EGB 5 08-12F		EGB 5 12-06F		EGB 5 12-12F		EGB 5 16-06F		EGB 5 16-12F		EGB 5 25-12F		EGB 5 25-16F		EGB 5 25-25F	
Rated voltage	kV	24										36																	
Rated lightning impulse withstand voltage 1,2/50 μs	kV	125										170																	
Rated power frequency withstand voltage 1 min	kV	50										70																	
Rated normal current	A	630	1250	630	1250	630	1250	630	1250	630	1250	630	1250	630	1250	630	1250	630	1250	630	1250	1600	2500	1600	2500	1600	2500	1600	2500
Rated short circuit breaking current	kA	12,5				16				20				8				12,5				16				25			
Rated short circuit making current	kA	31,5				40				50				20				31,5				40				63			
Rated cable-charging breaking current	A	31,5										50																	
DC component	%	32																											
Rated no-load transformer breaking current	A	20																											
Rated single capacitor bank breaking current	A	500																											
Rated operating sequence		0 - 0.3 s - CO - 3 min. - CO/CO - 15 s - CO																											

Table 1: Range of types and technical features from the company which design SF6 circuit breaker.

ELİMSAN Şalt Cihazları ve Elektromekanik San. ve Tic. A.Ş.
 pb: 295 • Uzuntarla • İZMİT • Phone: +90 262 375 28 10 • Fax: +90 262 375 28 08
 e-mail: elimsanuretim @ elimsangroup.com

ELİ İthalat - İhracat ve Dış Tic. A.Ş.
 pb: 295 • Uzuntarla • İZMİT • Phone: +90 262 375 23 60 (pbx) • Fax: +90 262 375 23 22
 e-mail: eli @ elimsangroup.com

www.elimsangroup.com



The characteristics of the used grading capacitors in electric substations of 30 KV

Part Number	Rated Voltage kVdc	Rated Voltage kVrms	Test Voltage kVrms	Corona Inception Voltage (kVrms) (<10pc)	Capacitance ±20% (pF) ±10% on request	Dimensions millimeters (inches)				Packaging Unit
						Ø ± 1	d	L ± 1	H ± 2	
HP30EX0561M --	15	10	12	6	560	28 (1.100)	12 (0.472)	22 (0.866)	16 (0.630)	40
HP30EX0751M --					750	28 (1.100)	12 (0.472)			40
HP30EX0102M --					1000	28 (1.100)	12 (0.472)			40
HP40EX0152M --					1500	38 (1.500)	12 (0.472)			40
HP40EX0182M --					1800	38 (1.500)	12 (0.472)			40
HP40EX0202M --					2000	38 (1.500)	12 (0.472)			40
HP50EX0252M --					2500	48 (1.900)	12 (0.472)			45
HP50EX0272M --					2700	48 (1.900)	12 (0.472)			45
HP50EX0332M --					3300	48 (1.900)	12 (0.472)			45
HP60EX0372M --					3700	58 (2.283)	15 (0.591)			20
HP60EX0402M --					4000	58 (2.283)	15 (0.591)			20
HP60EX0502M --					5000	58 (2.283)	15 (0.591)			20
HP60EX0562M --					5600	58 (2.283)	15 (0.591)			20
HP30EY0501M --	20	15	18	9	500	28 (1.100)	12 (0.472)	24 (0.945)	18 (0.709)	40
HP30EY0561M --					560	28 (1.100)	12 (0.472)			40
HP30EY0751M --					750	28 (1.100)	12 (0.472)			40
HP40EY0102M --					1000	38 (1.500)	12 (0.472)			40
HP40EY0132M --					1300	38 (1.500)	12 (0.472)			40
HP40EY0152M --					1500	38 (1.500)	12 (0.472)			40
HP50EY0202M --					2000	48 (1.900)	12 (0.472)			45
HP50EY0222M --					2200	48 (1.900)	12 (0.472)			45
HP50EY0252M --					2500	48 (1.900)	12 (0.472)			45
HP60EY0302M --					3000	58 (2.283)	15 (0.591)			20
HP60EY0332M --					3300	58 (2.283)	15 (0.591)			20
HP60EY0372M --					3700	58 (2.283)	15 (0.591)			20
HP60EY0402M --					4000	58 (2.283)	15 (0.591)			20
HP30E30561M --	30	20	24	12	560	28 (1.100)	12 (0.472)	26 (1.024)	20 (0.787)	40
HP40E30821M --					820	38 (1.500)	12 (0.472)			40
HP40E30102M --					1000	38 (1.500)	12 (0.472)			40
HP40E31121M --					1120	38 (1.500)	12 (0.472)			40
HP50E30152M --					1500	48 (1.900)	12 (0.472)			45
HP50E30172M --					1700	48 (1.900)	12 (0.472)			45
HP50E30202M --					2000	48 (1.900)	12 (0.472)			45
HP60E30272M --					2700	58 (2.283)	15 (0.591)			20
HP60E30302M --					3000	58 (2.283)	15 (0.591)			20
HP60E30332M --					3300	58 (2.283)	15 (0.591)			20
HP30E40391M --	40	28	33	17	390	28 (1.100)	12 (0.472)	30 (1.180)	24 (0.945)	40
HP40E40751M --					750	38 (1.500)	12 (0.472)			40
HP50E40102M --					1000	48 (1.900)	12 (0.472)			30
HP50E40142M --					1400	48 (1.900)	12 (0.472)			30
HP60E40172M --					1700	58 (2.283)	15 (0.591)			20
HP60E40202M --					2000	58 (2.283)	15 (0.591)			20
HP60E40242M --					2400	58 (2.283)	15 (0.591)			20

Table 2: The parameters used in the substation indicated with a red color



People's Democratic Republic of Algeria
Ministry of Higher Education and Scientific Research
University M'Hamed BOUGARA – Boumerdes



Institute of Electrical and Electronic Engineering
Department of Power and Control

Final Year Project Report Presented in Partial Fulfilment of
the Requirements for the Degree of

MASTER

In Electrical and Electronic Engineering
Option: Power Engineering

Title:

**Mitigating Ferroresonance in MV Power
System Involving Power Transformer
and Circuit Breaker Capacitance using
Alternating Transient Program**

Presented by:

- **BEDDA ZEKRI Sad**
- **MEKKAOUI Tarek**

Supervisor:

Mrs.BOUTORA.S

Registration Number:...../2016

Dedication

On the occasion of finishing my final year project, it gives me immense pleasure to express my gratitude to:

*Who helped me to reach this degree, who I cannot live without them **My Mother** and **My Father**.*

As Allah the Highest says: “And lower to them the wing of humility out of mercy” and say, “My Lord, have mercy upon them as they brought me up when I was small.”

My uncles and My aunts

***My Brothers:** Abdelmounem, Ilyes, Foudil, Ziad and especially to my heart Ahmed.*

***My lovely Sister:** “Atika”.*

***My Future Wife:** “Sara”.*

***My Supervisor:** BOU TORAJA for her help, and all who learned me even a letter.*

***My Friends:** ((especially my roommates Khaled M, Oussama T and Med ramzi CH))
My partner and best friend Tarek MEKKA OUI
and others Ali K, Bilal G, Djilani G, Hamza Z, Khaled B, ... and the list is so long.*

With Love 🌸

SAD

Dedication

*All praise to Allah, today we fold the days' tiredness and the errand
summing up between the cover of this humble work,*

*To the utmost knowledge lighthouse, to our greatest and most honored
prophet Mohamed - May peace and grace from Allah be upon him-*

*To the spring that never stops giving, to my mother who weaves my
happiness with strings from her merciful heart... to my mother.*

(Mama and Yama)

*To whom he strives to bless comfort and welfare and never stints, what he
owns to push me in the success way who taught me to promote life stairs
wisely and patiently, to my dearest father.*

*To whose love flows in my veins and my heart always remembers them, to my
brothers and sisters.*

(Mustapha, M.ishak, Hadjer, Hibaallah and Halla)

*To those who taught us letters of gold and words of jewel of the utmost and
sweetest sentences in the whole knowledge. Who reworded to us their
knowledge simply and from their thoughts made a lighthouse guides us
through the knowledge and success path, To our honored teachers and
professors.*

*To my friends Abdullah, Bachir, Bader, Baki, Belgacem, Bilal, Chouaib,
djafer, Farouk, Hachimi, Mohammed, Hamza.Z, Hamza.H, Khaled,
Maki, Masouad, Nani, Nour eldine, Omer.G, Omer.B, Ridha, Sad,
Salem, Taher, Yacine, Yacine, Zakaria and the list is so long.*

With love

TAREK

Acknowledgment

We would like to express our very great appreciation to Mrs.BOUTORA.S, our supervisor, for her patient guidance, enthusiastic encouragement and useful critiques, and for her valuable and constructive suggestions during the planning and development of this search work. Her willingness to give her time so generously has been very much appreciated.

We would also like to extend our grateful thanks to our parents and friends for their invaluable support.

A great appreciation to the library supervisors for their help in providing us the references needed.

ABSTRACT

Ferroresonance is a phenomenon usually initiated by transients in power networks resulting from switching operations or ground faults or others. Nonlinear behavior of the core of a power transformer results in magnetic saturation. Long-lasting ferroresonant state is dangerous to the equipment due to prolonged overvoltage and large overcurrents in MV windings. In this thesis, a ferroresonance solution using Alternating Transient Program, was attempted. The ferroresonant oscillations analyzed result from interaction between the power transformer and a grading capacitance of a circuit breaker. Some practical solutions are suggested and introduced after creating a ferroresonance situation, they had a considerable effect on damping and eliminating the risk of ferroresonance.

TABLE OF CONTENTS

DEDICATION	I
ACKNOWLEDGMENT	III
ABSTRACT	IV
TABLE OF CONTENTS	V
LIST OF TABLES	VII
LIST OF FIGURES	VIII
GENERAL INTRODUCTION	1
CHAPTER 01: Identifying Ferroresonance Compared To Linear Resonance	
1.1. Introduction	2
1.2. Identifying Ferroresonance Compared To Linear Resonance	2
1.3. Conclusion	8
CHAPTER 02: Understanding Ferroresonance	
2.1. Introduction	9
2.2. Types of Ferroresonance Modes	9
2.2.1. Fundamental mode	9
2.2.2. Subharmonic mode	10
2.2.3. Quasi-periodic mode	10
2.2.4. Chaotic mode	11
2.3. Causes and Effects of Ferroresonance on Power Systems	11
2.3.1. Systems Vulnerable to Ferroresonance	12
2.3.1.1. Voltage Transformer Energized Through Grading Capacitance	12
2.3.1.2. Voltage Transformers Connected to an Isolated Neutral System	13
2.3.1.3. Voltage Transformers and HV/MV Transformers with Isolated Neutral	13
2.3.1.4. Transformer Supplied by a Highly Capacitive Power System with Low Short-Circuit Power	14
2.3.1.5. Transformer Accidentally Energized in Only One or Two Phases	15
2.3.1.6. Power system grounded through a reactor	16
2.3.2. Effect of Ferroresonance on Power Systems	17

2.4. Controlling Ferroresonance	18
2.4.1. Damping Ferroresonance in Voltage Transformers	19
2.4.1.1. Voltage Transformers with one Secondary Winding	19
2.4.1.2. Voltage Transformers with two Secondary Winding	19
2.4.2. Limiting the cable length switched	20
2.5 conclusion	20
CHAPTER 03: Simulation results	
3.1. Introduction	21
3.2. The electrical power network of Haoud Berkaoui	21
3.3. Highlights about Alternative Transient Program	22
3.3.1. What is ATP?	22
3.3.2. ATPDraw	22
3.4. The real electrical circuit of Haoud Berkaoui	23
3.4.1. Description of the circuit	23
3.4.2. The characteristics of the equipment used in the Substation	24
3.4.3. ATP simulation results	25
3.5. The Case study	27
3.5.1 The effect of changing grading capacitor (Cg)	27
3.6. Practical solution	36
3.6.1. increasing the value of shunt capacitance at the transformer primary side	36
3.6.2. installing a capacitor bank at the transformer secondary side	38
3.6.3. installing a damping resistor at the transformer secondary side	41
3.7. Conclusion	44
GENERAL CONCLUSION	45
REFERENCES	
APPENDIX	

LIST OF TABLES**CHAPTER 03: Simulation results**

Table 3.1: Ferroresonance simulations results summary of maximum overvoltage for C_g	34
Table 3.2: Simulation results of maximum overvoltage for shunt capacitors.....	36
Table 3.3: Simulation results of maximum overvoltage for bank capacitors.....	39
Table 3.4: Simulation results of maximum overvoltage for damping resistor.....	42

LIST OF FIGURES

CHAPTER 01: Identifying Ferroresonance Compared with Linear Resonance

Figure 1.1: Series LC Circuit with Sinusoidal Voltage Source	2
Figure 1.2: λ -I Characteristic for a linear inductor	2
Figure 1.3: Frequency Response of a Linear LC Circuit.....	3
Figure 1.4: λ -I Characteristic for a nonlinear inductance.....	3
Figure 1.5: Frequency Response of a Nonlinear LC Circuit.....	4
Figure 1.6: Jump phenomena for variation of the amplitude of the excitation.....	5
Figure 1.7: Ferroresonant Circuit.....	5
Figure 1.8: Graphical solution of the ferroresonance circuit.....	7

CHAPTER 02: Understanding Ferroresonance

Figure 2.1: Fundamental mode of ferroresonance.....	10
Figure 2.2: Subharmonic mode of ferroresonance.....	10
Figure 2.3: Quasi-periodic mode of ferroresonance.....	11
Figure 2.4: Chaotic mode of ferroresonance.....	12
Figure 2.5: Ferroresonance of a voltage transformer connected in series with an open circuit Breaker.....	12
Figure 2.6: Ferroresonance of a VT between phase and ground in an isolated neutral system.....	13
Figure 2.7: Faulty system.....	13
Figure 2.8: Ferro-resonance of voltage transformer between phase and ground with ungrounded/isolated neutral	14
Figure 2.9: Power transformer supplied by capacitive system.....	14
Figure 2.10: Examples of unbalanced systems.....	15
Figure 2.11: PIM inductance between neutral and ground.....	16
Figure 2.12: Resonant grounding system.....	16
Figure 2.13: Damping for voltage transformer with one secondary.....	19
Figure 2.14: Damping for voltage transformer with two secondaries.....	19

CHAPTER 03: Simulation results

Figure 3.1: the geographic location of Haoud Berkaoui.....	21
Figure 3.2: Main Window Multiple Circuit windows and the floating Selection menu.....	23
Figure 3.3: The one line diagram representation.....	24
Figure 3.4: ATPDraw representation of the circuit of Haoud Berkaoui station.....	25
Figure 3.5: The values of voltages at the point A	26
Figure 3.6: The values of voltages at the point TRS, B, C and D.....	26
Figure 3.7: Voltage transformer connected in series with an open circuit breaker.....	27
Figure 3.8: The ATP model circuit used for simulation.....	28

Figure 3.9: The voltages at point TRS with $C_g = 1\text{nF}$ and 100% V_s	28
Figure 3.10: The voltages at point TRS with $C_g = 600\text{nF}$ and 100% V_s	29
Figure 3.11: The voltages at point TRS with $C_g = 2\mu\text{F}$ and 100% V_s	29
Figure 3.12: The voltages at point TRS with $C_g = 5\mu\text{F}$ and 100% V_s	29
Figure 3.13: The voltages at point TRS with $C_g = 30\mu\text{F}$ and 100% V_s	30
Figure 3.14: The voltages at point TRS with $C_g = 1\text{nF}$ and 80% V_s	30
Figure 3.15: The voltages at point TRS with $C_g = 600\text{nF}$ and 80% V_s	31
Figure 3.16: The voltages at point TRS with $C_g = 2\mu\text{F}$ and 80% V_s	31
Figure 3.17: The voltages at point TRS with $C_g = 5\mu\text{F}$ and 80% V_s	31
Figure 3.18: The voltages at point TRS with $C_g = 30\mu\text{F}$ and 80% V_s	32
Figure 3.19: The voltages at point TRS with $C_g = 1\text{nF}$ and 120% V_s	32
Figure 3.20: The voltages at point TRS with $C_g = 600\text{nF}$ and 120% V_s	33
Figure 3.21: The voltages at point TRS with $C_g = 2\mu\text{F}$ and 120% V_s	33
Figure 3.22: The voltages at point TRS with $C_g = 5\mu\text{F}$ and 120% V_s	33
Figure 3.23: The voltages at point TRS with $C_g = 30\mu\text{F}$ and 120% V_s	34
Figure 3.24: The effect of the grading Capacitance on ferroresonance.	35
Figure 3.25: The effect of the Shunt Capacitance on ferroresonance.	36
Figure 3.26: The voltages at point TRS for Case 1 with $C_s = 0.5\mu\text{F}$	37
Figure 3.27: The voltages at point TRS for case 3 with $C_s = 2.7\mu\text{F}$	37
Figure 3.28: The voltages at point TRS for Case 5 with $C_s = 5\mu\text{F}$	37
Figure 3.29: Capacitor bank at the transformer TR1 secondary side.	38
Figure 3.30: The effect of the Bank Capacitance on ferroresonance.	39
Figure 3.31: The voltages at point TRS for Case 1 with $C_b = 10\mu\text{F}$	40
Figure 3.32: The voltages at point TRS for Case 4 with $C_b = 49\mu\text{F}$	40
Figure 3.33: The voltages at point TRS for Case 7 with $C_b = 100\mu\text{F}$	40
Figure 3.34: The damping resistor at the transformer TR1 secondary side.	41
Figure 3.35: The effect of the Damping resistor on ferroresonance.	42
Figure 3.36: The voltages at point TRS for Case 5 with $R = 30\Omega$	43
Figure 3.37: The voltages at point TRS for Case 4 with $R = 25\Omega$	43
Figure 3.38: The voltages at point TRS for Case 1 with $R = 12\Omega$	43

GENERAL INTRODUCTION

GENERAL INTRODUCTION

Power quality and power disturbances have become an important increasing factor throughout electrical networks. Ferroresonance is one of these disturbances that can occur on distribution systems, causing quality and security problems.

Ferroresonance is a non-linear resonance phenomenon that can affect power networks. The abnormal rates of harmonics and transients or steady state overvoltages and overcurrents that it causes are often dangerous for electrical equipment.

The term “Ferroresonance”, which appeared in the literature for the first time in 1920, refers to all oscillating phenomena occurring in an electric circuit which must contain at least:

- 1) a non-linear inductance (ferromagnetic and saturable).
- 2) a capacitor.
- 3) a voltage source (generally sinusoidal).
- 4) low losses. [1]

Power networks are made up of a large number of saturable inductances (power transformers, voltage measurement inductive transformers (VT), shunt reactors), as well as capacitors (cables, long lines, capacitor voltage transformers, series or shunt capacitor banks, voltage grading capacitors in circuit-breakers, metalclad substations). They thus present scenarios under which ferroresonance can occur. [1]

The aim of this thesis is to identify ferroresonance and to understand it better, when it is compared to linear LC resonance. Also to describe the effects of ferroresonance on power systems, because they are considered to be catastrophic when they occur, in addition the methods of mitigating them will be discussed.

In order to demonstrate the achievement of the stated aim, we strengthen our study with simulation of one of favorable cases of this phenomenon, which is the interaction between the power transformer and circuit breaker grading capacitor in MV power system, then we try to find some practical solutions.

Chapter 1

Identifying Ferroresonance Compared To Linear Resonance

1.1. Introduction

The trend toward using higher distribution voltages and underground feeders has increased the number of instances in which ferroresonance overvoltage have been reported. [2] The problem of ferroresonance can be categorized as a nonlinear resonance which can cause damage in power distribution and transmission systems. In simple terms, ferroresonance is an LC resonance involving a nonlinear inductance and a capacitance. [3] Ferroresonance can be better understood if it is compared to linear LC resonance.

1.2. Identifying Ferroresonance Compared to Linear Resonance

A typical linear LC resonant circuit consists of an ideal inductor connected in parallel or series with an ideal capacitor. There is no damping in the circuit and the behavior of this LC combination is observed as the frequency of an applied sinusoidal voltage or current is varied. Figure 1.1 shows an example of a series LC circuit with linear elements. In this circuit L is constant and independent of current, regardless of the flux linked λ by the inductor. The relationship between the flux and the current is shown in the Figure 1.2. [3]

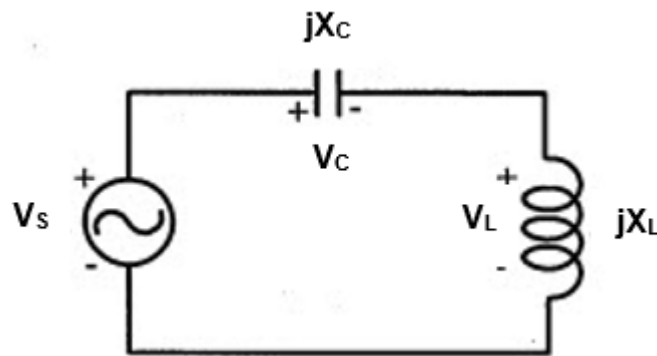


Figure 1.1: Series LC Circuit with Sinusoidal Voltage Source

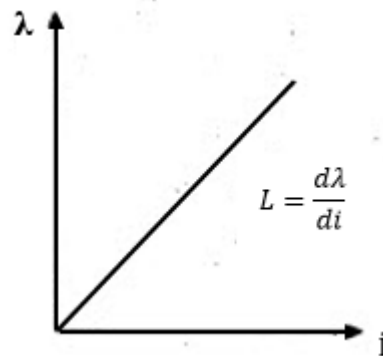


Figure 1.2: λ - i Characteristic for a linear inductor

In this circuit, the resonance occurs when the total impedance of the circuit $jX_L - jX_C$ equal to zero. The frequency at which this happens is $\omega_r = \frac{1}{\sqrt{LC}}$. Therefore as ω approaches ω_r , current i approaches ∞

Figure 1.3 shows the frequency response of a linear LC circuit. [3]

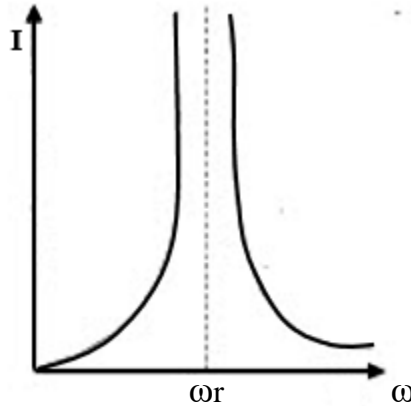


Figure 1.3: Frequency Response of a Linear LC Circuit

If damping is considered as a resistance in parallel with the inductor in the above case, the current will be limited to $i < \infty$ and the resonant frequency will be shifted to a new damped resonant frequency to $\omega = \omega_d$.

In the circuit of figure 1.1, if the linear inductance is replaced with a nonlinear saturable iron core inductor then ferroresonance can occur. A typical λ - i characteristic of such an inductor is shown in figure 1.4 which is typical for a transformer core. [3]

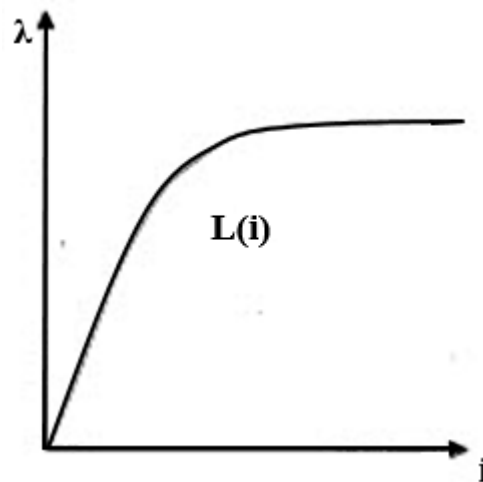


Figure 1.4: λ - i Characteristic for a nonlinear inductance

The circuit with a nonlinear inductance will have a much different type of frequency response. In this case, there is no single resonant frequency, since the frequency response characteristic will be multi-

valued. [3] Figure 1.5 shows the frequency response of a nonlinear LC circuit when there is no damping in the system.

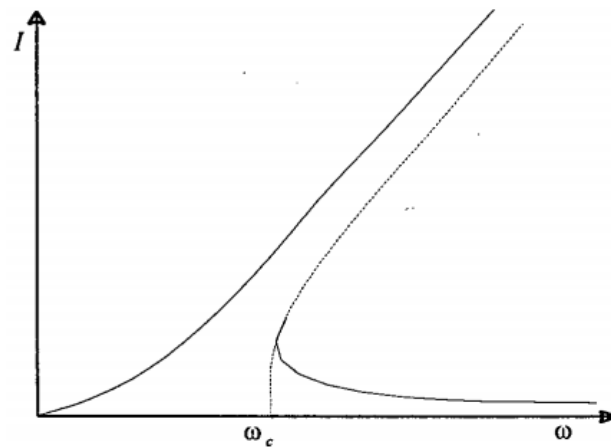


Figure 1.5: Frequency Response of a Nonlinear LC Circuit

- For $\omega > \omega_c$, there may be two stable modes of “Resonance” as well as a third unstable mode.
- For $\omega < \omega_c$ there is only one possible mode of operation.

As ω is decreased and its value passes ω_c , operation can make a sudden change or jump from one stable operating mode to another. This is one of the reasons why this type of behavior is sometimes called jump resonance.

Therefore, jump resonance refers to a condition in a sinusoidally excited system where an incremental change in the frequency of the input to the system or an incremental change in the driving voltage or in the magnitude of one of the parameters of the system causes a sudden jump in signal amplitude somewhere in the system. This jump can be one of voltage, current, flux linkage or all three.

Figure 1.6 shows the jump phenomenon when the amplitude of the excitation is varied slowly. In this diagram the effect of the damping is considered. In this figure, starting from point 1, as V_s is increased, V_L slowly increases through point 2 to point 3. As V_s is increased further, a jump takes place from point 3 to point 4 with an accompanying increase in V_L , after which V_L increases slowly with V_s . If the process is reversed, V_L decreases slowly as V_s decreases from point 5 to point 6. As V_s is decreased further, a jump from point 6 to point 2 takes place, with an accompanying decrease in V_L , after which V_L decreases slowly with decreasing V_s . Rudenberg gives a very clear explanation of this jump phenomenon based on a graphical method. [3]

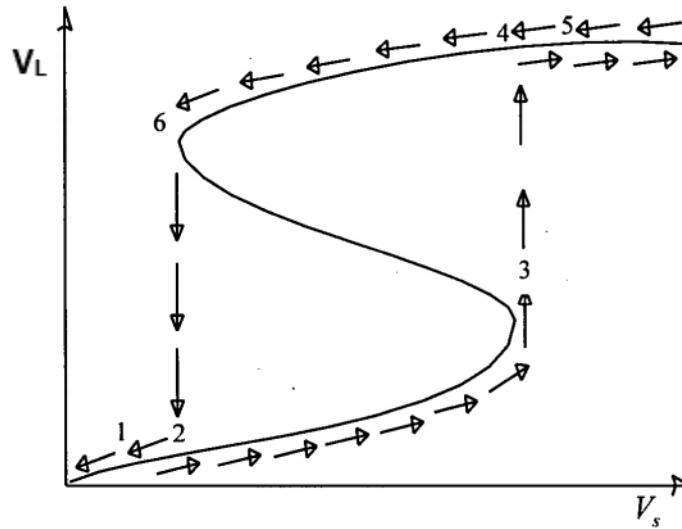


Figure 1.6: Jump phenomena for variation of the amplitude of the excitation

Consider the circuit of Figure 1.7, in which the linear inductance has been replaced with a nonlinear inductor

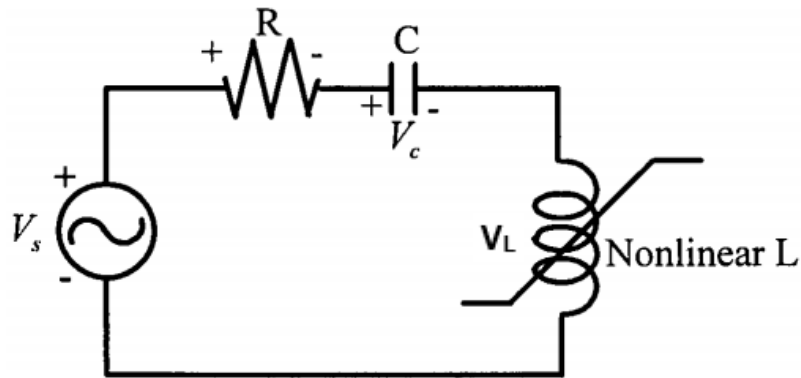


Figure 1.7: Ferroresonant Circuit

When the series resistance is ignored, the sum of the voltages around the only mesh of the circuit can be written as:

$$V_s(t) - V_c(t) - V_L(t) = 0 \quad (1.1)$$

The value of V_c can be replaced by its time-integral expression and V_L as the total derivative of $L(i)i(t)$. Then equation 1.1 can be written as:

$$V_s(t) - \frac{1}{C} \int i(t) dt - \frac{d}{dt} [L(i)i(t)] = 0 \quad (1.2)$$

Evaluating equation 1.2 and substituting $q(t) = \int i(t) dt$ will result in:

$$V_s(t) - \frac{1}{C}q(t) - L(i)\frac{d^2q(t)}{dt^2} - \frac{dq(t)}{dt}\frac{dL(i)}{di(t)} = 0 \quad (1.3)$$

From equation 1.3 it is evident that finding a closed-form solution for this nonlinear circuit will be quite difficult. This would be made more evident by adding a source impedance and by providing a complete equivalent of the transformer. Historically, methods of graphical solution represent one of the earliest attempts to explain ferroresonance. The graphical solution for the circuit of Figure 1.7, including the series resistance, can be obtained from two independent relationships for the voltage across the inductance and the capacitance. (Assuming sinusoidal variation of current). The voltage across the inductor is proportional to the frequency, and the voltage across the capacitance is proportional to the current and inversely proportional to the frequency and capacitance.

$$\begin{aligned} V_L &= \omega f(i) \\ V_C &= -\frac{I}{\omega C} \end{aligned} \quad (1.4)$$

The total magnitude of voltage for the circuit is:

$$V_s = \sqrt{(V_L + V_C)^2 + (RI)^2} \quad (1.5)$$

From equations 1.4 and 1.5, the voltage across the nonlinear inductor can be written as:

$$V_L = \sqrt{V_s^2 - (RI)^2} + \frac{I}{\omega C} \quad (1.6)$$

The first term in the right-hand side of Equation 1.6 $\sqrt{V_s^2 - (RI)^2}$ represents an ellipse whose main axes have the magnitude of V_s , and $\frac{V_s}{R}$ and the second term is a straight line having slope of $\frac{I}{\omega C}$. Adding these two quantities represents an oblique ellipse, whose intersection with the characteristic of V_L presents the three possible states of the oscillation of the circuit. Figure 1.8 shows the graphical solution for the ferroresonance circuit of Figure 1.7.

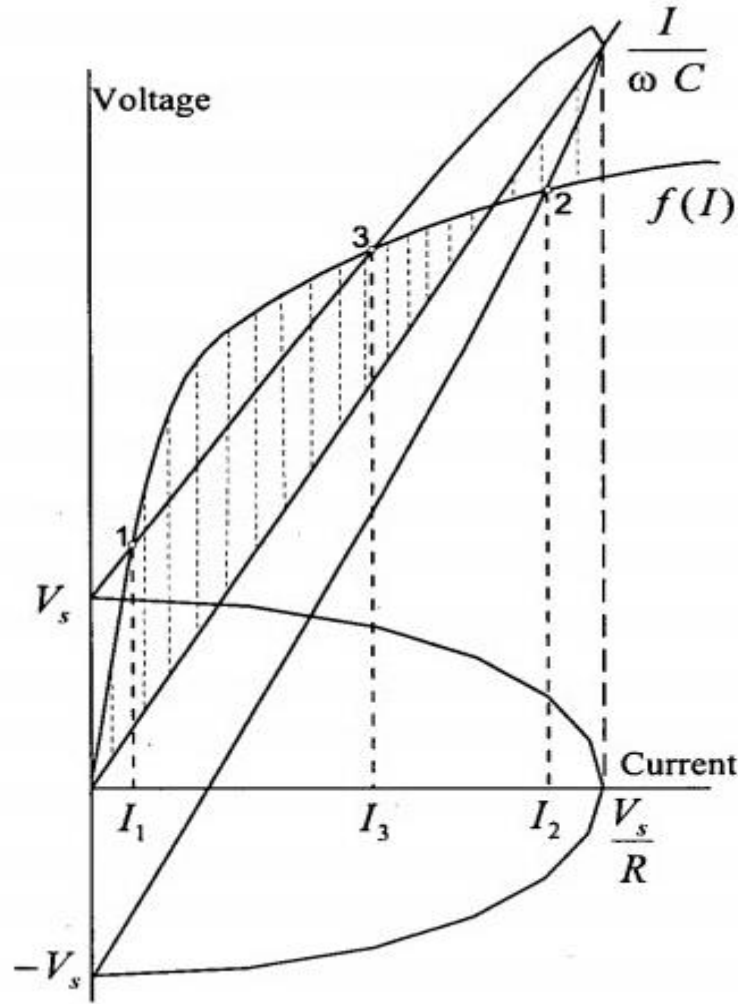


Figure 1.8: Graphical solution of the ferroresonance circuit

Points 1 and 2 in the Figure 1.8 represent the stable solutions, whereas point 3 represents an unstable solution. To show this, rewrite Equation 1.6 as:

$$(IR)^2 = V_s^2 - \left[f(I) - \frac{I}{\omega C} \right]^2 \quad (1.7)$$

If the quantity $\left[f(I) - \frac{I}{\omega C} \right]$ increases in magnitude with an increase in current, then according to equation 1.7, $(RI)^2$ tends to decrease, and this suppresses any further increase in current.

Thus stability is achieved. However, if the quantity $\left[f(I) - \frac{I}{\omega C} \right]$ decreases in magnitude, with an increase of current, the magnitude of $(RI)^2$ tends to increase and under this condition, the current continues to increase and the solution is unstable.

The dashed area in the Figure 1.8 shows the variation of the magnitude of $\left[f(I) - \frac{I}{\omega C}\right]$. And point 3 in corresponds to an unstable solution since $\left[f(I) - \frac{I}{\omega C}\right]$ decreases with an increase of current. In the same figure, points 1 and 2 represent the stable solutions. [3]

1.3. Conclusion

Therefore, we can conclude that the ferroresonance is a complex phenomenon in which there are several steady states for a given circuit, the appearance of these states is highly sensitive to system parameters values and the initial conditions. Small variations in a system parameters or a transient may cause a sudden jump between two very different steady states and initiate one of the ferroresonance modes. These modes will be discussed in next chapter with the causes of this phenomenon, and its effects on power system, then how to control it to prevent its happening.

Chapter 2

Understanding Ferroresonance

2.1. Introduction

In the previous chapter, the discriminative difference between the linear resonance and ferroresonance has been described. This chapter introduces types of ferroresonance modes, there are several modes of ferroresonance with varying physical and electrical displays, some have very high voltages and currents while others have voltages close to normal. In addition, it describes the effects of ferroresonance on power systems. Because they are considered to be catastrophic when they occur, finally the methods of mitigating them will be discussed.

2.2. Types of Ferroresonance Modes

All experience of waveforms appearing on power systems, experiments conducted on reduced system models together with numerical simulations, enable classification of ferroresonance states into four different types. This classification corresponds to the steady state condition, i.e. once the transient state is over, as it is difficult for a ferroresonant circuit to distinguish the normal transient state from ferroresonant transient states. However, this in no way implies that transient ferroresonance phenomena do not present a risk for electrical equipment. Dangerous transient overvoltages can occur during several system periods after an event (for example energizing of an unloaded transformer) and persist for several power system cycles. Basically, there are four types of steady-state responses, a ferroresonance circuit can possibly have, they are the fundamental mode, subharmonic mode, quasi-periodic mode and chaotic mode. [1] Each of the classifications and its characteristics are depicted in from Figure 2.1 to Figure 2.4.

The type of ferroresonance can be identified either by the spectrum of the current and voltage signals, or by a stroboscopic image obtained by measuring current I and voltage V at a given point of the system and by plotting in plane v, i the instantaneous values at instants separated by a system period. [1]

2.2.1. Fundamental mode

The periodic response has the same period, T as the power system. The frequency spectrum of the signals consists of fundamental frequency component as the dominant one followed by decreasing contents of 3rd, 5th, 7th and n^{th} odd harmonic. In addition, this type of response can also be identified by using the stroboscopic diagram of Figure 2.1 (c) which is also known as Poincarè plot, which can be obtained by simultaneously sampling of voltage, v and current, i at the fundamental frequency. [4] Figure 2.1 below shows the diagrams to explain fundamental mode.

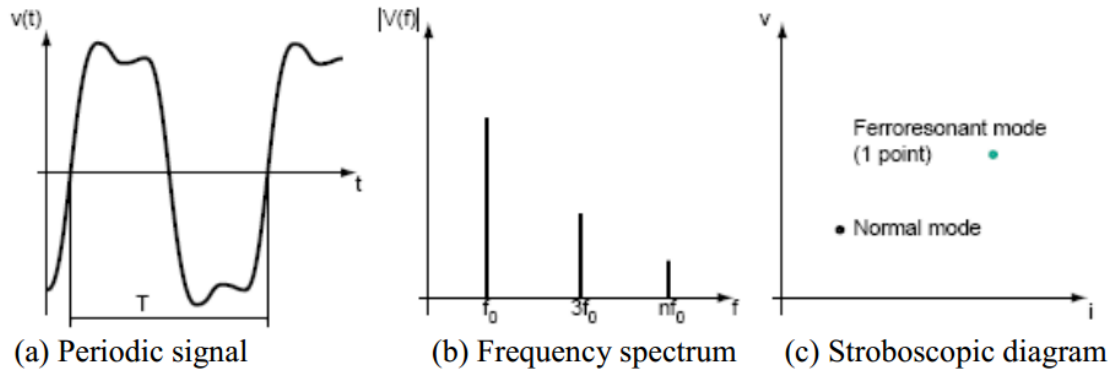


Figure 2.1: Fundamental mode of ferroresonance.

2.2.2. Subharmonic mode

In this type of ferroresonance signals has a period which is multiple of the source period, nT . The fundamental mode of ferroresonance is normally called a Period-1 (i.e. $f_0/1$ Hz) ferroresonance and a ferroresonance with a sub-multiple of the power system frequency is called a Period- n (i.e. f_0/n Hz) ferroresonance. Alternatively, the frequency contents are described having a spectrum of frequencies equal to f_0/n with f_0 denoting the fundamental frequency and n is an integer. With this signal, there are n points exist in the stroboscopic diagram which signifies predominant of fundamental frequency component with decreasing harmonic contents at other frequencies. [4] Figure 2.2 below shows the diagrams to explain Subharmonic mode.

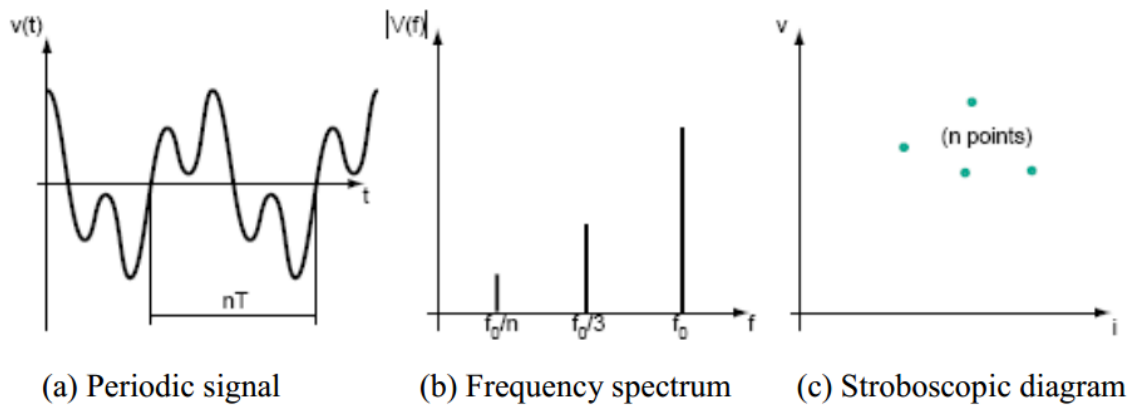


Figure 2.2: Subharmonic mode of ferroresonance.

2.2.3. Quasi-periodic mode

This kind of signal is not periodic. The frequency contents in the signal are discontinuous in the frequency spectrum, whose frequencies are defined as: $nf_1 + mf_2$ (where n and m are integers and f_1/f_2 an irrational real number). This type of response displays a feature employing a close cycle of dotted points on the stroboscopic plot.

The set of points (closed curve) in the diagram is called an attractor to which all close by orbits will asymptotically approach as $t \rightarrow \infty$, that is, in the steady state. [5] Figure 2.3 below shows the diagrams to explain Quasi-periodic mode.

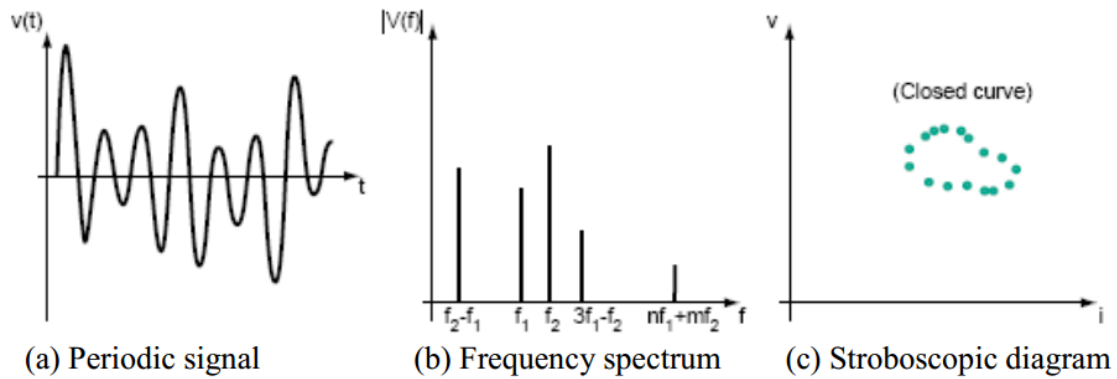


Figure 2.3: Quasi-periodic mode of ferroresonance.

2.2.4. Chaotic mode

This mode has a signal exhibiting non-periodic with a continuous frequency spectrum i.e. it is not cancelled for any frequency. The stroboscopic plot consists of n points surrounding an area known as the strange attractor which appears to skip around randomly. [4] Figure 2.4 below shows the diagrams to explain Chaotic mode.

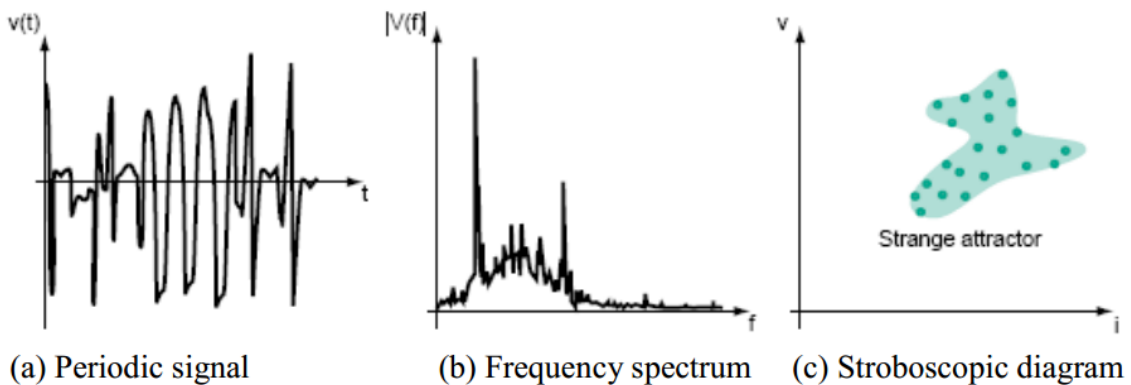


Figure 2.4: Chaotic mode of ferroresonance.

2.3. Causes and Effects of Ferroresonance on Power Systems

In the preceding section, the characteristics and features of each of the four distinctive ferroresonance modes have been highlighted. In this section we will focus firstly on causes of ferroresonance which are many but they can be generalized as below:

- Transients.
- Phase-to-ground , phase-to-phase faults.
- Circuit breaker opening and closing.
- Transformer energizing and de-energizing.

The main cause of ferroresonance cannot be known beforehand and it is generally found out by analyzing events in the power system prior to ferroresonant oscillations. [1] In addition, ferroresonance can cause undesirable effects on power system components which will be discussed.

2.3.1. Systems Vulnerable to Ferroresonance

In the modern power systems, there are many sources of capacitances, nonlinear inductances and wide range of operating setups. Configurations that may allow ferroresonance to happen are endless. But there are some typical configurations that may lead to ferroresonance. [1]

2.3.1.1. Voltage Transformer Energized Through Grading Capacitance

Switching operations may cause ferroresonance in voltage transformers which are connected between phases and ground. A sample case is illustrated in figure 2.5; Opening of circuit breaker D started ferroresonance by causing capacitance C (all the capacitances to ground) to discharge through voltage transformer. Through grading capacitance C_d , source delivers enough energy to maintain oscillation. [1]

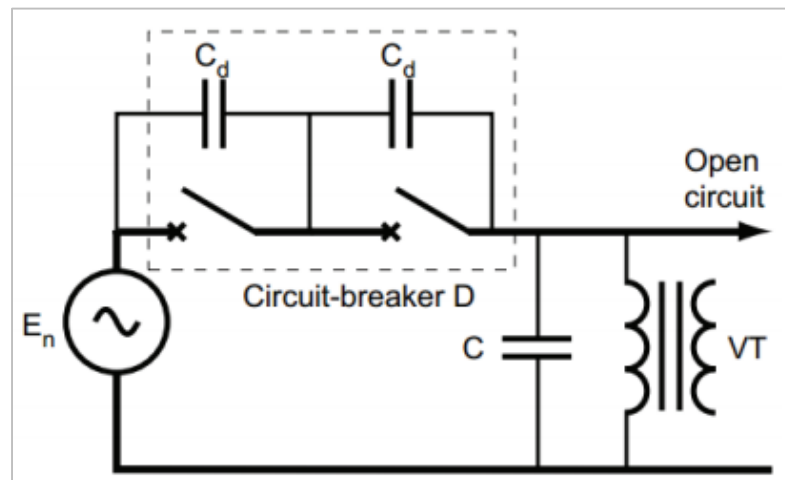


Figure 2.5: Ferroresonance of a voltage transformer connected in series with an open circuit breaker

2.3.1.2. Voltage Transformers Connected to an Isolated Neutral System

Transients due to switching operations or ground faults may start ferroresonance by saturating iron core of voltage transformers shown in figure 2.6. This grounding system can be chosen on purpose or the system can become neutral isolated from a loss of system grounding due to different reasons. A system operator may think there is a phase-to-ground fault in the system because of neutral point displacement and potential rise respect to ground on one or two phases. [1]

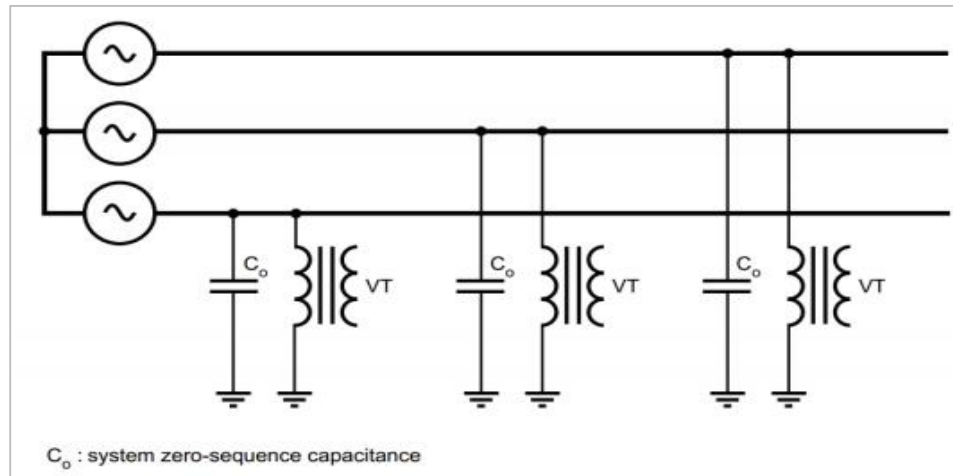


Figure 2.6: Ferroresonance of a VT between phase and ground in an isolated neutral system

2.3.1.3. Voltage Transformers and HV/MV Transformers with Isolated Neutral

There is possibility of ferroresonance when HV and MV neutrals are ungrounded. When a ground fault happens in HV side, high potential is obtained at HV neutral point. With the help of capacitive effect between primary and secondary, over-voltages appears on MV side. [1] Conditions for ferroresonance is formed with voltage source E_0 , capacitances C_e and C_0 and magnetizing inductance of a voltage transformer in figure 2.7 and figure 2.8.

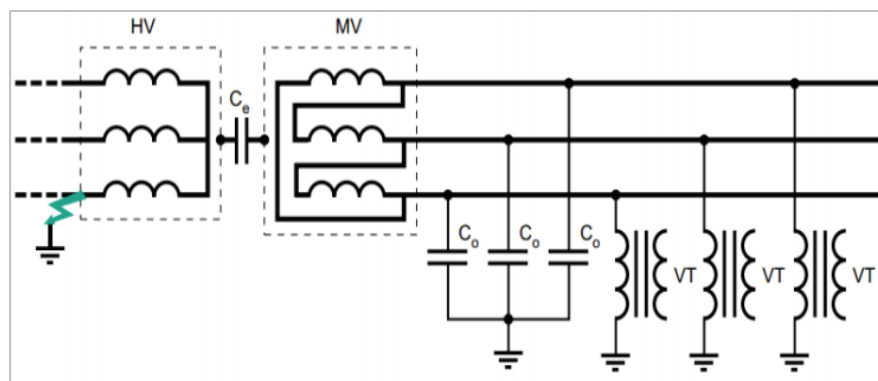


Figure 2.7: Faulty system

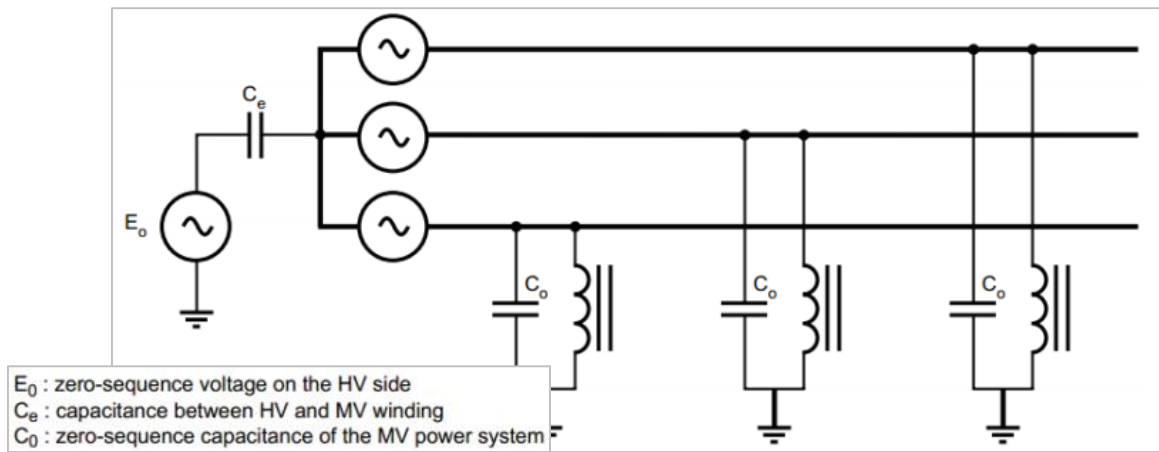


Figure 2.8: Ferro-resonance of voltage transformer between phase and ground with ungrounded/isolated neutral

2.3.1.4. Transformer Supplied by a Highly Capacitive Power System with Low Short-Circuit Power

As shown in figure 2.9 when an unloaded power transformer is connected to a relatively low short-circuit power source through underground cable or long overhead line, ferroresonance may happen. [1]

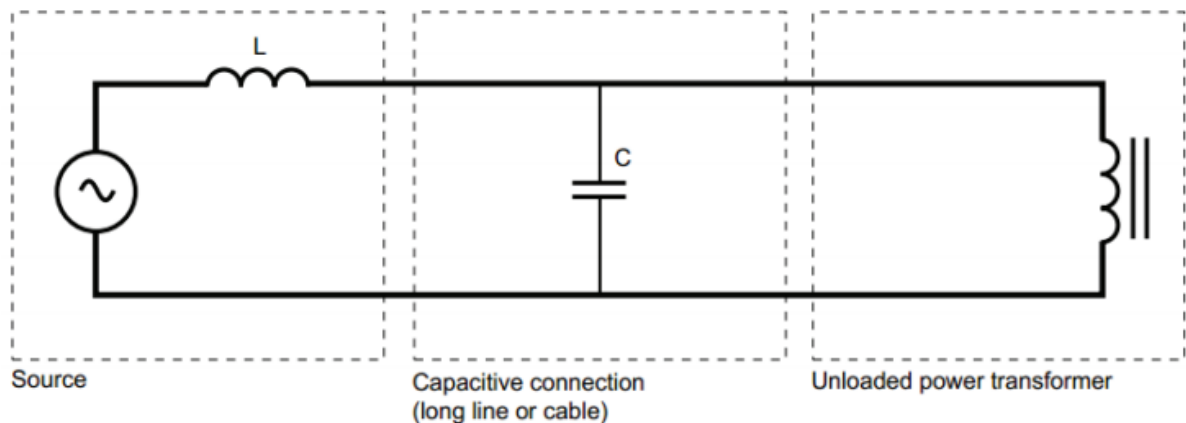


Figure 2.9: Power transformer supplied by capacitive system

With the experience from the past, it is concluded that system with features below are in danger of ferroresonance [1];

- Voltage transformer connected between phase and ground on an isolated neutral system
- Transformer fed through capacitive lines
- Non-multi pole breaking
- Unloaded or lightly loaded voltage transformers

2.3.1.5. Transformer Accidentally Energized in Only One or Two Phases

These setups can happen when one or two of the source phases are disconnected while the transformer is lightly loaded. System capacitances in figure 2.10 may consist of underground cables or overhead lines. Primary of the transformers can be delta connected or wye connected with isolated or grounded neutral. Because of switching operations, ferroresonant configurations are formed. Factors that are relevant is given below [1];

- Phase-to-phase and phase-to-ground capacitances
- Primary and secondary windings connections
- Voltage source grounding

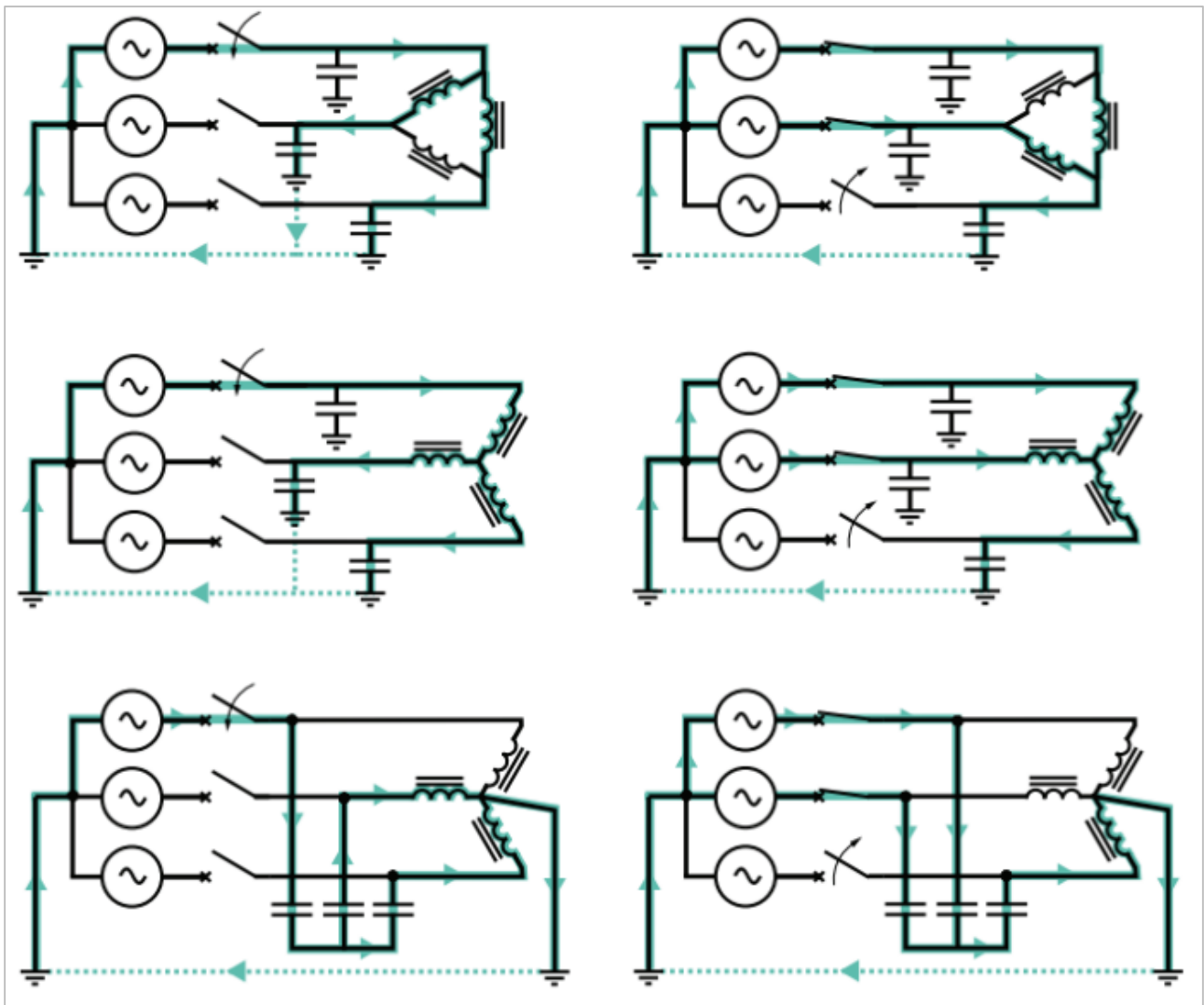


Figure 2.10: Examples of unbalanced systems

2.3.1.6. Powersystem grounded through a reactor

In LV systems, Permanent Insulation Monitors (PIMs) are used to measure insulation impedance by injecting direct current between system and ground. Their impedance is inductive and it may contribute to ferroresonance oscillations. Any potential rise in neutral point may cause ferroresonance between inductance of PIM and capacitances of the system. [1]

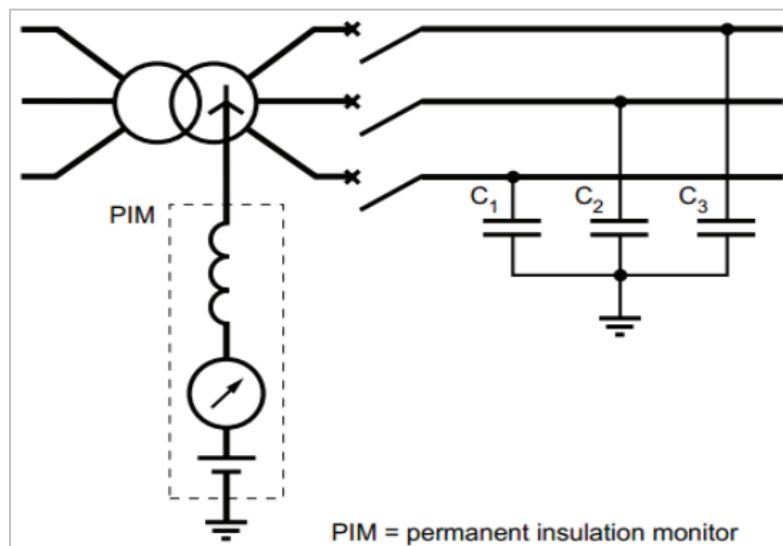


Figure 2.11: PIM inductance between neutral and ground

In MV systems, a coil of inductance L is used between MV neutral of a HV/MV transformer and ground to limit ground fault currents. Excitation of ferroresonance of the circuit consisting inductance L and zero-sequence capacitances may happen because of natural dissymmetry of transformer and capacitances shown in figure 2.12. [1]

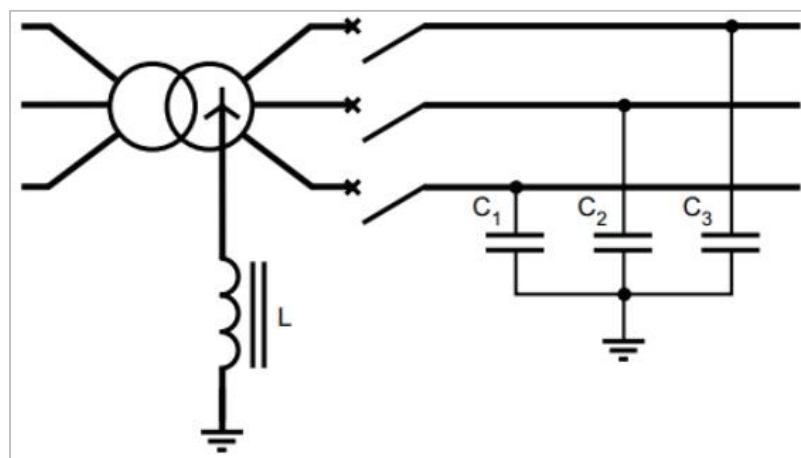


Figure 2.12: Resonant grounding system

2.3.2. Effects of Ferroresonance on Power Systems

As it may be seen hereinafter, due to the different factors involved in the ferroresonance phenomenon, when it occurs the situation can be rather disconcerting. That is why it is so important to identify the most common symptoms of a ferroresonance situation which are summarized as follows:

- High permanent over voltages of differential mode (phase-to-phase).
- High permanent over currents.
- High permanent distortions of voltage and current waveforms.
- Displacement of the neutral point voltage.
- Transformer heating.
- Loud noise in transformers and reactances.
- Damage of electrical equipments (capacitor banks, voltage transformers etc...).
- Untimely tripping of protection devices.

Some of the effects are not only special to ferroresonance; an initial analysis can be done by looking at voltage waveforms. If it is not possible to obtain recordings or if there are possible interpretations for effects, not only system configuration should be checked but also events prior to ferroresonance. Following step is to determine if three conditions are met in order ferroresonance to happen;

- Co-existence of capacitances and non-linear inductances
- Existence of a point whose potential is not fixed (isolated neutral, single phase switching)
- Lightly loaded system (unloaded power or voltage transformers)

If any of these conditions are not met, ferroresonance is said to be very unlikely [1].

In reference [6], ferroresonance occurred because of switching operations during commissioning new 400-kV substation where grading capacitance of a circuit breaker involved. It is reported that two voltage transformers are driven into sustained ferroresonance state. Ferroresonance experienced in Station Service Transformer during switching operations by firstly opening the circuit breaker and then the disconnecter switch located at the riser pole surge arrester [7]. Oscillations caused explosion of surge arrester.

In reference [8], explosion of a voltage transformer is reported. One of the buses was removed because of installing of new circuit breaker and current transformer, at the same time maintenance and line trip testing were conducted. Voltage transformers on the de-energized bus were energized by near on-operation bus bar through grading capacitors.

2.4. Controlling Ferroresonance

According to CIGRE technical brochure no. 569, mitigation techniques applicable to the power transformer are grouped into three basic approaches [18]:

- Avoid circuit parameters or operating conditions favouring ferroresonance
- Minimize the energy transfer that is required to sustain the ferroresonant oscillations
- Control the duration of ferroresonance by the operational switching

Based on these approaches, four kinds of the mitigation techniques are derived as follows:

- (a) An increase of the capacity of shunt capacitance at the transformer primary side.
- (b) An insertion of the capacitor bank at the transformer secondary side.
- (c) An installation of the resistive load bank at the transformer secondary side.
- (d) A change of the transformer saturation characteristics with the low flux density.

International standards state that resonance over voltages should be prevented or limited, those voltage values cannot be taken basis for insulation design. So in theory, current design of insulations and surge arresters do not provide protection against ferroresonance [9].

There are some researches on dynamical damping of ferroresonance, prototypes are introduced [10], [11] but the most common used practice is static damping with damping resistors.

In case of power transformers whose are fed through capacitive lines, the best solution proposed is avoiding risky situations when active power delivery is less than 10% of the transformer rated power [1]

For configurations in figure 2.10, following practical solutions are advised [1];

- Lowering capacitance between circuit breaker and transformer
- Avoiding use of transformers at 10% of its rated capacity
- Avoiding no-load energizing
- Prohibiting single-phase operations

For MV power systems grounded through a reactor figure 2.12, overcompensation of power frequency capacitance component of the ground fault current can be done or a resistive component to increase losses can also be added [1].

2.4.1. Damping Ferroresonance in Voltage Transformers

As mentioned before, voltage transformers connected between phase and ground in neutral isolated systems is dangerous for ferroresonance oscillations to happen. It is advised that avoid wye-connections of voltage transformer primaries with grounded neutral by leaving neutral of primaries ungrounded or using delta connection instead [12], [13]. If wye-connection for primaries is used, only way left to damp a possible oscillation is to introduce load resistances.

2.4.1.1. Voltage Transformers with one Secondary Winding

Even though resistors will consume power during operation, damping resistors are used to damp possible ferroresonant oscillations in figure 2.13. Recommended minimum values of resistance R and power rating of resistor P_R are calculated with rated values of transformer in (2.1) and (2.2) [13], [1].

$$R = \frac{U_s^2}{k \cdot P_t - P_m} \quad \text{..... (2.1)}$$

$$P_R = \frac{U_s^2}{R} \quad \text{..... (2.2)}$$

where; U_s : rated secondary voltage (V)

k : factor between 0.25 and 1 regarding errors and service conditions

P_t : voltage transformer's rated output (VA)

P_m : power required for measurement (VA)

2.4.1.2. Voltage Transformers with two Secondary Windings

There is also an option to have two secondaries in voltage transformers. One is for measurement and second one is especially for damping (tertiary winding). The advantage to have damping resistors in the open delta connected secondary winding is that it is only active during unbalanced operation. During the balanced operation no current circulates in open delta. Recommended minimum values of resistance R and power rating of resistor P_R are calculated with rated values of transformer in (2.3) and (2.4) [13], [1].

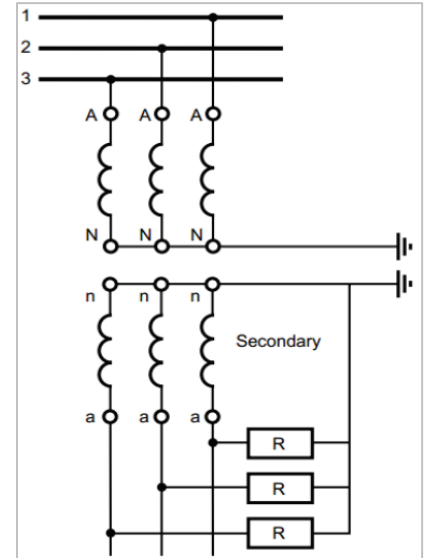


Figure 2.13: Damping for voltage transformer with one secondary.

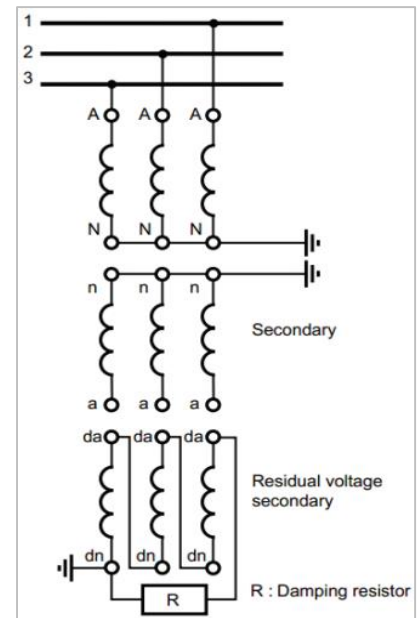


Figure 2.14: Damping for voltage transformer with two secondaries.

$$R = \frac{3\sqrt{3} U_s^2}{P_e} \dots\dots\dots (2.3)$$

$$P_R = \frac{(3U_s)^2}{R} \dots\dots\dots (2.4)$$

where; **Us**: rated voltage of the tertiary winding (V)

Pe: rated thermal burden of tertiary winding (VA) is the apparent power than voltage transformer can supply without exceeding thermal constraints.

2.4.2. Limiting the cable length switched

Limiting the cable length to be less than the length established by the Baitch Ferroresonance Critical Cable Length will limit the overvoltage that may occur to $(1 + \sqrt{3})$ times phase-to-earth voltage. The effect of iron losses will tend to result in the overvoltage being less than $(1 + \sqrt{3})$ times phase-to-earth voltage.

There are some issues on ferroresonance as follows:

- Isolating a power transformer from the grid during ferroresonance oscillations using a disconnector between the transformer and the circuit breaker
- Effectiveness of surge arresters for the actual ferroresonance.
- Varying residual flux of the iron core in a power transformer

2.5 conclusion

At the end of this chapter, the appearance of various types of ferroresonance oscillations in a power system was presented. Then we have discussed some typical configurations that may lead to destructive effects that make us care about it and looking hardly for controlling it. In the next chapter we will analyze and make simulation to the first vulnerable configuration to this phenomenon in section 2.3.1.1 using ATP program trying to damp it.

Chapter 3

Simulation results

3.1. Introduction

In practice the ferroresonant oscillations may be initiated by momentary saturation the core of the inductive element resulting from e.g. switching operation or other type of event resulting in a transient overvoltage in the system. The undamped ferroresonant oscillations in power system are dangerous to the equipment installed due to large overcurrents and/or overvoltages which may ultimately lead to permanent equipment damage. [14]

In this chapter numerical simulations of the ferroresonance phenomenon in the MV inductive voltage transformer are presented. The ferroresonant oscillations analyzed result from interaction between the voltage transformer and a grading capacitance of a circuit breaker. [14] our simulation will be analyzed on electrical power network of Haoud Berkaoui using Alternative Transient Program.

3.2. The electrical power network of Haoud Berkaoui

The region of Haoud Berkaoui represents one of ten principles hydrocarbons productive zones of Algerian desert. It is situated at 35 Km to south west of Wilaya of Ouregla. Figure 3.1 shows the geographic location of Haoud Berkaoui. [15]

The electrical power network implemented by Schneider Electric as part of the electrification project of Haoud Berkaoui is composed of three high-voltage substations. Which are located in Guellala, Haoud Berkaoui and Benkahla; they are powered by 60kV from the Algerian national electricity company Sonelgaz. Each substation is composed of control buildings, premises and equipment home building separate GIS and thus protecting the metal-clad high-voltage SF6. The transformers are located outside the boxes in walls separated by firewalls.[15]

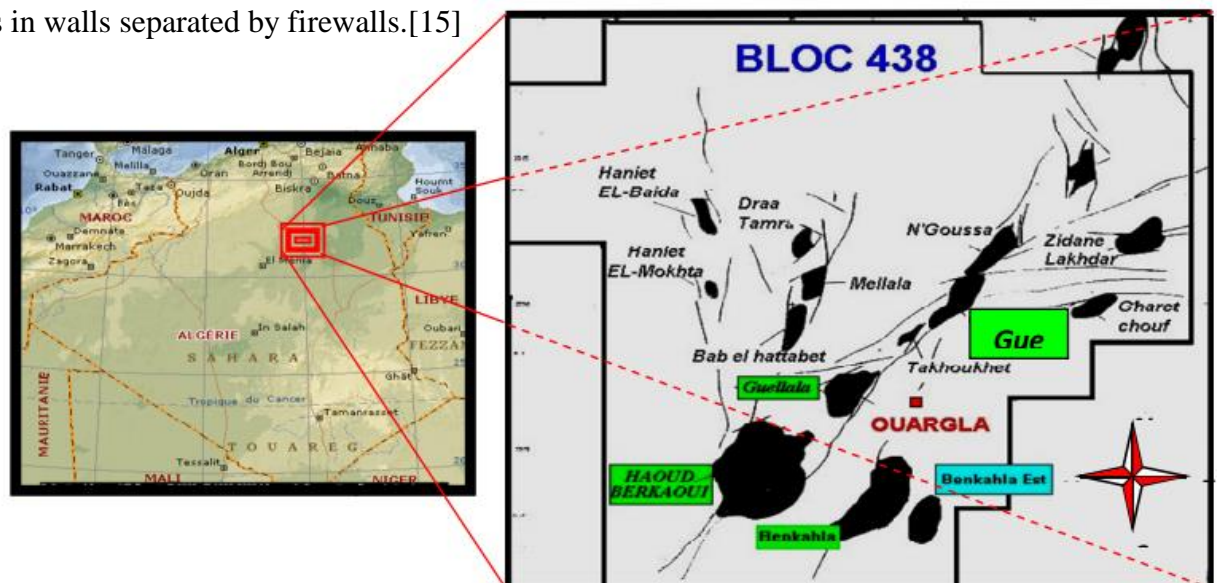


Figure 3.1: the geographic location of Haoud Berkaoui.

3.3. Highlights about Alternative Transient Program

Transient analysis of electrical circuits is as important as steady-state analysis. When transients occur, the currents and voltages in some parts of the circuit may many times exceed those that exist in normal behavior and may destroy the circuit equipment in its proper operation. A number of simulation tools have been developed in the last few years, especially for steady state simulations. Few programs are able to accurately determine the response of a system to a transient; one of these programs is ATP. [16]

3.3.1. What is ATP ?

ATP is a universal program system for digital simulation of transient phenomena of electromagnetic as well as electromechanical nature. With this digital program, complex networks and control systems of arbitrary structure can be simulated. ATP has extensive modelling capabilities and additional important features besides the computation of transients. It has been continuously developed through international contributions. ATP was formed after a disagreement over commercialization in 1984 and has been continuously developed by both Drs. W.Scott Meyer and Tsu-huei Liu. [17]

ATP program calculates variables of interest within electric power systems as functions of 3 to solve the differential equations of system components in the time domain. Non-zero initial conditions can be determined either automatically by a steady state, phasor solution or they can be entered by the user for some components.

ATP has many models including rotating machines, transformers, surge arresters, transmission lines and cables. With this digital program, complex networks of arbitrary structure can be simulated. Analysis of control systems, power electronics equipment and components with nonlinear characteristics such as arcs and corona are also possible. Symmetric or asymmetric disturbances are allowed, such as faults, lightning surges, or any kind of switching operations including commutation of valves. Calculation of the frequency response of phasor networks is also supported. [17]

3.3.2. ATPDraw

ATPDraw is a graphical, mouse- driven preprocessor to ATP. It helps creating and editing the model of the electrical circuit the user wants to simulate interactively. In the program the user can construct an electric circuit, by selecting predefined components from an extensive library. The preprocessor then creates the corresponding ATP input file, automatically in correct format.

ATPDraw has a standard Windows user interface. Figure 3.2 shows the main window of ATPDraw containing two open circuit windows. ATPDraw supports multiple documents and offers the user to work on several circuits simultaneously along with the facility to copy information between the circuits. The size of the circuit window is much larger than the actual screen, as is indicated by the scroll bars of each circuit window. [17]

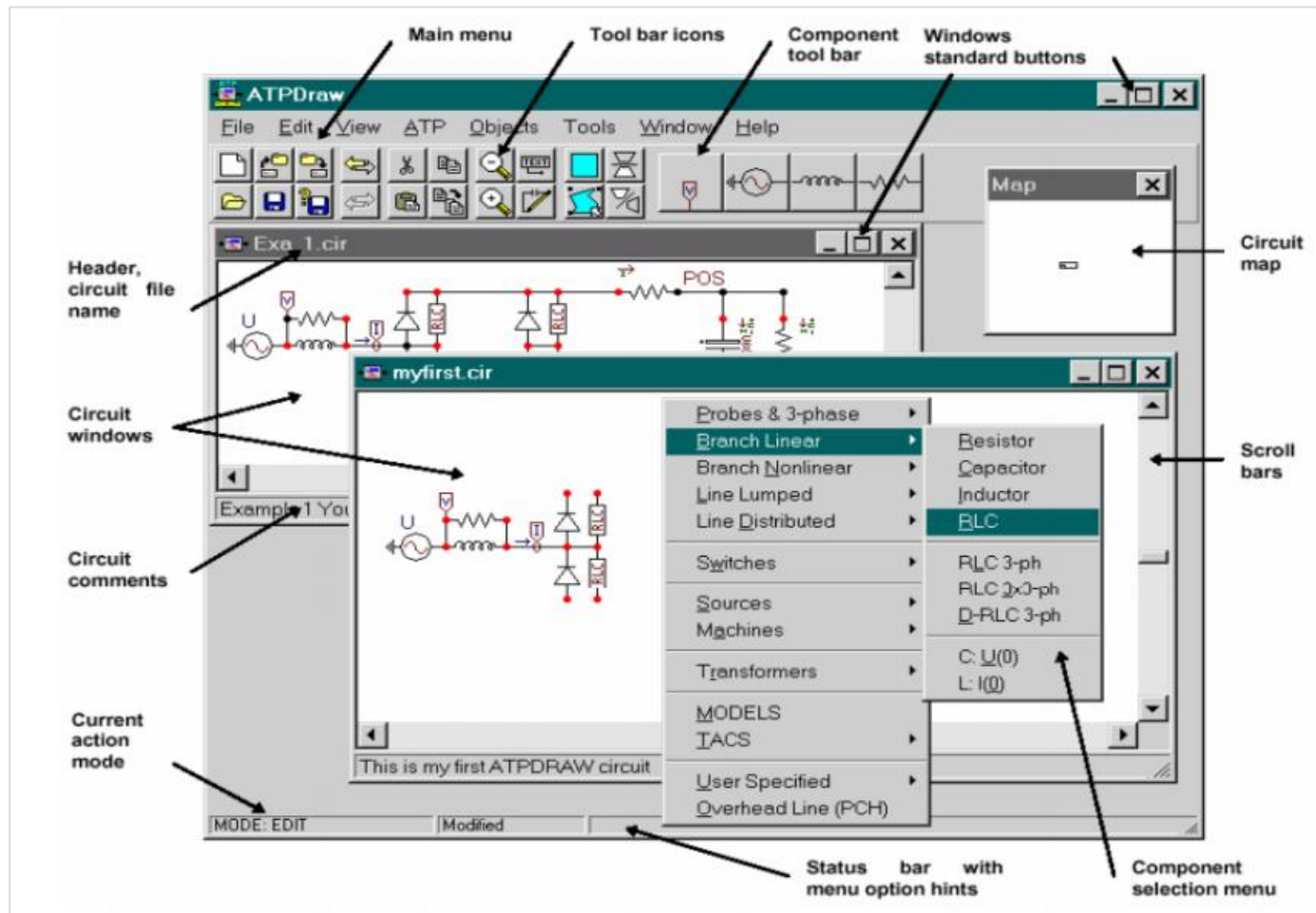


Figure 3.2: Main Window Multiple Circuit windows and the floating Selection menu.

3.4. The real electrical circuit of Haoud Berkaoui

3.4.1. Description of the circuit

Figure 3.3 shows the single line diagram of Haoud Berkaoui. It is formed by a generator as source followed by transmission line connected to two big transformers in parallel, there are two transformers 30/5.5 KV with rated power 6300 KVA each, both connected to 5.5KV bus bare. This bus bare feeds:

- Two motors of the compressors of rated power 2060 KW for each one.
- Two transformers 5.5/0.4 KV of rated power 500 KVA used for lightning, motors, air conditioning, 220 volts sources.

- One motor feeds pump Security 315KW.
- Water injection unit which feeds three electro-pumps of rated power 560 KW. [15]

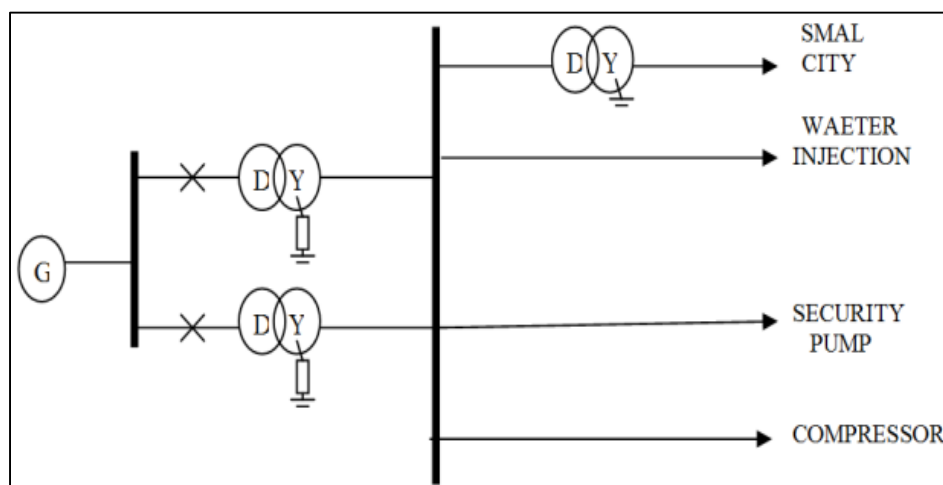


Figure 3.3: The one line diagram representation.

3.4.2. The characteristics of the equipment used in the Substation:

All important parameters which have been taken even from the station or from the Web site of the companies that have made those instruments are listed below:

❖ Two transformer TR1 and TR2 (MV):

- Rated power: 6300 KVA - Primary voltage: 30000 V - Secondary voltage: 5750 V
- Primary current: 121,24 A - Secondary current: 632,57 A

❖ A Transformers TR3 (LV):

- Rated power: 250 KVA - Primary voltage: 5500 V
- Secondary voltage: 400 V - Primary current: 24 A
- Secondary current: 358.9 A

❖ Three motors feed three pumps for water injunction:

- Number of phases: Three - Rated power: 560 KW - Voltage: 5500 V
- Current: 69,5 A - Frequency: 50 Hz - Cos Φ : 0,88
- Rotation speed: 1494 rev/min -Weight: 4600 Kg -Type of connection: Star

❖ Two motors feed two compressors:

- Number of phases: Three - Rated power: 2060 KW - Voltage: 5500 V
- Current: 242,7 A - Frequency: 50 Hz - Cos Φ : 0,93
- Rotation Speed: 2986 rev/min -Weight: 8400 Kg -Type of connection: Star

❖ **One motor feeds a security pump:**

- | | | |
|-----------------------------------|-----------------------|----------------------------|
| - Number of phases: Three | - Rated power: 315 KW | - Voltage: 5500 V |
| - Current: 40,6 A | - Frequency: 50 Hz | - Cos Φ : 0,86 |
| - Speed of rotation: 1488 rev/min | - Weight: 2420 Kg | - Type of connection: Star |

❖ **The consumption parameters of the city (RLC):**

- | | |
|------------------------------|---------------------------------|
| - The real power: 103.09 KW | - The reactive power: 49.93 VAR |
| - The rated power: 114.55 VA | - Power factor: 90.0% |
| | - The efficiency: 97.0% |

3.4.3. ATP simulation results

In our simulation, ATPDraw software has been used to draw the circuit which is shown in figure 3.4. Synchronous machine has been represented as source of 30KV, the two transformers are 30/5.5KV, the small transformers are 5.5/0.4KV, the induction motor of 0.4KV and the loads are the RL equivalent circuit of the used light, pumps water injection...etc. The detailed elements of the ATPDraw circuit are given in the appendix.

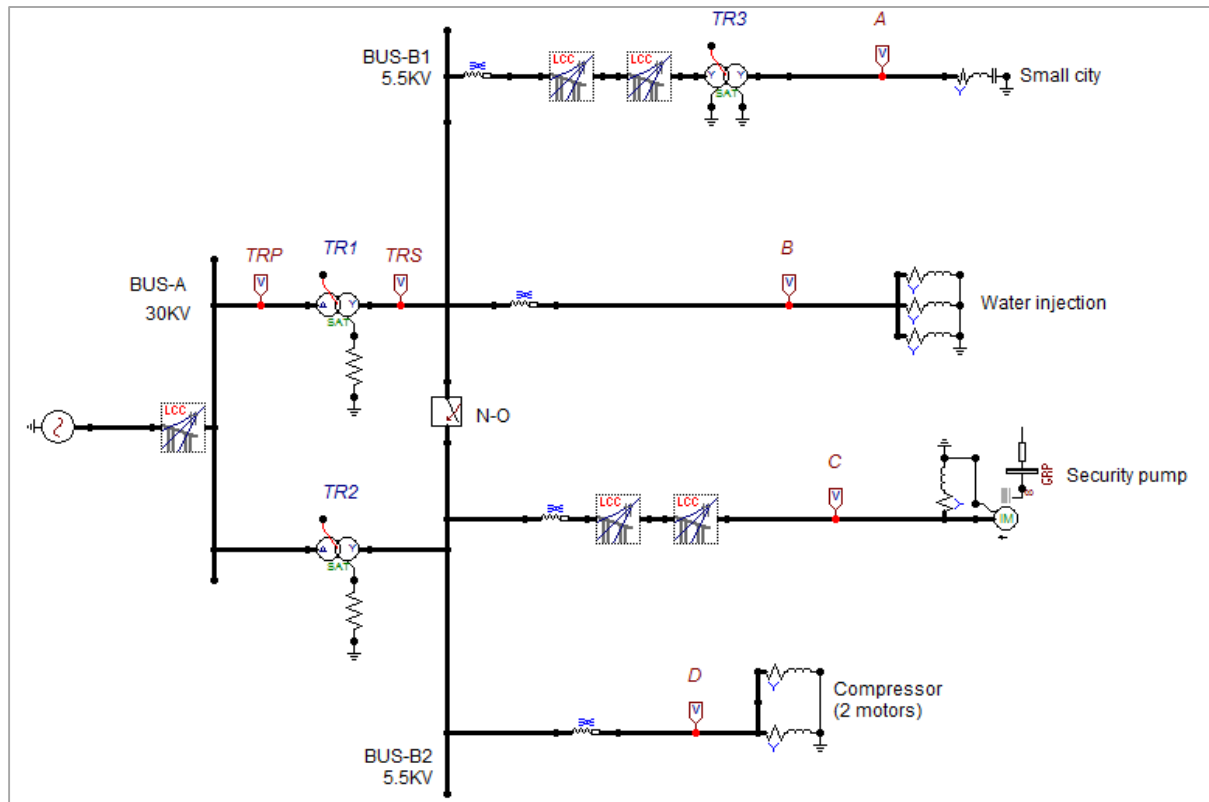


Figure 3.4: ATPDraw representation of the circuit of Haoud Berkaoui station.

Figures 3.5 and 3.6 below show the steady state of the network, after checking the voltage waveform at points TRS, A, B, C and D for the loads.

➤ **The simulation result at point A:**

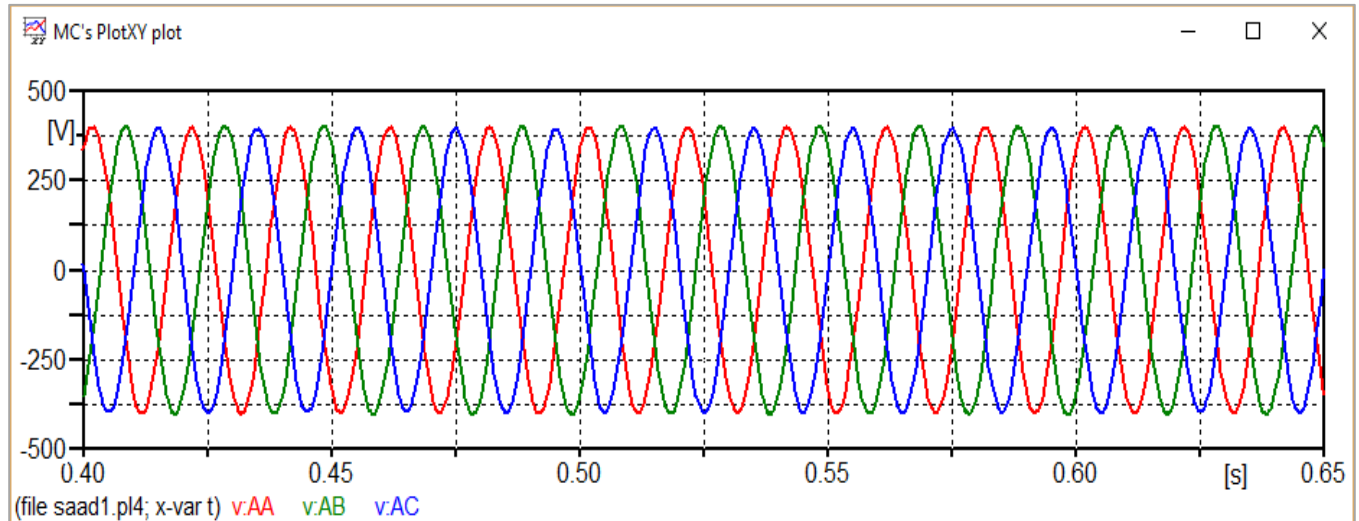


Figure 3.5: The values of voltages at the point A.

Where the peak values of the three phases (A, B and C) at point A are: $V_A = 380 \text{ V}$

➤ **The simulation result at points TRS, B, C and D:**

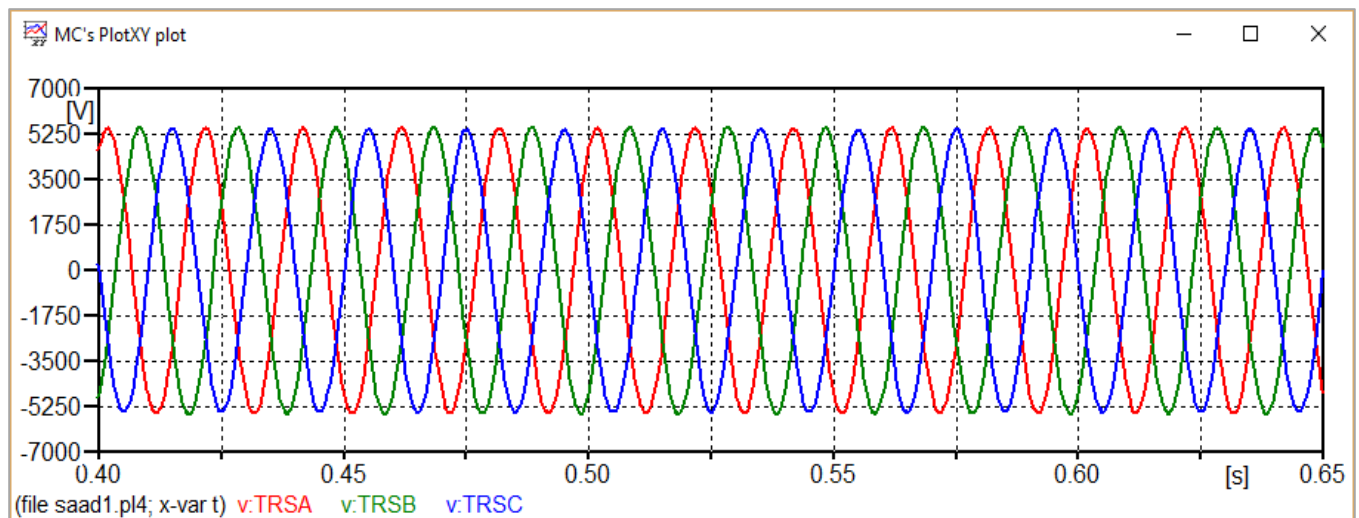


Figure 3.6: The values of voltages at the point TRS, B, C and D.

Where the peak values of the three phases (A, B and C) are: $V_{TRS} = V_B = V_C = V_D = 5.5 \text{ KV}$

3.5. The Case study

Switching operations may cause ferroresonance in voltage transformers which are connected between phases and ground. A sample case of voltage transformer energized and de-energized through Grading capacitance of circuit breaker is illustrated in Figure 3.7.

Opening of circuit breaker D starts ferroresonance by causing capacitance C (all the capacitances to ground) to discharge through voltage transformer. Through grading capacitance C_d , source delivers enough energy to maintain oscillation.

Following is the circuit equipment condition:

- i. Before switching (Transformer energized)
 - Circuit breaker was close.
- ii. After switching (Transformer de-energized)
 - Circuit breaker was open.

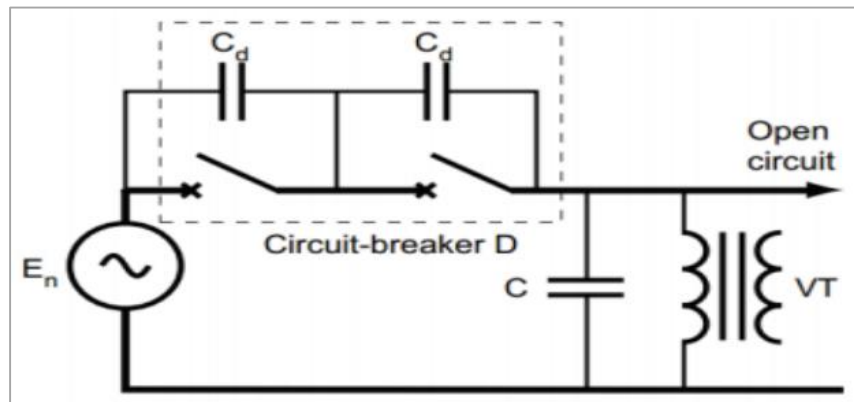


Figure 3.7: Voltage transformer connected in series with an open circuit breaker.

3.5.1 - The effect of changing grading capacitor (C_g):

In order to see the effect of the circuit breaker grading capacitance values on the occurrence of ferroresonance we have connected a circuit breaker consisting of its grading capacitance (C_g) at the primary side of the big transformers as shown in the gray area in Figure 3.8.

The commissioning of the system of Figure 3.8 was conducted as follows: the energization of the VT's from the 30 kV busbar when the circuit breaker (CB) were close and then de-energized the VT's by opening the circuit breaker (CB). The effect after the switching events has thus reconfigured the circuit into ferroresonance condition involving the interaction between the circuit breaker's grading capacitor and the transformers.

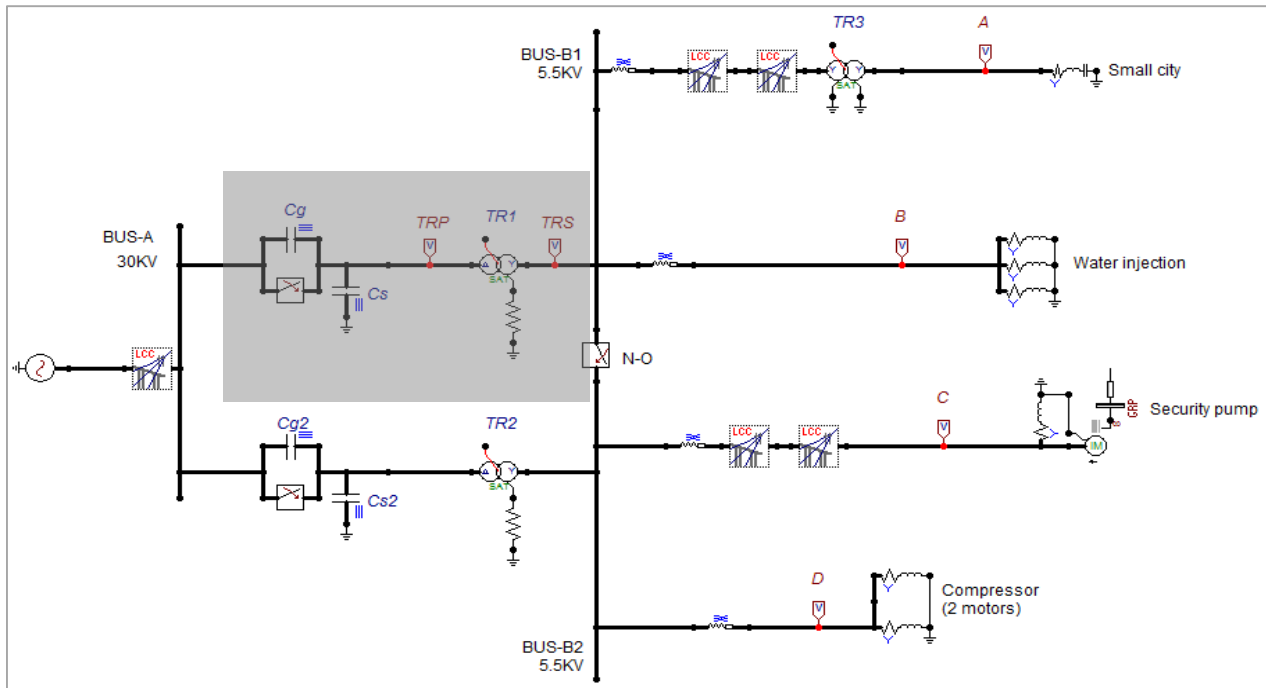


Figure 3.8: The ATP model circuit used for simulation

- Simulation results:

In order to look into the effect of grading capacitance on ferroresonance, let us look at a wider view by having the grading capacitance (C_g) varied. We assume also the variation of the coming voltage from the generation station, the network voltage values for which the ferroresonance risk will be verified are: 80%, 100% and 120% of the rated voltage V_s (30Kv). The ferroresonant response was verified for opening the switch parallel to the C_g at the $t = 0.5$ s.

The voltage waveforms across the transformer TR1 (MV power transformer) with network voltage 100% $V_s = 30$ Kv are recorded as shown below:

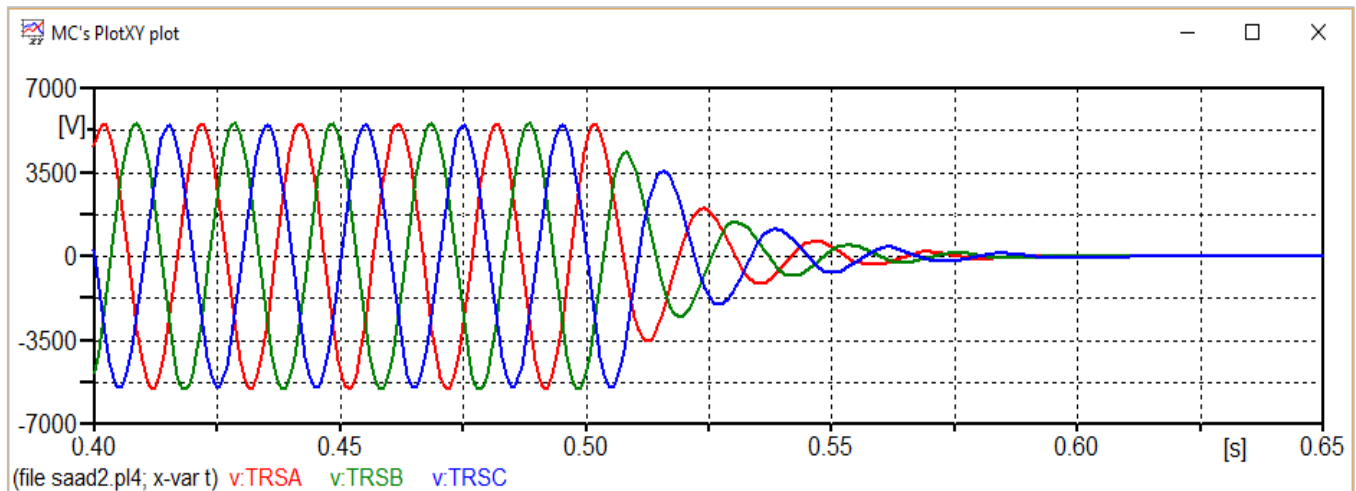


Figure 3.9: The voltages at point TRS with $C_g = 1\text{nF}$ and 100% V_s

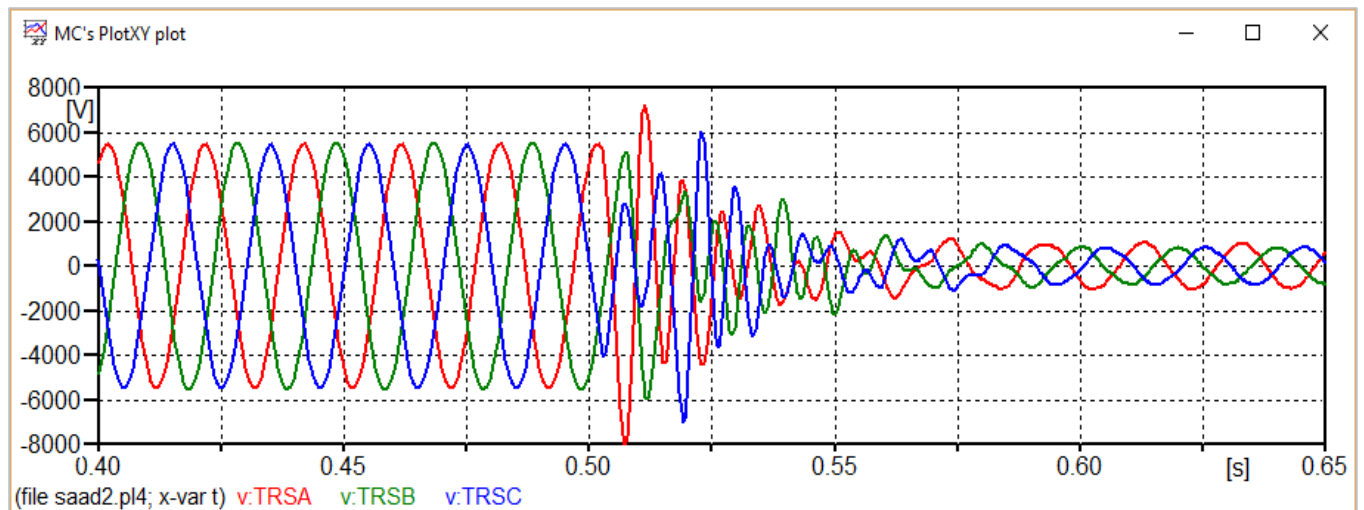


Figure 3.10: The voltages at point TRS with $C_g = 600\text{nF}$ and 100% V_s

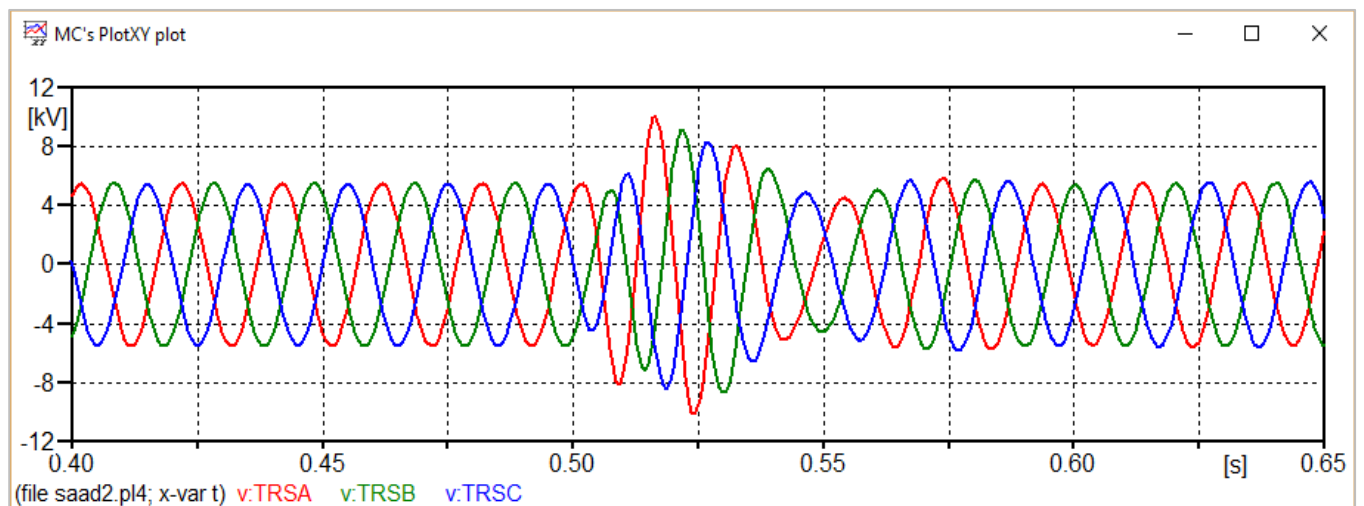


Figure 3.11: The voltages at point TRS with $C_g = 2\mu\text{F}$ and 100% V_s

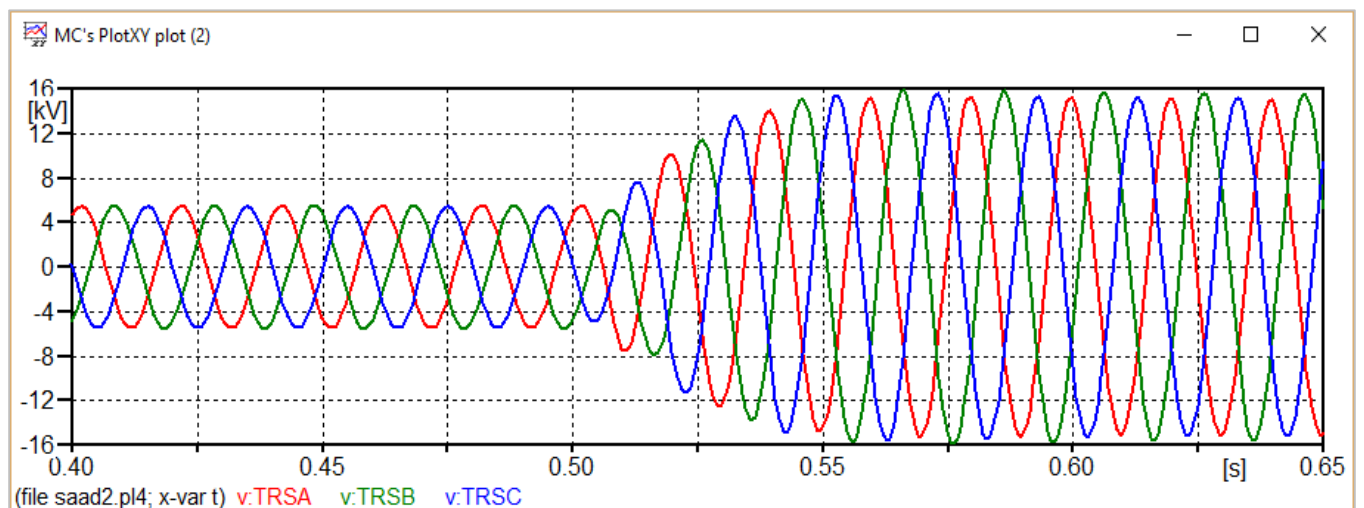


Figure 3.12: The voltages at point TRS with $C_g = 5\mu\text{F}$ and 100% V_s

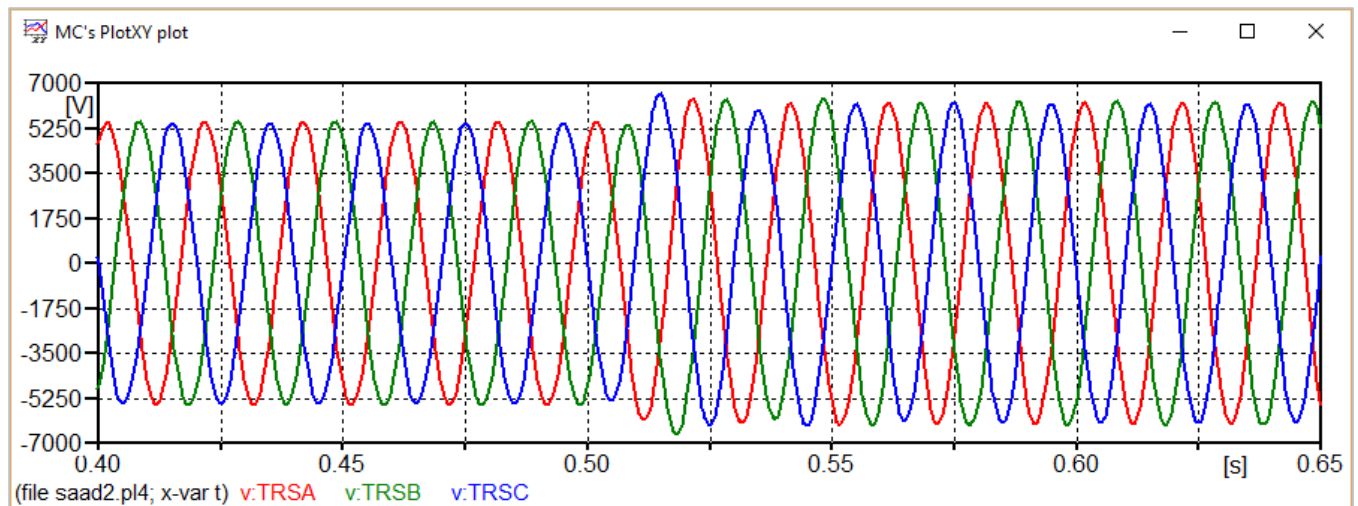


Figure 3.13: The voltages at point TRS with $C_g = 30\mu\text{F}$ and 100% V_s .

Comments: In all the above waveforms. It could be seen that for V_s values of 100%, the ferroresonance may exist for $C_g = 0.6\mu\text{F}$ and above until the value $C_g = 30\mu\text{F}$, it will appear overvoltage start to be less and extremely equal to the secondary voltage of TR1.

Now we vary the network voltage down to 80% $V_s = 24\text{ Kv}$, then we record the voltage waveforms across the transformer TR1 as shown below:

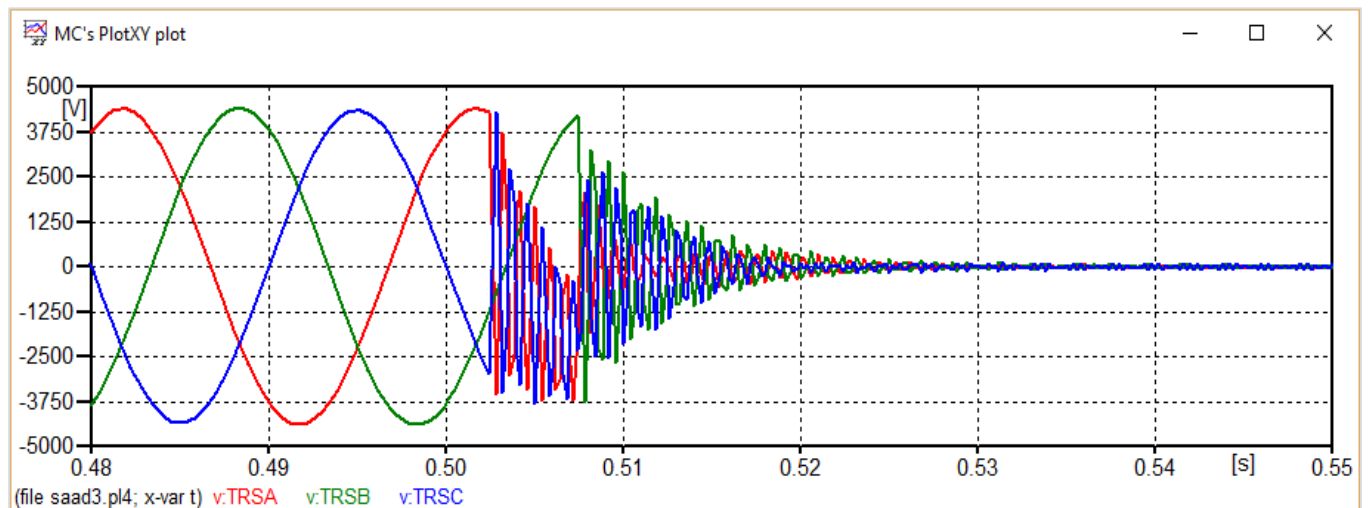


Figure 3.14: The voltages at point TRS with $C_g = 1\text{nF}$ and 80% V_s .

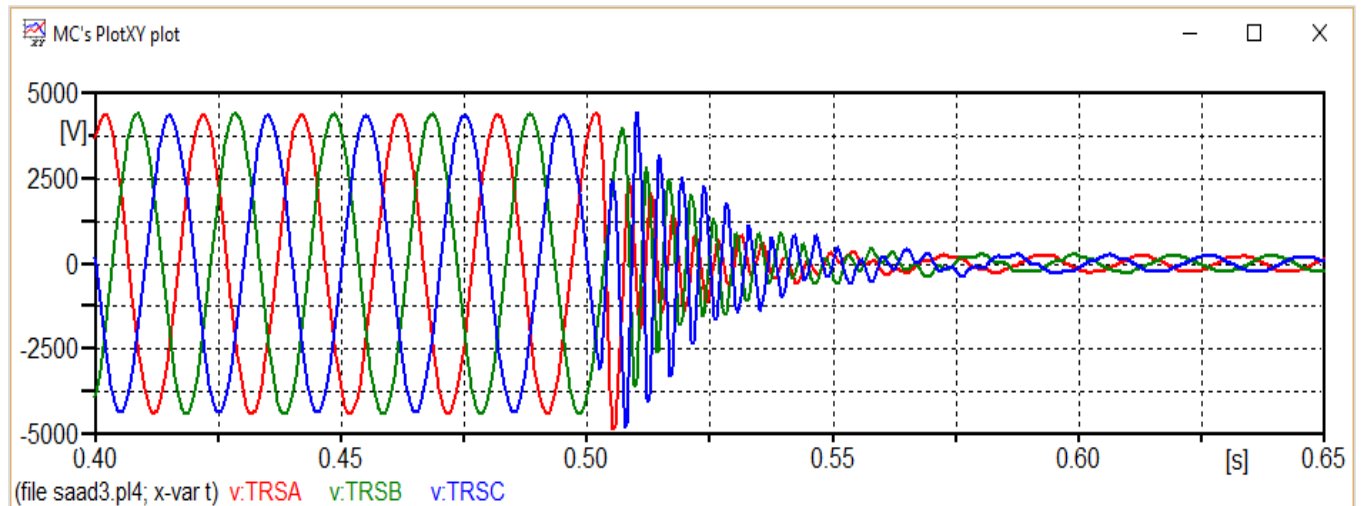


Figure 3.15: The voltages at point TRS with $C_g = 600\text{nF}$ and 80% V_s .

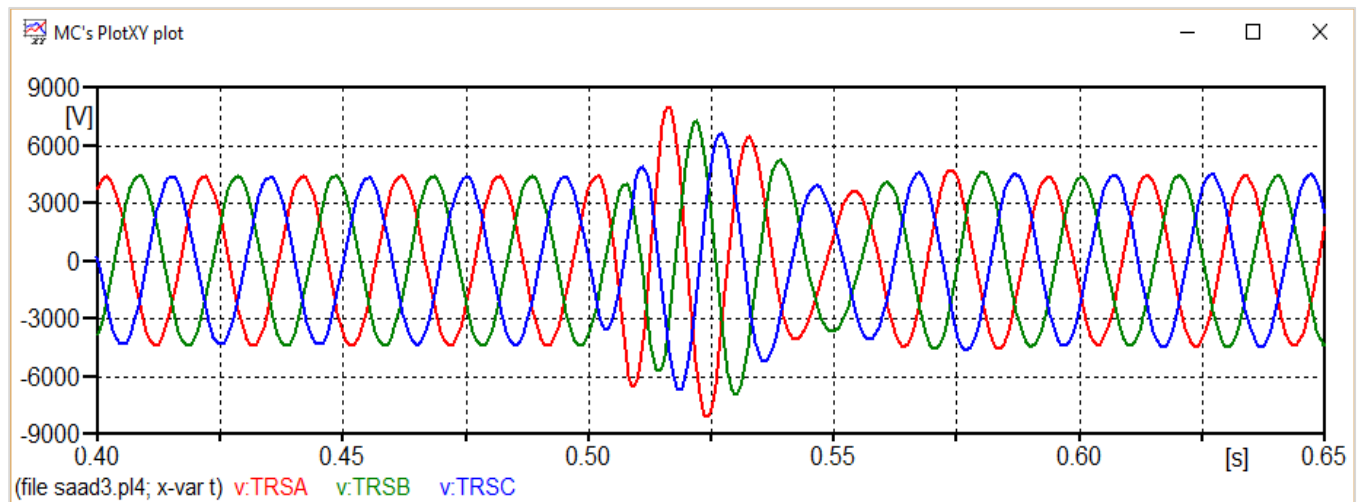


Figure 3.16: The voltages at point TRS with $C_g = 2\mu\text{F}$ and 80% V_s .

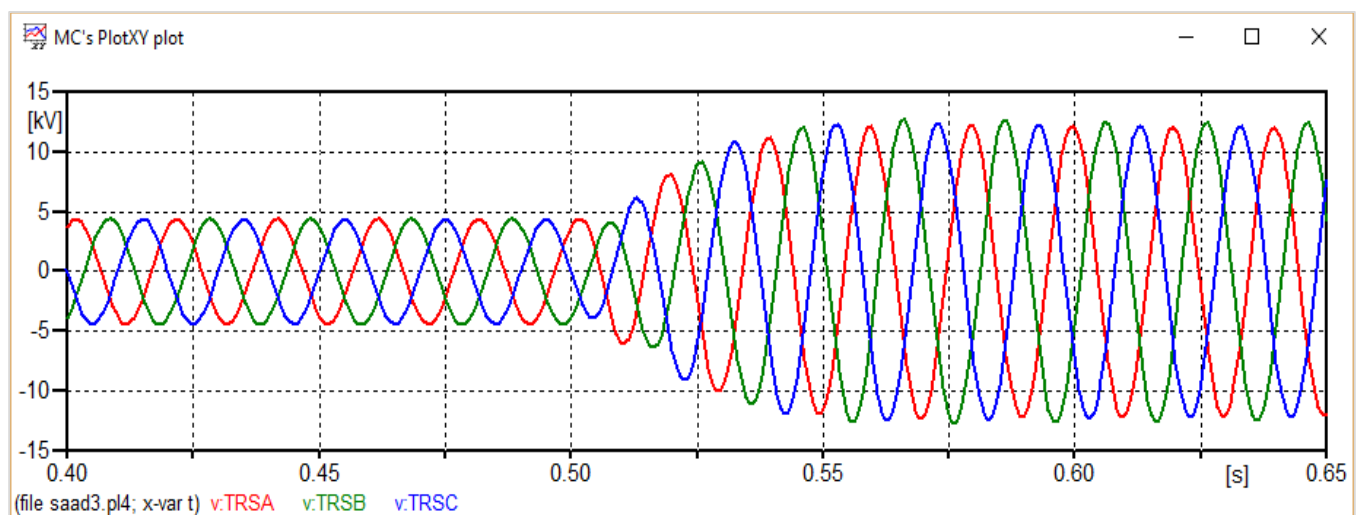


Figure 3.17: The voltages at point TRS with $C_g = 5\mu\text{F}$ and 80% V_s .

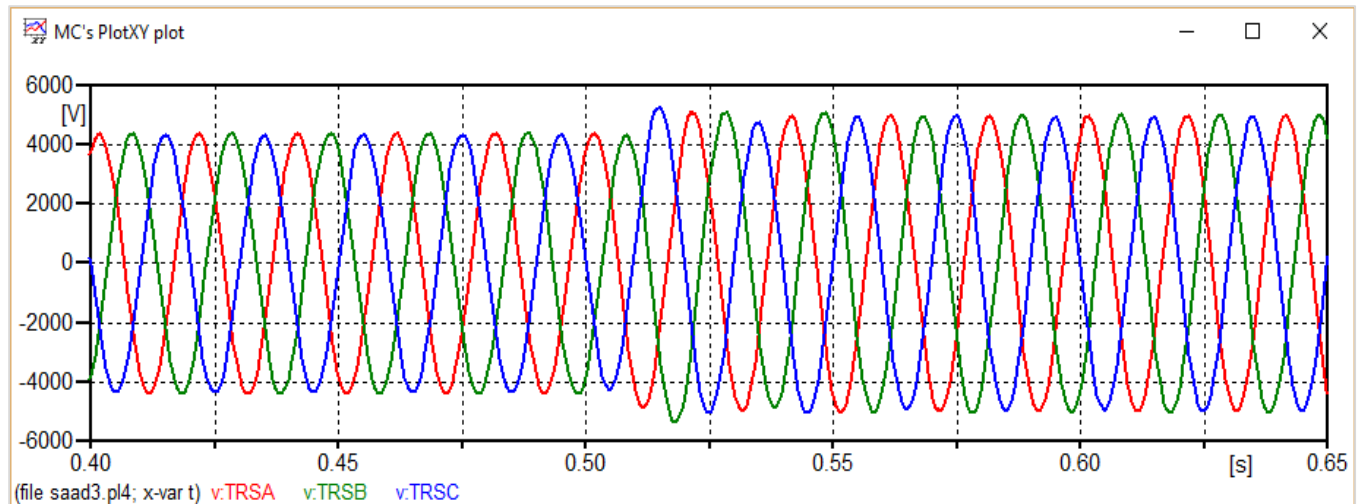


Figure 3.18: The voltages at point TRS with $C_g = 30\mu\text{F}$ and 80% V_s .

Comments: In the above waveforms from figure 3-14 to 3-18. It could be seen that for V_s values of 80%, the ferroresonance doesn't exist for $C_g = 0.6\mu\text{F}$ as it is for V_s values of 100%, it exists for $C_g = 2\mu\text{F}$ and above until the value $C_g = 30\mu\text{F}$, it will appear overvoltage start to be less and extremely equal to the secondary voltage of TR1.

Now we vary the network voltage up to 120% $V_s = 36\text{ Kv}$, then we record the voltage waveforms across the transformer TR1 as shown below:

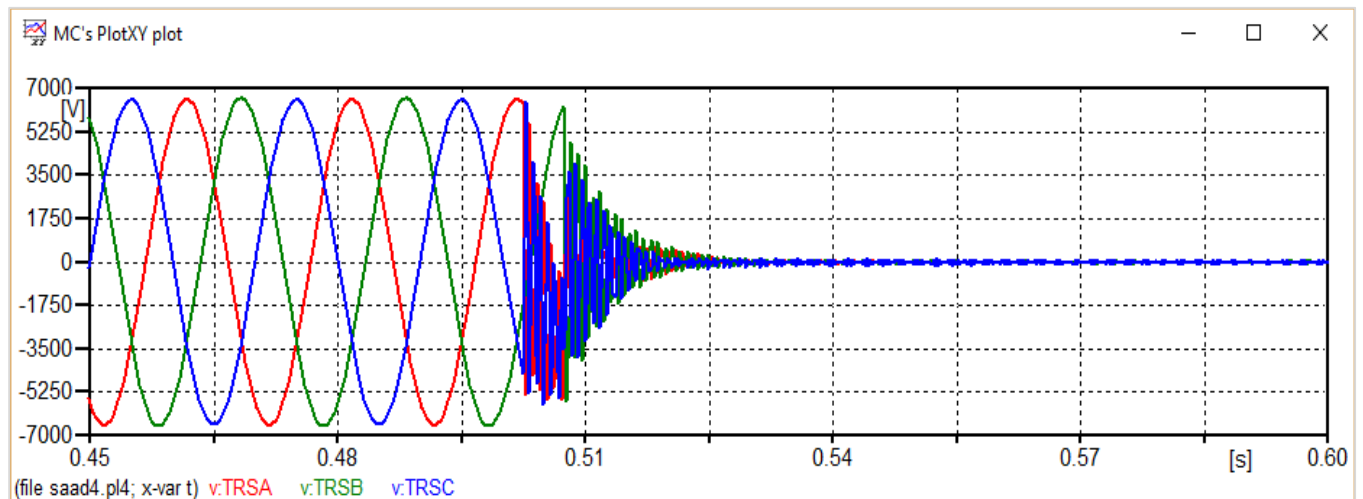


Figure 3.19: The voltages at point TRS with $C_g = 1\text{nF}$ and 120% V_s .

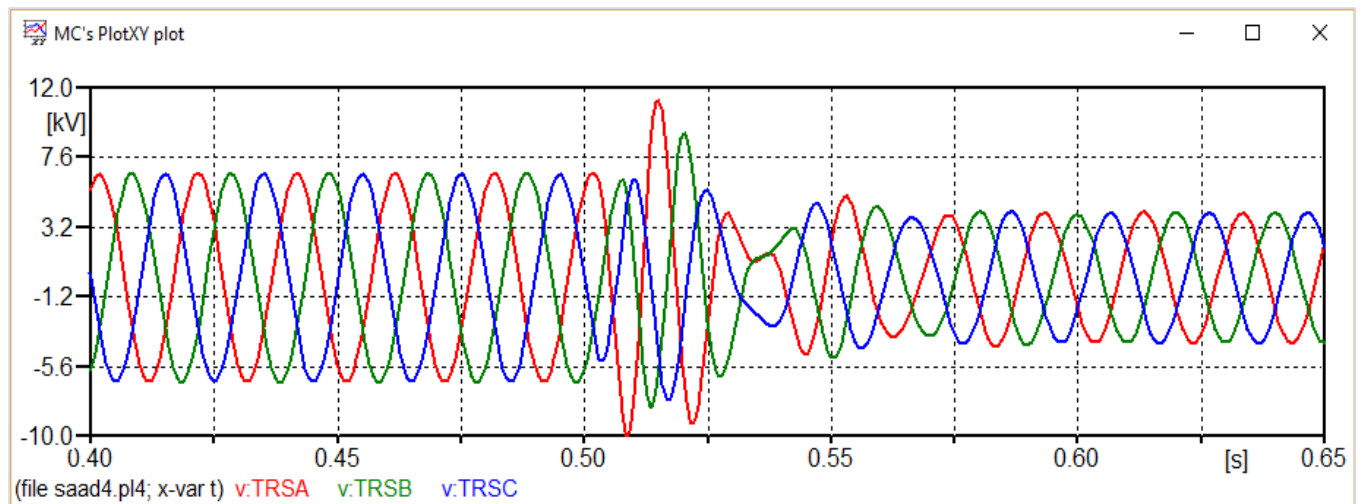


Figure 3.20: The voltages at point TRS with $C_g = 10\text{nF}$ and 120% V_s .

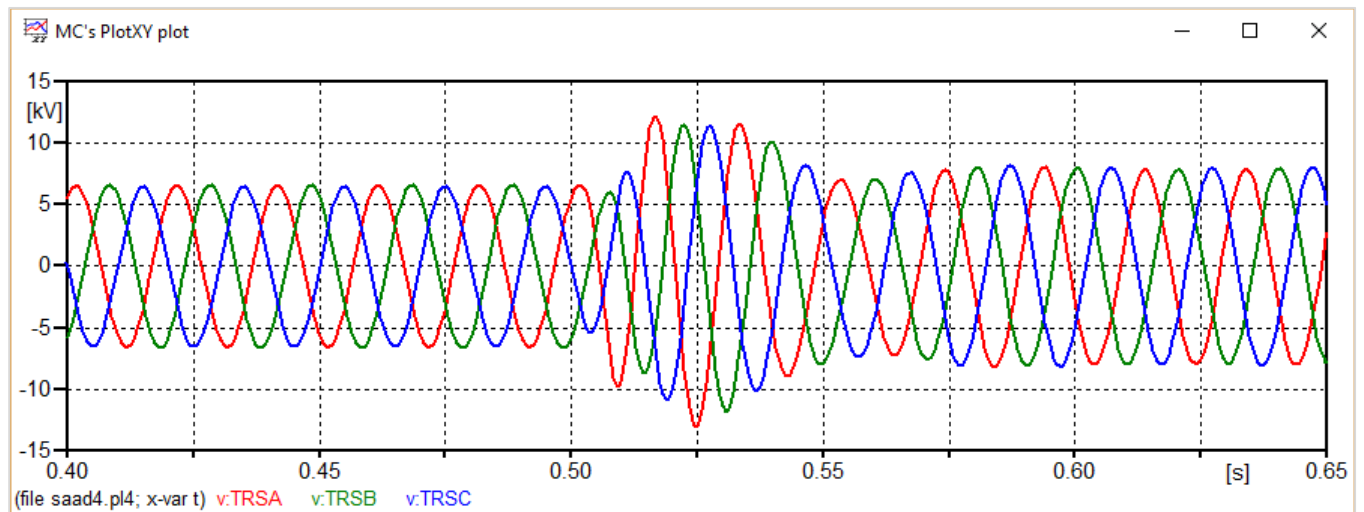


Figure 3.21: The voltages at point TRS with $C_g = 2\mu\text{F}$ and 120% V_s .

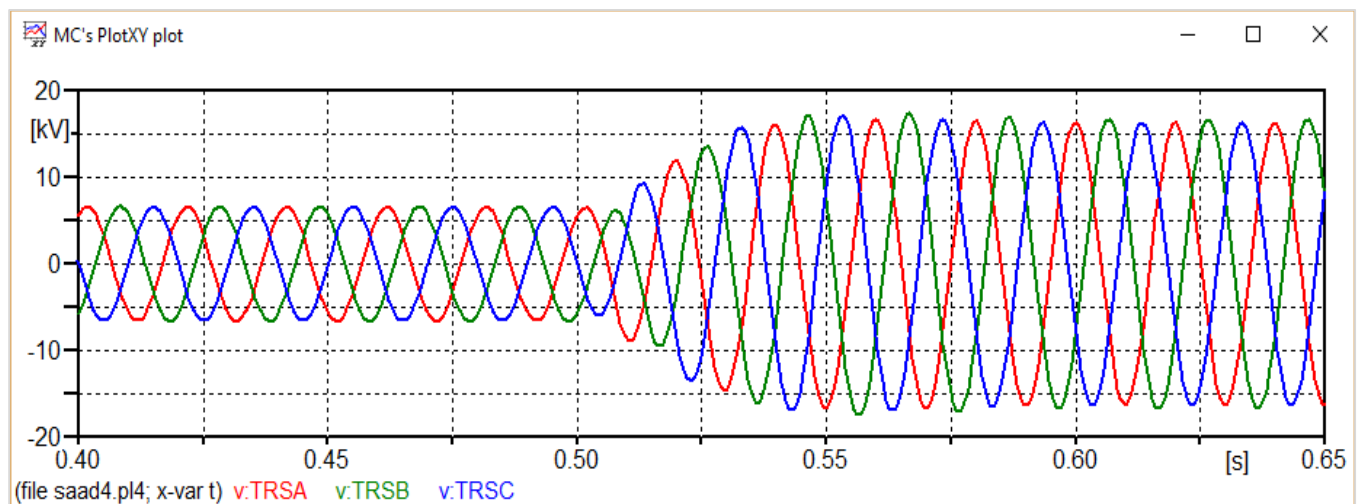


Figure 3.22: The voltages at point TRS with $C_g = 5\mu\text{F}$ and 120% V_s .

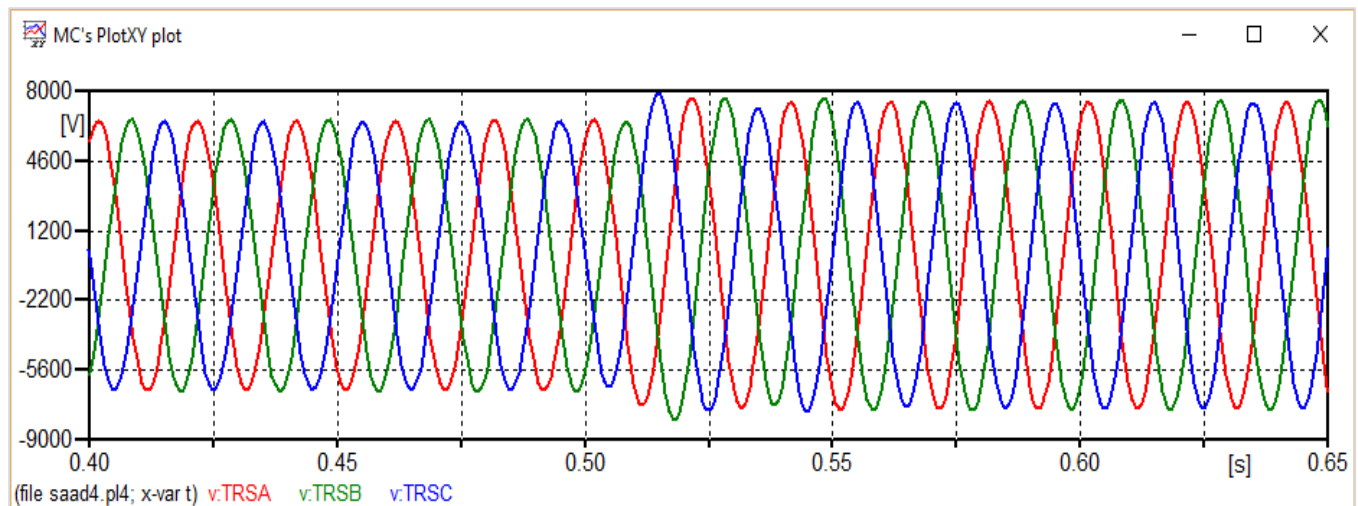


Figure 3.23: The voltages at point TRS with $C_g = 30\mu\text{F}$ and 120% V_s .

Comments: In the above waveforms from figure 3-19 to 3-23. It could be seen that for the extreme value of $V_s = 120\%$ however, a potential risk of ferroresonance was identified for $C_g = 10\text{nF}$ and above, until the value $C_g = 50\mu\text{F}$, it will appear overvoltage start to be less and extremely equal to the secondary voltage of TR1.

After performing all the simulations to identify the ferroresonant combination of V_s and C_g values. This ferroresonant region is clearly shown in Table 1 below, summarizing the results of the peak value of overvoltage.

	80% V_s	100% V_s	120% V_s
1nF	NO (0 pu)	NO (0 pu)	NO (0 pu)
10nF	NO (0 pu)	NO (0 pu)	YES (1.3 pu)
600nF	NO (0 pu)	YES (1.5 pu)	YES (1.6 pu)
2 μF	YES (1.8 pu)	YES (2 pu)	YES (2.1 pu)
2.5 μF	YES (2.1 pu)	YES (2.3 pu)	YES (2.5 pu)
5 μF	YES (2.85 pu)	YES (2.9 pu)	YES (3.1 pu)
10 μF	YES (2.1 pu)	YES (2.2 pu)	YES (2.3 pu)
15 μF	YES (1.35 pu)	YES (1.4 pu)	YES (1.6 pu)
30 μF	NO (1.2 pu)	NO (1.25 pu)	YES (1.4 pu)
50 μF	NO (1 pu)	NO (1 pu)	NO (1.2 pu)

Table 3.1: Ferroresonance simulations results summary of maximum overvoltage for C_g .

We have plotted the corresponding graph of this table:



Figure 3.24: The effect of the grading Capacitance on ferroresonance.

General comments:

Finally, we conclude that the best values of grading capacitor which insure a high speed switching for the circuit breaker are: $C < 1\text{nF}$ for the three cases of Vs

Also the interval of grading capacitance which causes overvoltage more than 1.5 per unit:

$$2\mu\text{F} < C < 10\mu\text{F}$$

The Figure 3.24 referred that for values greater than $15\mu\text{F}$ it will appear overvoltage start to be less and less because the resistance of the capacitor was being smaller every time which damp out the extra power of the system.

Varying the value of the source voltage has its effect on ferroresonance especially at the small values of C_g as shown above in the red region (Figure 3.24) and table 3.1, which in the case of 80% Vs the risk

of ferroresonance is suppressed at $C_g = 600\text{nf}$, unlike what exist in the other cases. Also the opposite in the case of 120% V_s , which the risk of ferroresonance extended to $C_g = 10\text{nf}$.

3.6. Practical solution

3.6.1. Increasing the value of shunt capacitance at the transformer primary side

As mentioned in section 2.4, increasing the capacity of shunt capacitance at the transformer primary side is one of the ferroresonance mitigation techniques.

In order to confirm its effectiveness, we create a ferroresonance situation at it is optimum, by fixing the value of grading capacitor $C_g = 5\mu\text{F}$ as we see in figure 3.12, then we try to change the value of the shunt capacitor C_s at the transformer primary side. The simulation results are summarized in Table 3.2, and Figures 3.26, 3.27 and 3.28 show voltage waveforms at transformer secondary side for case 1 with ferroresonance, the threshold in case 3 and its elimination in case 5.

Industry analysts have empirically assumed that when the voltage exceeds 1.25 pu, the system is said to be “in ferroresonance” [19].

Cases	Capacitor (μF)	Maximum overvoltage (pu)	state
1	0.5	2.4	In ferroresonance
2	2.5	1.3	In ferroresonance
3	2.7	1.25	Threshold
4	3	1.15	Non ferroresonance
5	5	0.8	Non ferroresonance

Table 3.2: Simulation results of maximum overvoltage for shunt capacitors.

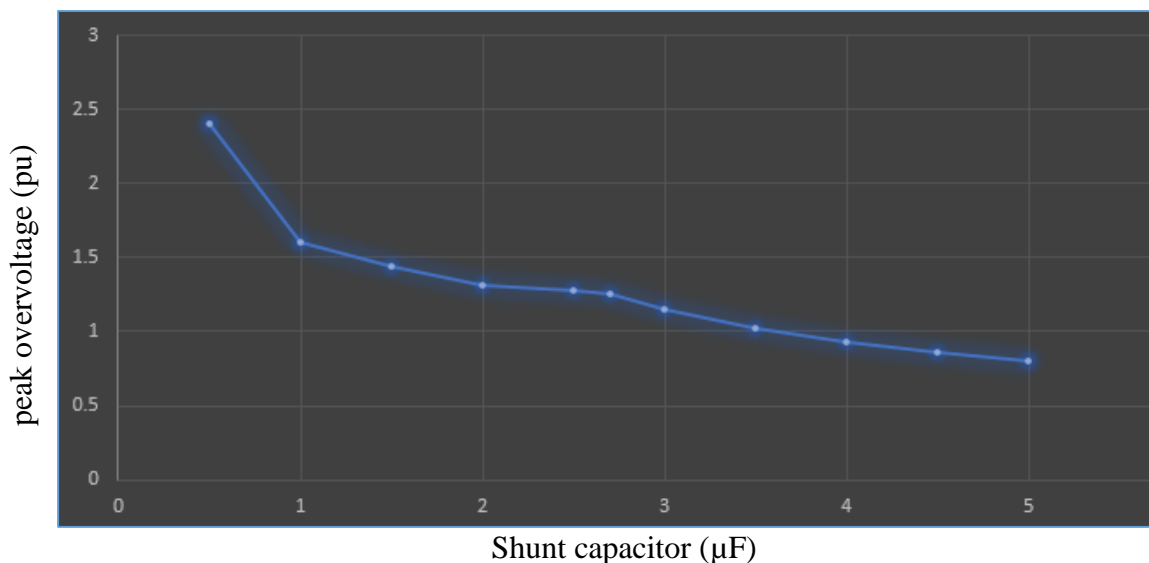
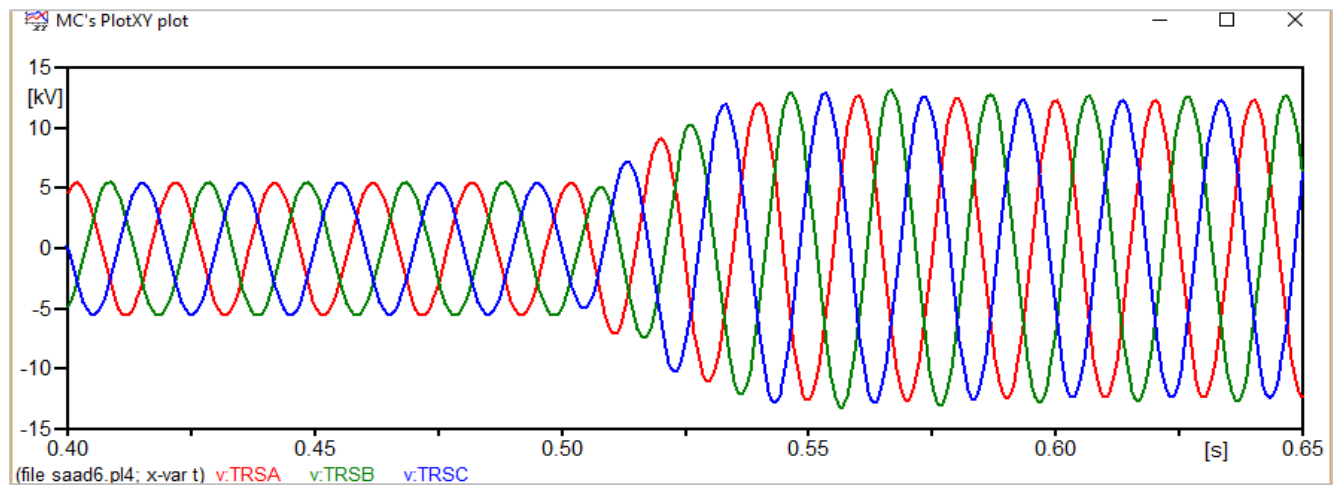
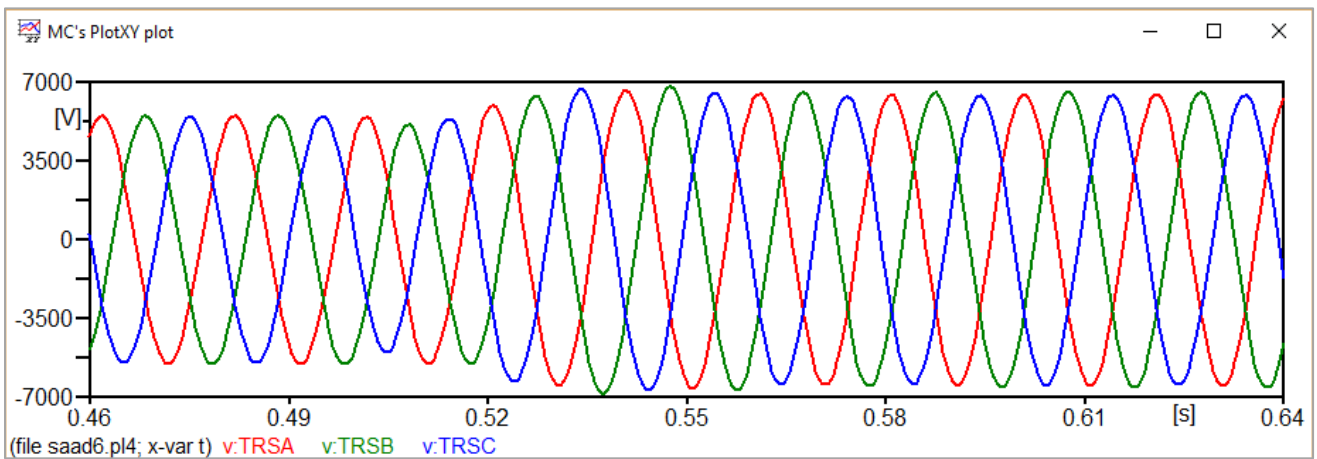
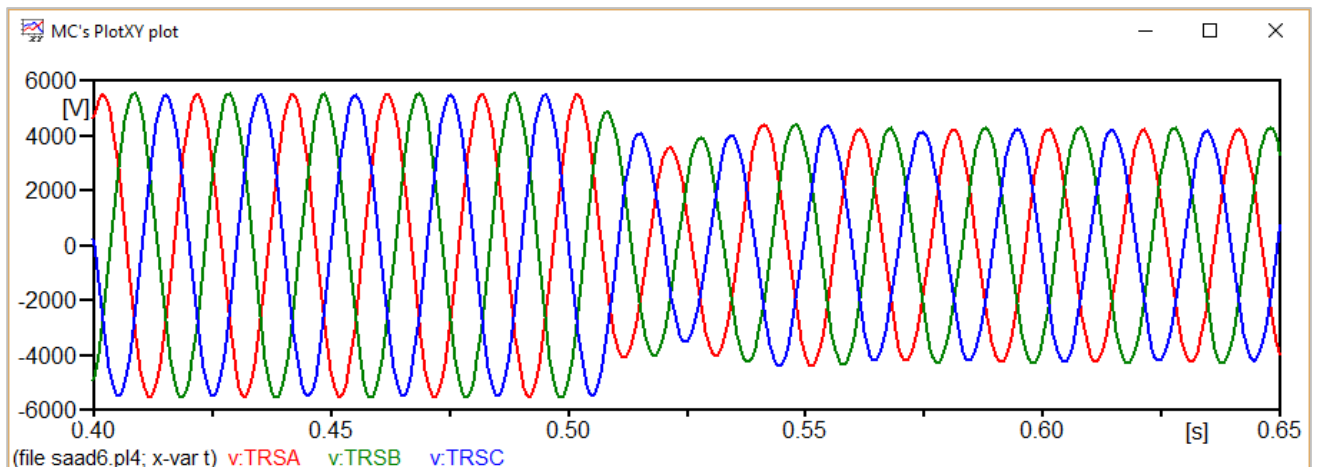


Figure 3-25: The effect of the Shunt Capacitance on ferroresonance.

Figure 3.26: The voltages at point TRS for Case 1 with $C_s = 0.5 \mu\text{F}$ Figure 3.27: The voltages at point TRS for case 3 with $C_s = 2.7 \mu\text{F}$ Figure 3.28: The voltages at point TRS for Case 5 with $C_s = 5 \mu\text{F}$

Comments:

According to industry analysts, we see from the table 3.2 and figure 3.25 above that the value of **Cs = 2.7 μF** is the threshold value, and ferroresonance can be avoided by installing the shunt capacitor **Cs ≥ 2.7μF** in this study case. But in the case of **Cs < 2.7 μF** the ferroresonance is reduced slowly when Cs increased from small values until 2.7 μF.

The increasing at the value of shunt capacitance connected in the transformer primary side is very effective to reduce the risk of ferroresonance. Despite the high cost of implementation, it is one of the best solutions if the transformer secondary side is not accessible.

3.6.2. Installing a capacitor bank at the transformer secondary side

The second solution is to install the capacitor bank to suppress ferroresonance. As many papers and technical reports propose the insertion of the capacitor bank at the delta connected tertiary winding [20]. This can only be applicable to the power transformers with tertiary winding terminals. It is considered that the capacitor bank C_b is located at the transformer secondary side in the study because the transformer applied to this study does not have tertiary winding as shown in gray region in figure 3.29.

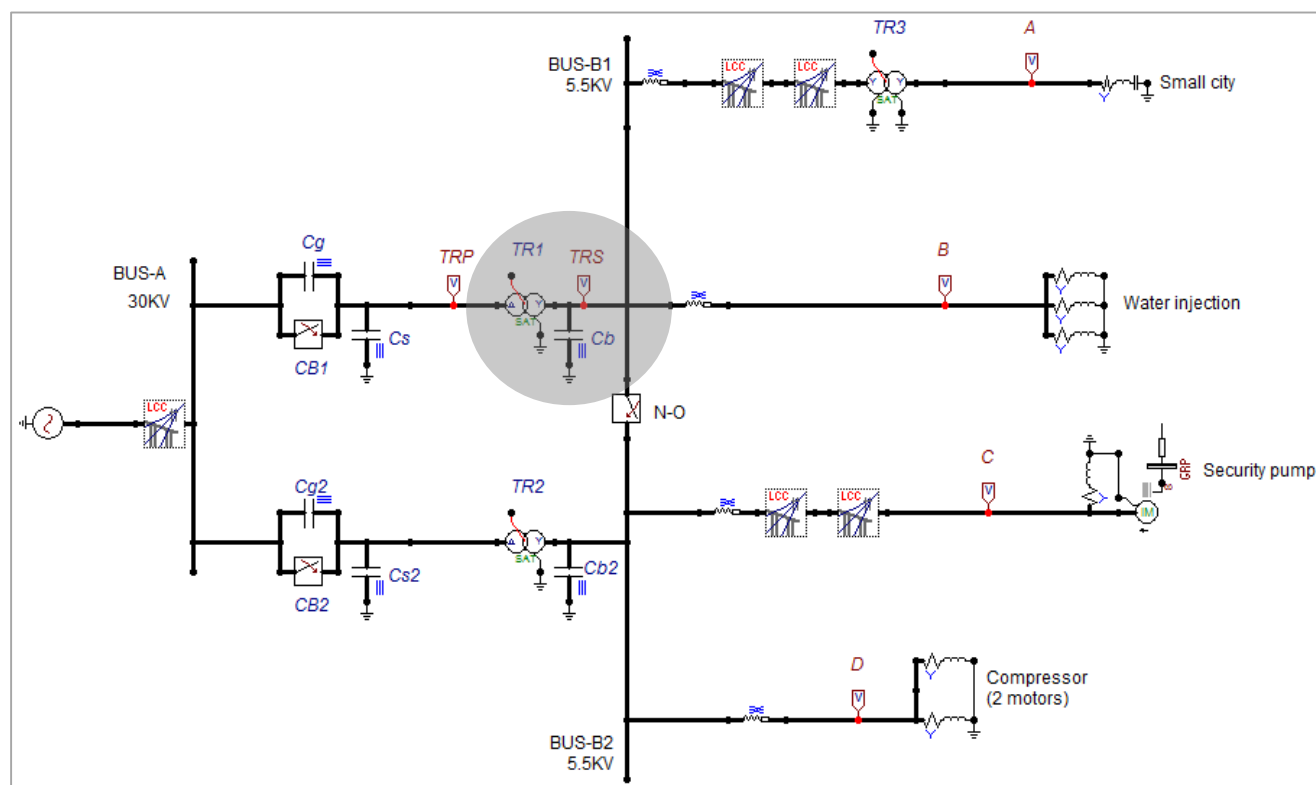


Figure 3.29: Capacitor bank at the transformer TR1 secondary side.

In order to confirm its effectiveness, we create a ferroresonance situation at it is optimum, by fixing the value of grading capacitor $C_g = 5\mu\text{F}$ as we see in figure 3.12, then we try to change the value of the bank capacitor C_b at the transformer secondary side (see figure 3-29). The simulation results are summarized in Table 3.3, and Figures 3.31, 3.32 and 3.33 show voltage waveforms at transformer secondary side for case 1 with ferroresonance, the threshold in case 4 and its elimination in case 7.

Cases	Capacitor (μF)	Maximum overvoltage (pu)	state
1	10	1.8	In ferroresonance
2	40	1.35	In ferroresonance
3	45	1.29	In ferroresonance
4	49	1.25	Threshold
5	50	1.24	Non ferroresonance
6	60	1.15	Non ferroresonance
7	100	0.87	Non ferroresonance

Table 3.3: Simulation results of maximum overvoltage for bank capacitors.

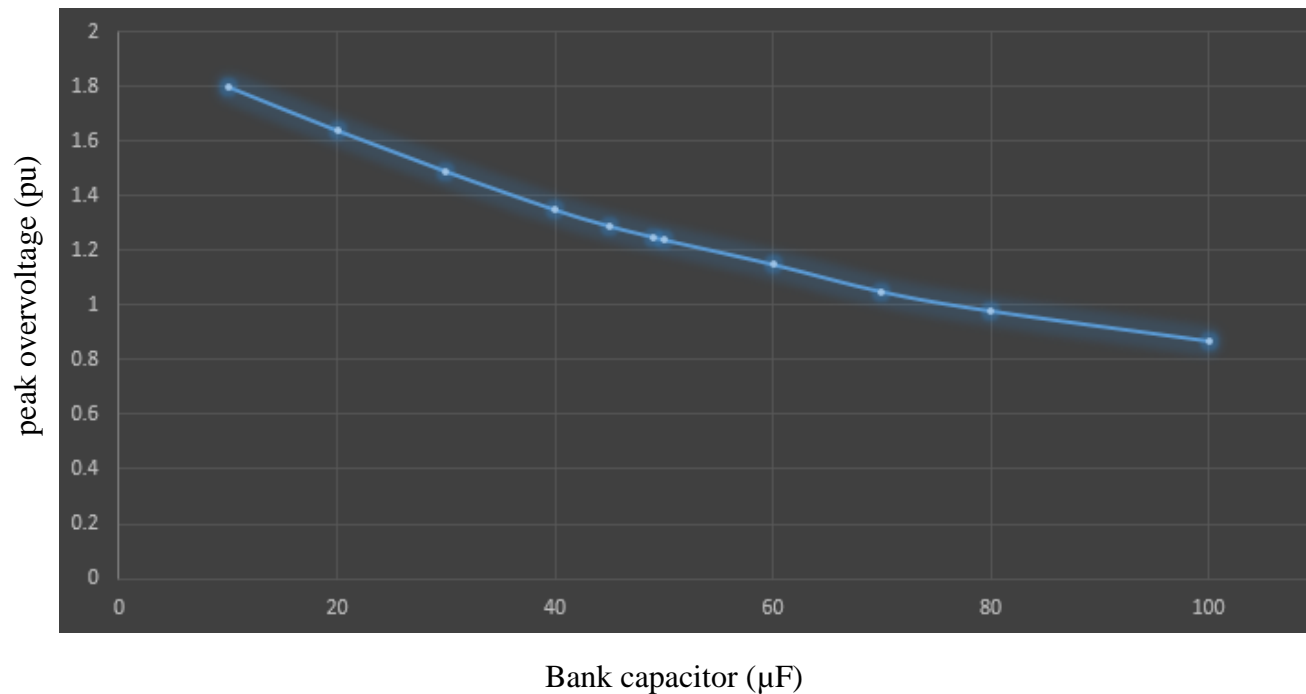


Figure 3.30: The effect of the Bank Capacitance on ferroresonance.

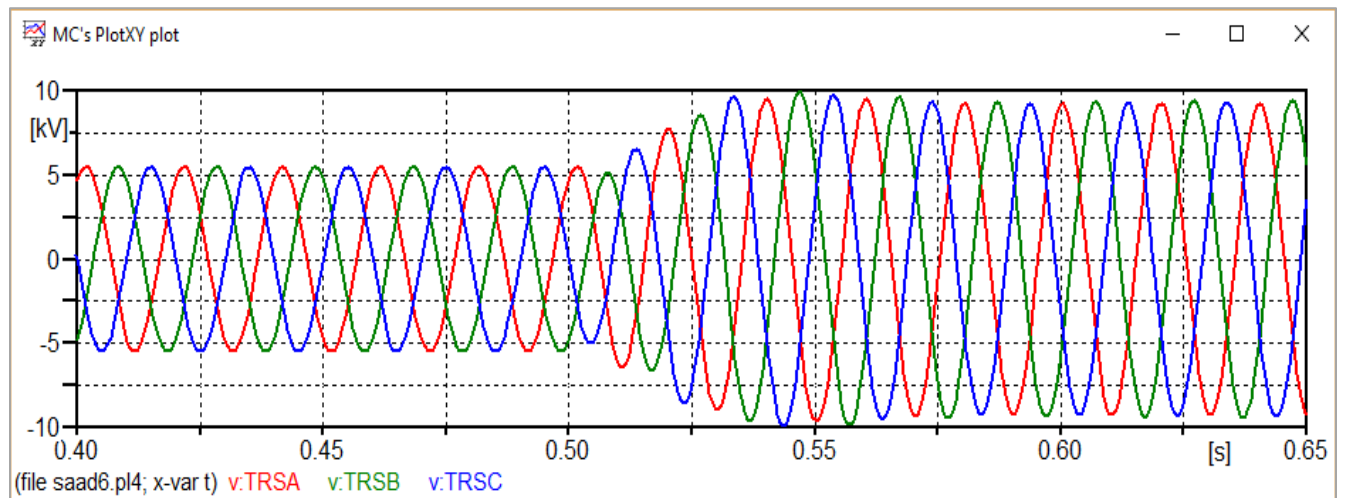


Figure 3.31: The voltages at point TRS for Case 1 with $C_b = 10 \mu\text{F}$

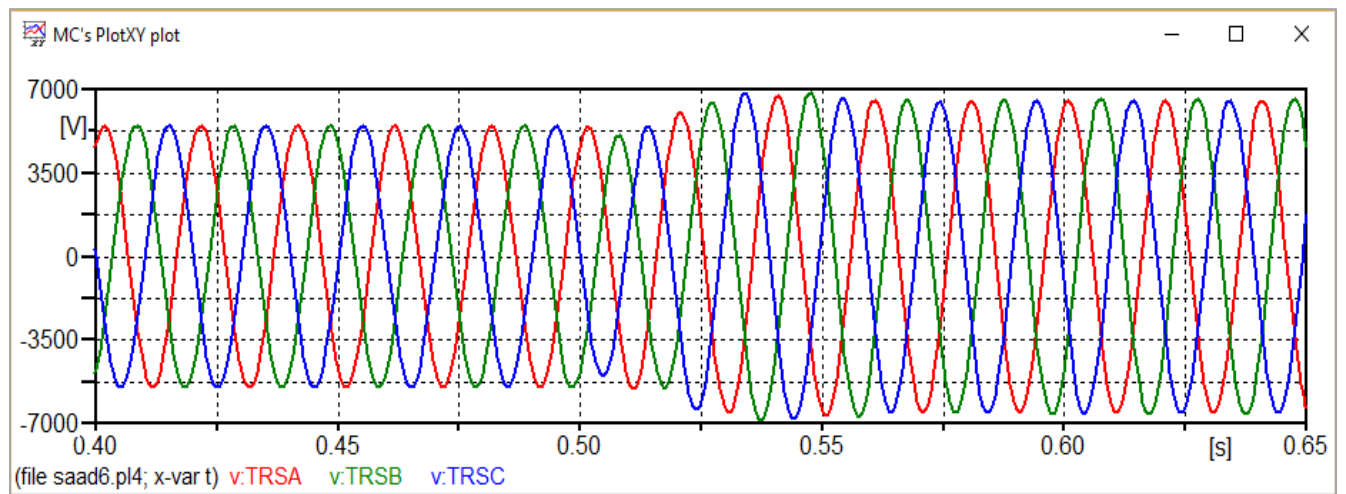


Figure 3.32: The voltages at point TRS for Case 4 with $C_b = 49 \mu\text{F}$

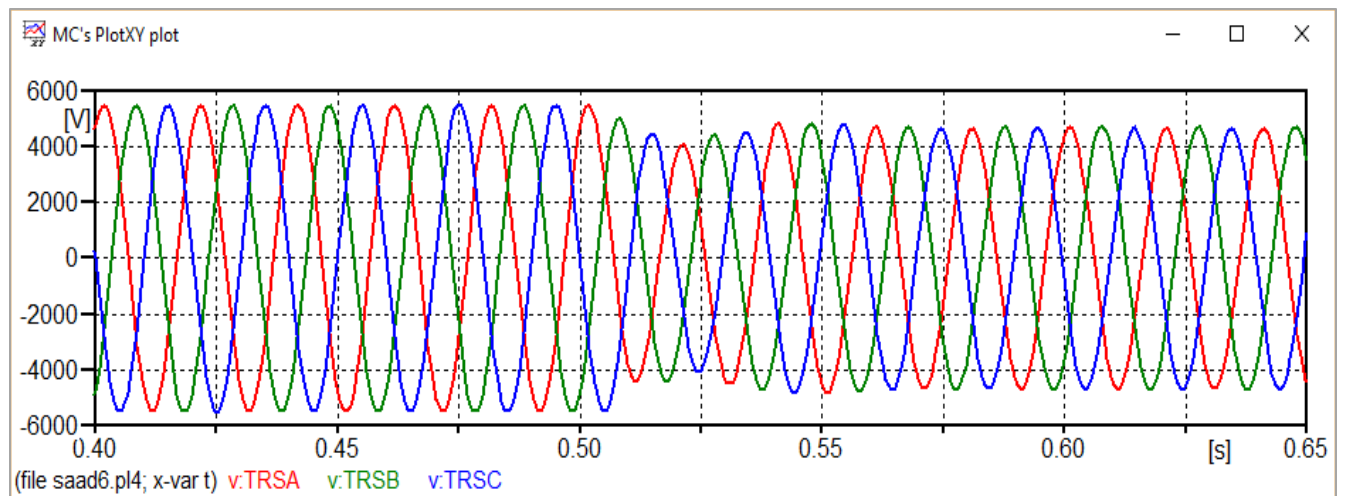


Figure 3.33: The voltages at point TRS for Case 7 with $C_b = 100 \mu\text{F}$

Comments:

According to industry analysts, we see from the table 3.3 and Figure 3.30 above that the value of $C_b = 49 \mu\text{F}$ is the threshold value, and ferroresonance can be avoided by installing the bank capacitor $C_b \geq 49 \mu\text{F}$ in this study case. But in the case of $C_b < 49 \mu\text{F}$ the ferroresonance is reduced slowly when C_s increased from small values until $49 \mu\text{F}$.

It can be observed that the high capacity of the capacitor bank is very effective on the suppression of ferroresonance. This countermeasure has the disadvantages such as its higher cost and the possibility of explosion in practice. In other words, the capacitor bank at the transformer secondary side can significantly reduce the risk of ferroresonance, however it also has disadvantages as well.

3.6.3. Installing a damping resistor at the transformer secondary side

Historically, the most commonly used mitigation method is a resistor connected to the transformer TR1 secondary side as shown in figure 3.34. The zero-sequence voltage present at the resistor terminals results in the zero-sequence current resulting from the ferroresonant oscillations.

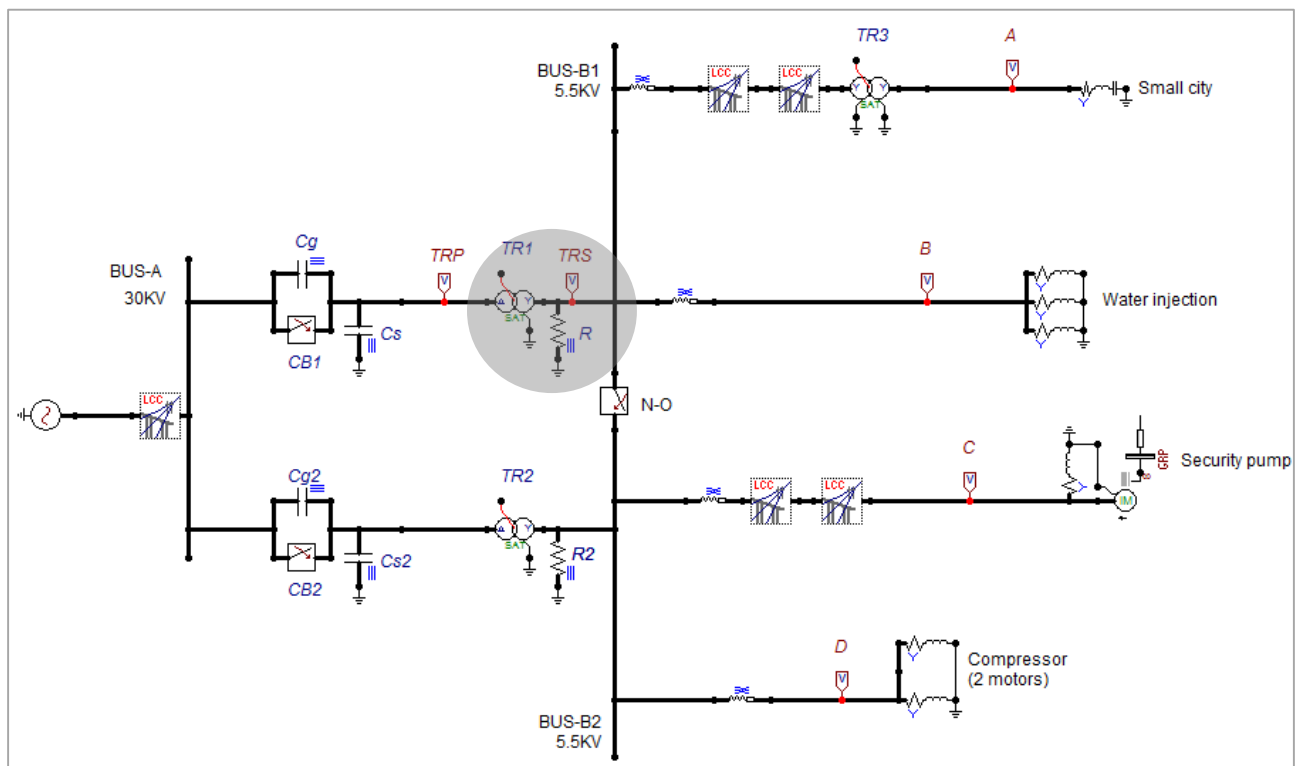


Figure 3.34: The damping resistor at the transformer TR1 secondary side.

This simple method, however, has a limited applicability in the case of the modern, compact constructions of the VTs, utilizing low-loss magnetic materials since typical core losses (oriented steel) are lower than 50 W, which has little effect on the damping properties.

Both computer simulations and experiments showed in many cases that the resistance value needed for efficient damping of the ferroresonant oscillations is very small ($R < 20 \Omega$) and the resulting power dissipated in the damping resistor is greater than several hundreds of watts.

Now we try to see the effect of this method we try to vary R around the value of 20Ω , table 3.4 summarizes the simulation results and figures 3.36, 3.37 and 3.38 show voltage waveforms at transformer secondary side for case 5 with ferroresonance, the threshold in case 4 and its elimination in case 1.

Cases	Resistor (Ω)	Maximum overvoltage (pu)	state
1	12	0.9	Non ferroresonance
2	15	1.1	Non ferroresonance
3	20	1.18	Non ferroresonance
4	25	1.25	Threshold
5	30	1.29	In ferroresonance

Table 3.4: Simulation results of maximum overvoltage for damping resistor.

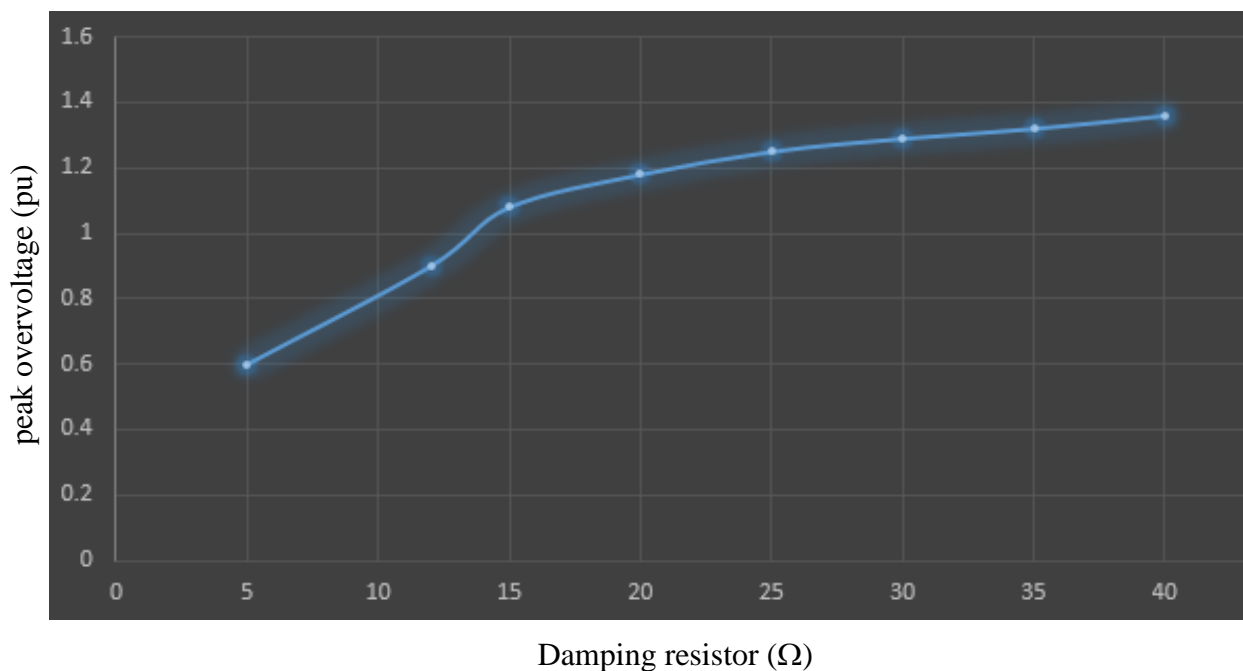


Figure 3.35: The effect of the Damping resistor on ferroresonance.

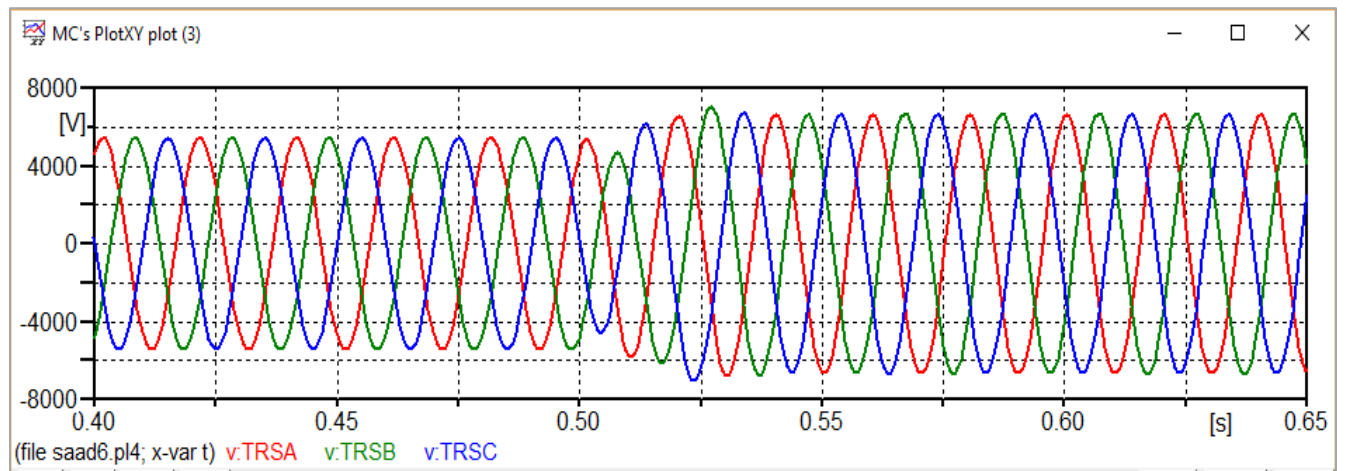


Figure 3.36: The voltages at point TRS for Case 5 with $R = 30 \, \Omega$

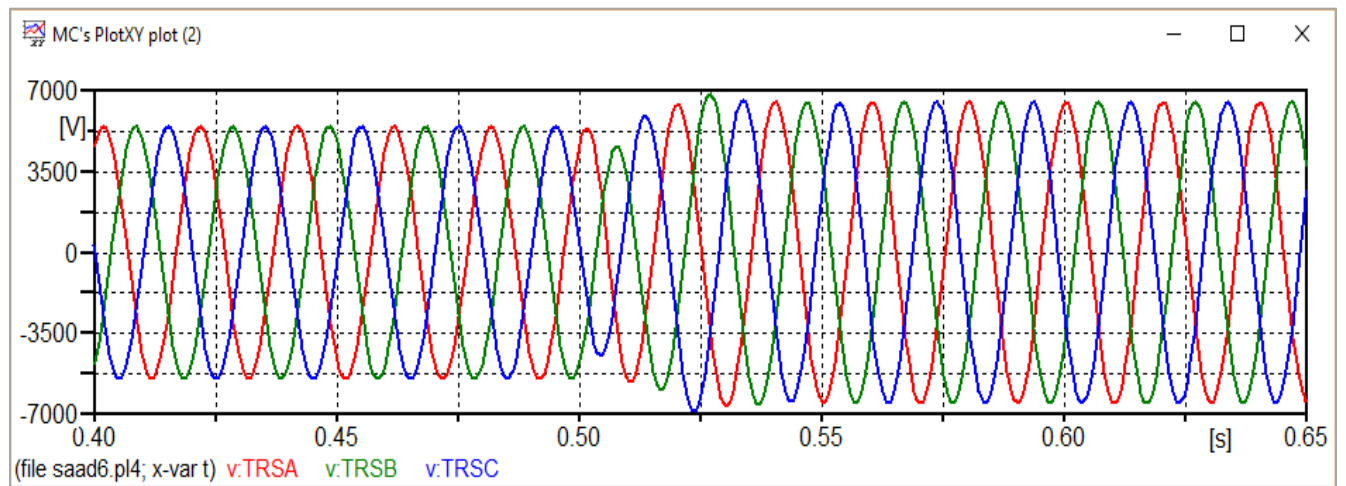


Figure 3.37: The voltages at point TRS for Case 4 with $R = 25 \, \Omega$

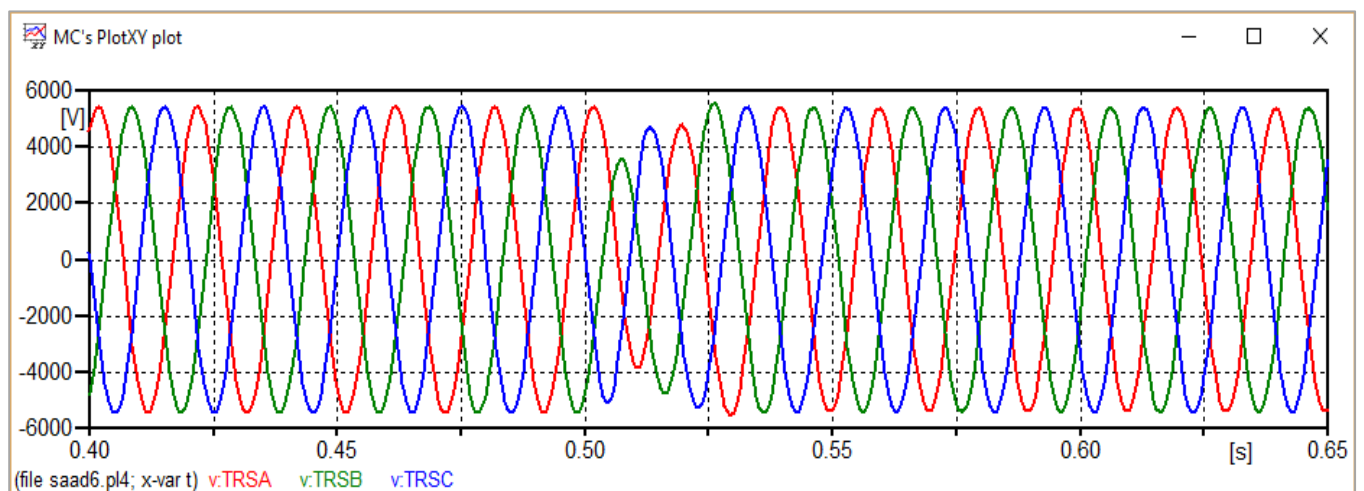


Figure 3.38: The voltages at point TRS for Case 1 with $R = 12 \, \Omega$

Comments:

Table 3.4 and Figure 3.35 shows the simulated effectiveness of the ferroresonant oscillations damping with the resistor. It can be seen that the use of the resistor $R = 12\Omega$ eliminate the ferroresonance with peak voltage $V = 0.9$ pu, and the use of the value of R larger than approximately 12Ω has a small influence on avoiding the ferroresonance, until the threshold $R = 25\Omega$ the ferroresonance is observed.

However, in practice, using a damping resistor of such a low value results in a risk of thermal damage of the VTs during abnormal network asymmetry resulting from prolonged earth faults. There are other known methods of preventing ferroresonance, such as the use of a saturable inductor in series with a damping resistor.

This approach, despite its applicability in high-voltage (HV) capacitive VTs with an intermediate inductive VT, is practically not used in the MV voltage transformers. The use of the R–L circuit overcomes the thermal problem in the case of the earth fault situation. However, the efficiency of damping is limited (it conducts current only above the saturation level of the inductor) and, thus, a very precise design of the damping circuit for a specific VT type is required.

3.7. Conclusion

The analysis presented in this chapter on the case study example showed the approach applicable to studying the potential of the ferroresonant behavior of the real power network. we have seen almost the parameters that can affect ferroresonance which are the grading capacitor of the circuit breaker and the source voltage.

The use of the ATP environment can be used to identify the potential ferroresonant combinations of parameters (voltage and capacitance) and allows one to select appropriate mitigation scheme as we have seen in section 3.6.

GENERAL CONCLUSION

GENERAL CONCLUSION

Even though ferroresonance is not very common, it is a problem in power systems. To get familiar with it, it is compared to linear resonance. The ferroresonance has dangerous consequences like stable overvoltages and overcurrents. Risky configurations are mentioned and prevention of ferroresonance is discussed, because they are considered to be catastrophic when they occur.

In addition, ATPDraw software has been developed to simulate one of the critical situations for the ferroresonance to appear, which is the interaction between the grading capacitor of circuit breaker and MV power transformer. The influence of capacitance values has been analyzed through several software simulations, considering the critical capacitance values.


Some practical solutions are suggested and introduced in the ATPDraw representation of the circuit of Haoud Berkaoui station after creating a ferroresonance situation, such as installing a shunt capacitor at the transformer primary side and installing a capacitor bank or a damping resistor at the secondary side, they had a considerable effect on damping and eliminating the risk of ferroresonance.

REFERENCES

- [1] Philippe FERRACCI, "Group Schneider Cahier technique n°190, Ferroresonance", ECT190, first issued March 1998.
- [2] Schultz, R.A., "Ferroresonance in Distribution Transformer Banks on 8/34.5 kV Systems," Presented at 1964 Spring Conference, Rocky Mountain Elec. League.
- [3] Rudenberg, R., transient performance of electrical power system, McGraw-Hill Book Company, New York, NY, Copyright @ 1949.
- [4] Swee Peng Ang "Ferroresonance simulation studies of transmission systems", the university of Manchester 2010, p 20-22.
- [5] T. D. Burton, Introduction to Dynamic System Analysis, International Edition ed.: McGraw-Hill.
- [6] M. Val Escudero, I. Dudurych, and M.A. Redfern, "Characterization of ferroresonant modes in HV substation with CB grading capacitors", Electric Power Systems Research, vol. 77, pp. 1506-1513, 2007.
- [7] K. Pattanapakdee and C. Banmongkol, "Failure of Rise Pole Arrester Due to Station Service Transformer Ferroresonance", Proceedings of International Conference on Power Systems Transients, Lyon, 4-7 June 2007.
- [8] D.A.N. Jacobson, D.R. Swatek and R.W. Mazur, "Mitigating Potential Transformer Ferroresonance in a 230 kV Converter Station", Proceedings of IEEE Transmission and Distribution Conference, pp. 269-275, Los Angeles, 1996.
- [9] IEC 71 International Standard, "Insulation Co-ordination", 1996
- [10] Yunge Li, Wei Shi, Rui Qin and Jilin Yang, "A Systematical Method for Suppressing Ferroresonance at Neutral-Grounded Substations", IEEE Transactions on Power Delivery, vol. 18, no.3, July 2003.
-

- [11] L. X. Zhou and Z. D. Yin, "Research on PT Ferromagnetic Resonance and the Controllable Damping", Proceedings of IEEE Power Tech Conference, pp. 413-418, Lausanne, 1-5 July 2007.
 - [12] P. Sakarung, T. Bunyagul and S. Chatratana, "Investigation and Mitigation of Overvoltage Due to Ferroresonance in the Distribution Network", Journal of Electrical Engineering and Technology, vol. 2, no. 3, pp. 300-305, 2007.
 - [13] T. Van Craenenbroeck, D. Van Dommelen and N. Janssens, "Damping Circuit Design for Ferroresonance in Floating Power Systems", European Transactions on Electrical Power, vol. 10, no. 3, May/June 2000.
 - [14] M StoSur, W PiaSecki . M FlorkoWSki, M Fulczyk "Electrical Power Quality and Utilization, Journal Vol. XIV, No. 2, pp 49 2008.
 - [15] B. Djaafar R. Taoufik 'Investigation on Power Transformer Design' Final Year Project Report 2015.
 - [16] Earthing systems in LV, B. LACROIX, R. CALVAS, Cahier Technique Merlin Gerin n 172.
 - [17] Bienvenido Rodríguez – Medina, Marianela Santiago- Luna, "Electric Power Engineering Group UPR- Mayagüez" "ATP/EMTP Quick Guide", Mayagüez, P.R. June 18,2002.
 - [18] CIGRE Working Group C4.307, "Resonance and ferroresonance in power networks," CIGRE, Tech. Bro. TB-569, Feb. 2014.
 - [19] S. Santoso, R. C. Dugan, and P. Nedwick, "Modeling ferroresonance phenomena in an underground distribution system," in Proc. 2001 IPST.
 - [20] A. V. Ranst, J. M. Dumoulin, and N. Mabrouk, "Insulation coordination and ferroresonance study for EMAL phase II project," Tractebel Eng., Brussels, BE, Apr. 2012.
-

The definitions and parameters

➤ **Source :** 

Name: ACSOURCE - Steady-state (cosine) function (voltage) Grounded; TYPE 14.

Component: ACSOURCE

DATA	UNIT	VALUE
AmplitudeA	Volt	30000
Frequency	Hz	50
PhaseAngleA	degrees	0
StartA	sec	-1
StopA	sec	100

NODE	PHASE	NAME
AC	ABC	X0019

Copy Paste entire data grid Reset Order: 0 Label:

Comment:

Type of source: ☐ Current ☒ Voltage

Num phases: ☐ Single ☒ 3-phase ☐ 3*1-phase

Angle units: ☒ Degrees ☐ Seconds

Amplitude: ☒ Peak L-G ☐ RMS L-G ☐ RMS L-L

Grounding: ☒ Grounded ☐ Ungrounded

☐ Hide

Edit definitions OK Cancel Help

➤ **Transformer:** 

Name: Sat-Trafo - General saturable transformer. 3 phase. 2 windings, Delta, Wye .with 30° phase shifts.

Component: SATTRAFO

	Prim.	Sec.
U [V]	30000	3180
R [ohm]	0.0005	0.0005
L [mH,ohm]	0.05	0.05

Coupling: D Y

Phase shift: 30

I(0)= 0 Rm= 00000000 ☒ 3-leg core

F(0)= 2 R0= 11500 ☐ RMS ☐ 3-winding

NODE	PHASE	NAME
Primary	ABC	X0045
Secondary	ABC	S
Starpoint	ABC	X0038
Sec-N	1	X0039

Order: 0 Label:

Comment:

Output: 0 - No ☐ Hide

Edit definitions OK Cancel Help



Model: PI **Unit system:** Metric

Line/Cable Data: XLPE120

Model Data Nodes

System type

Overhead Line

#Ph: 3

☐ Transposed
☐ Auto bundling
☒ Skin effect
☐ Segmented ground
☐ Real transf. matrix

Units

Metric

English

Standard data

Rho [ohm*m] 20

Freq. init [Hz] 50

Length [km] 0.7

☐ Set length in icon

Model

Type

☐ Bergeron
☒ PI
☐ JMart
☐ Semlyen
☐ Noda

Data

☐ Printed output
☐ [C] print out

Comment:

Order: 0

Label:

☐ Hide

OK

Cancel

Import

Export

Run ATP

View

Verify

Edit defin.

Help

Line/Cable Data: XLPE120

Model Data Nodes

#	Ph.no	Rin	Rout	Resis	Horiz	Vtower	Vmid
		[cm]	[cm]	[ohm/km DC]	[m]	[m]	[m]
1	1	0	0.545	0.303	-0.75	10	8
2	2	0	0.545	0.303	0	10	8
3	3	0	0.545	0.303	0.75	10	8

Add row

Delete last row

Insert row copy

Move

OK

Cancel

Import

Export


Run ATP

View

Verify

Edit defin.

Help

➤ **Induction Motor (Security pump):** 

Component: UM_3

Attributes

General Magnet Stator Rotor Init

Stator coupling

Y

Pole pairs:

2

Rotor coils

d: 1 q: 1

☐ Automatic
☐ Prediction

Frequency:

50

Tolerance:

0.1885

Order: 0

Label:

Comment:

Output

TQOUT

0 1 2 3

OMOUT

0 1 2 3

☒ THOUT
☒ CURR

☐ Hide

Edit definitions

OK

Cancel

Help

Component: UM_3

Attributes

General Magnet Stator Rotor Init

LMUD: 0.003533

LMUQ: 0.003533

Saturation

☒ none
☐ d
☐ q
☐ both
☐ symm

Stator

ABC

Pole pairs:

2

Frequency:

50

Tolerance:

0.1885

Order: 0

Label:

Comment:

Output

TQOUT

0 1 2 3

OMOUT

0 1 2 3

☒ THOUT
☒ CURR

☐ Hide

Edit definitions

OK

Cancel

Help

Component: UM_3

Attributes

General Magnet Stator Rotor Init

	R [ohm]	L [H/pu]
0	0	0
d	0.01673	0.1968
q	0.01673	0.1968

NODE	PHASE	NAME
Stator	ABC	P
M_NODE	1	XX0026
Neut	1	

Order: 0 Label:

Comment:

Output

TQOUT 0 1 2 3 OMOUT 0 1 2 3 ☒ THOUT ☐ Hide ☒ CURR

Edit definitions OK Cancel Help

Component: UM_3

Attributes

General Magnet Stator Rotor Init

	R [ohm]	L [H/pu]
1	0.017405	0.1968
2	0.017405	0.1968

NODE	PHASE	NAME
Stator	ABC	P
M_NODE	1	XX0026
Neut	1	

Order: 0 Label:

Comment:

Output

TQOUT 0 1 2 3 OMOUT 0 1 2 3 ☒ THOUT ☐ Hide ☒ CURR

Edit definitions OK Cancel Help

Component: UM_3

Attributes

General Magnet Stator Rotor Init

Manual

Stator	I [A]	Rotor	I [A]
0	0	1	0
d	0	2	0
q	0		

OMEGM [rad/s]: 0 THETAM: 0

NODE	PHASE	NAME
Stator	ABC	P
M_NODE	1	XX0026
Neut	1	

Order: 0 Label:

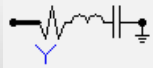
Comment:

Output

TQOUT 0 1 2 3 OMOUT 0 1 2 3 ☒ THOUT ☐ Hide ☒ CURR

Edit definitions OK Cancel Help

➤ **RLC load of the Small City:**



Name: RLCY3. Y-coupling

Independent values in phases.

Component: RLCY3

Attributes

DATA	UNIT	VALUE
L_1	mH	9.4
C_1	μF	0.01
R_2	Ohm	1.5
L_2	mH	9.4
C_2	μF	0.01
R_3	Ohm	1.5
L_3	mH	9.4
C_3	μF	0.01

NODE	PHASE	NAME
IN	ABC	RLC
OUT	1	

Copy Paste entire data grid Reset Order: 0 Label:

Comment:

Output 0 - No ☐ Hide ☐ \$Vintage,1

Edit definitions OK Cancel Help

Component: RLCY3

DATA	UNIT	VALUE	NODE	PHASE	NAME
R_1	Ohm	78	IN	ABC	W
L_1	mH	407	OUT	1	
C_1	F	0			
R_2	Ohm	78			
L_2	mH	407			
C_2	F	0			
R_3	Ohm	78			
L_3	mH	407			

Copy Paste entire data grid Reset Order: 0 Label:

Comment:

Output: 0 - No ☐ Hide ☐ \$Vintage,1

Edit definitions OK Cancel Help

Component: RLCY3

DATA	UNIT	VALUE	NODE	PHASE	NAME
R_1	Ohms	47.65	IN	ABC	SP
L_1	mH	580	OUT	1	
C_1	F	0			
R_2	Ohms	20			
L_2	mH	580			
C_2	F	0			
R_3	Ohms	20			
L_3	mH	580			

Copy Paste entire data grid Reset Order: 0 Label:

Comment:

Output: 0 - No ☐ Hide ☐ \$Vintage,1

Edit definitions OK Cancel Help

➤ **RL load of Water Injection:**



Name: RLCY3; Y-coupling,
Independent values in phases.

➤ **RL load of Security Pump:**



Name: RLCY3; Y-coupling,
Independent values in phases.

Component: RLCY3

DATA	UNIT	VALUE	NODE	PHASE	NAME
R_1	Ohm	13.55	IN	ABC	C
L_1	mH	80	OUT	1	
C_1	F	0			
R_2	Ohm	13.55			
L_2	mH	80			
C_2	F	0			
R_3	Ohm	13.55			
L_3	mH	80			

Copy Paste entire data grid Reset Order: 0 Label:

Comment:

Output: 0 - No ☐ Hide ☐ \$Vintage,1

Edit definitions OK Cancel Help

Component: LINESY_3

DATA	UNIT	VALUE	NODE	PHASE	NAME
R ₀	Ohm/m	0.5	IN1	ABC	F
L ₀	mH/m	0.1	OUT1	ABC	W1
R ₊	Ohm/m	0.005			
L ₊	mH/m	0.001			

Copy Paste entire data grid Reset Order: 4 Label:

Comment:

Lines: Length 100 [m] ☐ Hide

Edit definitions OK Cancel Help

➤ **RL load of compressor:**



Name: RLCY3; Y-coupling,
Independent values in phases.

➤ **Cable:**

Name: LINESY_3 - Symmetric RL
coupled line. Data given in positive
and zero sequence.

The parameters of the circuit breaker used in the electric substation of HAOUD BERKAOUI

TYPE		S																															
		EGB 1 20-06F		EGB 1 20-12F		EGB 1 28-06F		EGB 1 28-12F		EGB 2 12-06F		EGB 2 12-12F		EGB 2 16-06F		EGB 2 16-12F		EGB 3 12-06F		EGB 3 12-12F		EGB 3 16-06F		EGB 3 16-12F		EGB 3 25-12F							
Rated voltage	kV	7,2								12								17,5															
Rated lightning impulse withstand voltage 1,2/50 μs	kV	60								75								95															
Rated power frequency withstand voltage 1 min	kV	22								28								38															
Rated normal current	A	630	1250	630	1250	630	1250	630	1250	630	1250	630	1250	630	1250	630	1250	630	1250	630	1250	630	1250	630	1250	630	1250						
Rated short circuit breaking current	kA	20				28				12,5				16				25				12,5				16				25			
Rated short circuit making current	kA	50				70				31,5				40				63				31,5				40				63			
Rated cable-charging breaking current	A	10								25								31,5															
DC component	%	30																31															
Rated no-load transformer breaking current	A	20																															
Rated single capacitor bank breaking current	A	500																															
Rated operating sequence		0 - 0.3 s - CO - 3 min. - CO/CO - 15 s - CO																															

TYPE		SL						S						LM															
		EGB 4 12-06F		EGB 4 12-12F		EGB 4 16-06F		EGB 4 16-12F		EGB 4 20-12F		EGB 5 08-06F		EGB 5 08-12F		EGB 5 12-06F		EGB 5 12-12F		EGB 5 16-06F		EGB 5 16-12F		EGB 5 25-12F		EGB 5 25-16F		EGB 5 25-25F	
Rated voltage	kV	24										36																	
Rated lightning impulse withstand voltage 1,2/50 μs	kV	125										170																	
Rated power frequency withstand voltage 1 min	kV	50										70																	
Rated normal current	A	630	1250	630	1250	630	1250	630	1250	630	1250	630	1250	630	1250	630	1250	630	1250	630	1250	1600	2500	1600	2500	1600	2500	1600	2500
Rated short circuit breaking current	kA	12,5				16				20				8				12,5				16				25			
Rated short circuit making current	kA	31,5				40				50				20				31,5				40				63			
Rated cable-charging breaking current	A	31,5										50																	
DC component	%	32																											
Rated no-load transformer breaking current	A	20																											
Rated single capacitor bank breaking current	A	500																											
Rated operating sequence		0 - 0.3 s - CO - 3 min. - CO/CO - 15 s - CO																											

Table 1: Range of types and technical features from the company which design SF6 circuit breaker.

ELİMSAN Şalt Cihazları ve Elektromekanik San. ve Tic. A.Ş.
 pb: 295 • Uzuntarla • İZMİT • Phone: +90 262 375 28 10 • Fax: +90 262 375 28 08
 e-mail: elimsanuretim @ elimsangroup.com

ELİ İthalat - İhracat ve Dış Tic. A.Ş.
 pb: 295 • Uzuntarla • İZMİT • Phone: +90 262 375 23 60 (pbx) • Fax: +90 262 375 23 22
 e-mail: eli @ elimsangroup.com

www.elimsangroup.com



The characteristics of the used grading capacitors in electric substations of 30 KV

Part Number	Rated Voltage kVdc	Rated Voltage kVrms	Test Voltage kVrms	Corona Inception Voltage (kVrms) (<10pc)	Capacitance ±20% (pF) ±10% on request	Dimensions millimeters (inches)				Packaging Unit
						Ø ± 1	d	L ± 1	H ± 2	
HP30EX0561M --	15	10	12	6	560	28 (1.100)	12 (0.472)	22 (0.866)	16 (0.630)	40
HP30EX0751M --					750	28 (1.100)	12 (0.472)			40
HP30EX0102M --					1000	28 (1.100)	12 (0.472)			40
HP40EX0152M --					1500	38 (1.500)	12 (0.472)			40
HP40EX0182M --					1800	38 (1.500)	12 (0.472)			40
HP40EX0202M --					2000	38 (1.500)	12 (0.472)			40
HP50EX0252M --					2500	48 (1.900)	12 (0.472)			45
HP50EX0272M --					2700	48 (1.900)	12 (0.472)			45
HP50EX0332M --					3300	48 (1.900)	12 (0.472)			45
HP60EX0372M --					3700	58 (2.283)	15 (0.591)			20
HP60EX0402M --					4000	58 (2.283)	15 (0.591)			20
HP60EX0502M --					5000	58 (2.283)	15 (0.591)			20
HP60EX0562M --					5600	58 (2.283)	15 (0.591)			20
HP30EY0501M --	20	15	18	9	500	28 (1.100)	12 (0.472)	24 (0.945)	18 (0.709)	40
HP30EY0561M --					560	28 (1.100)	12 (0.472)			40
HP30EY0751M --					750	28 (1.100)	12 (0.472)			40
HP40EY0102M --					1000	38 (1.500)	12 (0.472)			40
HP40EY0132M --					1300	38 (1.500)	12 (0.472)			40
HP40EY0152M --					1500	38 (1.500)	12 (0.472)			40
HP50EY0202M --					2000	48 (1.900)	12 (0.472)			45
HP50EY0222M --					2200	48 (1.900)	12 (0.472)			45
HP50EY0252M --					2500	48 (1.900)	12 (0.472)			45
HP60EY0302M --					3000	58 (2.283)	15 (0.591)			20
HP60EY0332M --					3300	58 (2.283)	15 (0.591)			20
HP60EY0372M --					3700	58 (2.283)	15 (0.591)			20
HP60EY0402M --					4000	58 (2.283)	15 (0.591)			20
HP30E30561M --	30	20	24	12	560	28 (1.100)	12 (0.472)	26 (1.024)	20 (0.787)	40
HP40E30821M --					820	38 (1.500)	12 (0.472)			40
HP40E30102M --					1000	38 (1.500)	12 (0.472)			40
HP40E31121M --					1120	38 (1.500)	12 (0.472)			40
HP50E30152M --					1500	48 (1.900)	12 (0.472)			45
HP50E30172M --					1700	48 (1.900)	12 (0.472)			45
HP50E30202M --					2000	48 (1.900)	12 (0.472)			45
HP60E30272M --					2700	58 (2.283)	15 (0.591)			20
HP60E30302M --					3000	58 (2.283)	15 (0.591)			20
HP60E30332M --					3300	58 (2.283)	15 (0.591)			20
HP30E40391M --	40	28	33	17	390	28 (1.100)	12 (0.472)	30 (1.180)	24 (0.945)	40
HP40E40751M --					750	38 (1.500)	12 (0.472)			40
HP50E40102M --					1000	48 (1.900)	12 (0.472)			30
HP50E40142M --					1400	48 (1.900)	12 (0.472)			30
HP60E40172M --					1700	58 (2.283)	15 (0.591)			20
HP60E40202M --					2000	58 (2.283)	15 (0.591)			20
HP60E40242M --					2400	58 (2.283)	15 (0.591)			20

Table 2: The parameters used in the substation indicated with a red color

